Федеральное государственное автономное образовательное учреждение
высшего образования «Уральский федеральный университет имени
первого Президента России Б. Н. Ельцина»

Уральский энергетический институт
Кафедра «Атомные станции и возобновляемые источники энергии»

На правах рукописи

САЛИХ САДЖАД АБДУЛАЗИМ

ЭКСПЕРИМЕНТАЛЬНОЕ И ЧИСЛЕННОЕ ИССЛЕДОВАНИЕ ДВИГАТЕЛЯ ГАММА-СТИРЛИНГА С ИСПОЛЬЗОВАНИЕМ СЛОЖНОГО РАБОЧЕГО ТЕЛА

2.4.5. Энергетические системы и комплексы

ДИССЕРТАЦИЯ
на соискание ученой степени
кандидата технических наук

Научный руководитель:
Доктор технических наук, профессор,
Щеклеин Сергей Евгеньевич

Екатеринбург – 2024

Federal State Autonomous Educational Institution Higher Education «Ural Federal University named after the first President of Russia B.N. Yeltsin»

Ural Power Engineering Institute

Department of «Nuclear Power Plants and Renewable Energy Sources»

As a manuscript

SALIH SAJJAD ABDULADHEEM

EXPERIMENTAL AND NUMERICAL INVESTIGATION OF GAMMA STIRLING ENGINE UTILIZING COMPOUND WORKING FLUID

2.4.5. Energy systems and complexes

DISSERTATION

Degree of Candidate of Technical Sciences

Scientific supervisor:

Doctor of Technical Sciences, Professor,

Shcheklein Sergey Evgenievich

Yekaterinburg – 2024

ACKNOWLEDGMENT

I want to begin by expressing my gratitude to God for assisting me in every aspect of my life. Without the guidance and help of my supervisor, the support of my family, and the assistance of my friends, I would not have been able to complete my study.

I would like to express my deepest thanks and appreciation to my supervisor, Prof. Sergey Evgenvich Shcheklein, Head of Department of Nuclear and Renewable Energy, Ural Power Engineering Institute of Ural Federal University, for his exceptional guidance, kindness, understanding, and creation of an optimal environment for doing my thesis.

I would want to express my gratitude to Dr. Naseer T. Alwan, who continually motivated me, clarified my understanding of ideas, and pushed me to carry out this study work. Also, many thanks to Dr. Mohammed A. Qasim for his constant advice and help.

I would also like to express my gratitude to my family, specifically to my great mother, my wonderful wife, who is both my soulmate and partner in this life, and my brothers. Throughout both the positive times and the difficult times, they were there for me, providing me with support and encouragement.

Lastly, and of the greatest importance, I dedicate this work to the spirit of my father.

TABLE OF CONTENTS

LIST OF FIGURES

LIST OF TABLES

OVERVIEW AND DESCRIPTION OF THE RESEARCH

The relevance of the research topic and the degree of its development: The increase in energy demand is the result of a complex interaction between demographic, economic, technological, and societal factors. In order to address this challenge, it is typically necessary to implement a combination of energy efficiency measures, technological innovation, policy interventions, and shifts towards cleaner and more sustainable energy sources.

Currently, oil and gas activities provide about 15% of the overall energy-related emissions worldwide, which is equal to 5.1 billion tons of greenhouse gas emissions. According to the International Energy Agency's Net Zero Emissions by 2050 Scenario, the emissions intensity of these activities will decrease by 50% by the end of the current decade. When the decrease in oil and gas use is taken into account, it leads to a 60% reduction in emissions from oil and gas activities by 2030.

Stirling engine is among the most ancient heat engines, the combination of its efficiency, silent operation, flexibility, low emissions, reliability, scalability, and ability to utilize a variety of heat sources makes it a very attractive option for applications that emphasize sustainable and efficient power generation. Stirling engines have a broad variety of applications across industries and sectors because of their unique advantages. Some typical uses are power generation, space exploration, automotive, aerospace, marine, industrial, renewable energy systems, residential heating and cooling. Optimizing the efficiency of Stirling engine requires addressing a number of various aspects of their design, operation, and effectiveness. By choosing or creating the working fluid to satisfy Stirling engine and application requirements, we may improve performance and efficiency and enhance Stirling engine technology. Its ability to work with renewable sources makes it an essential technology for sustainable energy production and a crucial element in moving towards a cleaner and more sustainable energy future.

The purpose of the study: To enhance the performance of the Stirling engine, both numerical and experimental studies are conducted on a Gamma type Stirling engine through the addition of low-boiling point liquids into the working fluid.

The object of the study: The process of evaluating and investigating the performance of the Stirling engine via the study of the characteristics of the working fluid.

Subject of research: Adding low-boiling point liquids to the working fluid of the gamma engine provides prospects for enhanced heat transfer, thermal energy storage, and performance

improvement. However, it also raises concerns about fluid compatibility, control, handling, and efficiency trade-offs, which must be carefully addressed throughout design and implementation.

Research methods: Exploring the working fluids of Stirling engines involves studying a variety of fluid characteristics, performance, and compatibility in order to enhance the efficiency and dependability of the engine. Experimental study includes analyzing the behavior of volume and pressure variations in gas chambers containing air with additional low-boiling liquids such as acetone and spirit, depending on the impact of changing the temperature and test this experiment on Gamma Stirling engine. The research conducted a numerical study that included both first- and second-order analysis. All of these models were solved using algebraic and differential equations, which were programmed using MATLAB software. Moreover, through the use of the ASPEN-HYSYS software, a numerical simulation was carried out in order to investigate the operation of the ideal cycle of the Stirling engine with different compound working fluids.

The main provisions of the dissertation submitted for defense:

1. The use of compound working fluid in Stirling engine has the potential to enhance its performance in comparison to design that employs a single working fluid.
2. The results from experimental studies performed on Gamma Stirling engine to evaluate the influence of using various fluids with different concentrations.
3. The results of the mathematical modelling that was solved and in MATLAB code for first and second order significant models.
4. The results of numerical simulation that was carried out with the help of the ASPEN-HYSYS in order to investigate the ideal cycle of the Stirling engine.

Scientific novelty of the dissertation research:

1. Within the scope of this study, an innovative method was utilized in order to enhance the performance of the Stirling engine.
2. In this study, the efficiency and power of the Stirling engine were improved using a new method, which is the use of compound working fluids. Compound working fluids have the potential to improve the efficiency of Stirling engine by facilitating more effective heat transfer and achieving greater rates of energy conversion.
3. A mathematical model was developed in MATLAB for the purpose of this investigation. The model contains a study into the utilization of a compound working fluid rather than single working fluid.

4. The numerical simulation was built in ASPEN-HYSYS for the purpose of this research. The simulation comprises a study of the ideal cycle of the Stirling engine.
5. The use of compound working fluids opens the way for further research and development in Stirling engine technology. Researchers can explore new combinations of fluids to enhance performance and efficiency.
6. Regarding the challenges, The Stirling engine design becomes advanced when compound working fluids are included. To guarantee dependable and efficient working, it must take into account issues such as fluid compatibility, phase transitions, and temperature characteristics.

The theoretical and practical significance of the work: In the context of this research, the performance of Gamma-type Stirling engine will be investigated and analyzed. This will be accomplished by establishing the influence of the working fluid. By incorporating low-boiling-point fluids into a combination of the working fluids, an experiment was conducted, and the results showed that the engine performance was significantly enhanced as a result of this procedure. Moreover, empirical investigations carried out using MATLAB included solving complex algebraic equations, while ASPEN-HYSYS was used to determine the ideal cycle behavior. This research shows that engine performance may be enhanced by increasing power output and efficiency. The theoretical importance lies in understanding the effect of the working fluid and using advanced modeling techniques, while the practical importance lies in enhancing engine performance and promoting technological progress in Stirling engine technology.

Personal contribution: The following aspects illustrate the author's participation and contribute in the development of the research:

1. Conducted an extensive investigation and analysis of the Stirling engine performance to identify the specific parameters that contribute to its enhanced efficiency.
2. Practical investigations were carried out on the Stirling engine to assess the impact of involving different fluids and achieving a uniform mixture in order to enhance its performance.
3. A theoretical study was carried out in MATLAB for different mathematical models in order to compare the results of these various models.
4. The numerical simulation was conducted using the ASPEN-HYSYS software to analyze the ideal operating cycle of Stirling engine, which is well recognized as a significant software for evaluating the characteristics of different chemical compounds and mixtures.

5. Research and experiments demonstrated that the use of low-boiling fluids enhanced the performance of the Stirling engine, resulting in higher efficiency and power.

Approbation of Work: In a number of research papers and international scientific conferences, the results of the study were presented and discussed further:

1. Fourth International Conference on Recent Advances in Materials and Manufacturing (ICRAMM 2022) held at the Department of Mechanical Engineering, Velalar College of Engineering and Technology, Erode, Tamil Nadu, India during 08-09 December 2022.
2. Fourth International Conference on Emerging Electrical Energy, Electronics and Computing Technologies (ICE4CT 2022) held at the Faculty of Electrical Engineering & Technology, University Malaysia Perlis, conducted jointly with the Nandha Engineering College, India and Centre of Excellence for Renewable Energy (CERE) during 28- 29 December 2022. At this conference, we were awarded the best research paper that was presented.
3. International scientific and practical conference of students, graduate students and young scientists “ENERGY AND RESOURCE SAVING. ENERGY SUPPLY. NON-TRADITIONAL AND RENEWABLE ENERGY SOURCES. NUCLEAR POWER" held at Ural Federal University (UrFU) Russia, Ekaterinburg (December 12-16, 2022).
4. Fifth International Youth Conference on Radio Electronics, Electrical and Power Engineering (REEPE 2023), National Research University Moscow Power Engineering Institute (NRU MPEI) MOSCOW, RUSSIAN FEDERATION, March 16-18, 2023.

Publications: The total number of papers published during this study is 13 articles. Eight of these papers were published in the international databases Scopus and Web of Science and five papers were published in the Russian VAK journals recommended by the Higher Attestation Commission of the Russian Federation and the UrFU Attestation Council. Four articles were presented at international and Russian scientific conferences.

The structure and scope of the thesis: The dissertation includes an introduction, five chapters, a conclusion, 231 bibliography, a list of abbreviations, and supplemental appendices. The dissertation additionally consists of 200 pages, 96 figures, and 15 tables.

CHAPTER 1. INTRODUCTION, HISTORY, ANALYSIS OF STIRLING ENGINE PERFORMANCE

1.1. Introduction

Energy is the primary force behind the functioning of the contemporary world. The need for affordable energy and electricity has risen continuously due to the growing population and our relentless drive for development. Nevertheless, the remarkable expansion seen in the 20th and 21st centuries has also introduced a significant number of hazards and challenges. Energy is a fundamental aspect of several significant difficulties and challenges that the world is now confronting. Pollution and global warming pose significant challenges that have the potential to profoundly alter the Earth in unforeseeable and irreversible ways. As population grows and new industrial units are installed, power consumption is rising quickly worldwide. Advancements in technology need the use of electricity for electronic devices, hybrid vehicles, and robots. The available electricity producing sources experience increased load demand[10][11][12].

Global governments and companies must collaborate to effectively counteract this prevailing pattern[13].The significant reliance on fossil fuels as the primary energy source in many countries has resulted in several adverse environmental effects, including an increase of global warming and a rise of air pollution. Air pollution is responsible for several health issues and has adverse effects on society and the economy. Global efforts are currently being implemented to reduce the impacts of global warming by establishing international accords, which then inform the implementation of specific local policies in each country[14][15].

Renewable energy sources have grown essential in enhancing energy supply, particularly for electricity generation. The use of unlimited energy resources derived from the environment, with the objective of turning them into electrical energy, while preserving environmental considerations, presents an abundance of benefits for

renewable energy sources, primarily in terms of environmental preservation. This is clearly shown by the fact that renewable energy sources contribute little or zero percent to greenhouse gas emissions and other forms of air pollution[16].

Renewable energy harnesses energy sources that are perpetually renewed by natural processes, including sun, wind, water, geothermal energy, and plants. Renewable energy technologies transform these fuels into practical forms of energy, mostly electricity, but also heat, chemicals, or mechanical energy[17]. The combustion of fossil fuels for energy production leads to a substantial release of greenhouse gases, which in turn contributes to the phenomenon of global warming. The majority of renewable energy sources release little or no emissions, even when taking into account the whole life cycle of the technology. Stirling engines are external combustion engines that utilize different compressible fluids and consist of two working pistons linked to a crankshaft by connecting rods. Stirling engines are reciprocating external combustion engines that employ external heat to enable productive work using one or more pistons[18]. The performance of this thermodynamic machine is produced by the expansion and compression of the working fluid during heating and cooling. The engine defined amount of gas is moved in the direction between the engine hot and cold ends[19].

The compressible fluids utilized in engine construction may include air, hydrogen, helium, nitrogen, or even vapor. The engine can be powered by any heat source, ranging from hard coal to oil to solar energy. The only requirement is that the heat source must be compatible with the engine. In a solar energy model, the solar concentrator and absorber need to be incorporated into the heating component of the storage tank. The Stirling engine is an efficient way of decreasing reliance on fossil fuels since it may be fueled by many heat sources like biomass and sunlight. It is certain that the interest in this kind of engine will endure[20]. Stirling engines, being externally heated, are very ecologically friendly engines with a high theoretical cycle efficiency. They may be operated utilizing varied range of fuels and heat sources,

including combustible materials, solar radiation, geothermal hot water, and radioisotope energy[21].

A solar Stirling engine is very effective technique for converting solar energy into electricity and favored due to its exceptional performance and affordable price, it is very suitable option for converting concentrated solar thermal energy into electrical power. Additionally, this type of equipment can be utilized in various capacities, such as functioning as coolers or heat pumps. This machine has the capability to operate in many modes, thanks to its design and thermodynamic cycle[22]. It can function as a heat pump or refrigerator, depending on whether it is powered by cold or warm source and if it is producing mechanical work.

The adoption of the word "Stirling engine" as the overarching designation for a regenerative thermal cycle engine is a relatively recent development. The origin of this is thought to be in the Research Laboratories of Philips in Eindhoven in 1954. Prior to that, it was customary to designate it as a hot air engine. The substitution of air with helium or hydrogen as the working fluid at Phillips in the mid-1950s rendered the phrase "hot air engines" unsuitable. The alternative name Philips Stirling engine was deemed even more unsuitable than Stirling Engine or Stirling Cycle Engine, leading to its widespread usage[23].

1.2. Heat engine and Carnot cycle

A heat engine is a term that can be applied to all engines that produce any sort of work from energy. They have direct or indirect by-product of heat; even some entities that may not appear at first glance to be any sort of engine can involve the heat to energy process and thus be loosely classified as a kind of heat engine[24]. Heat engine is a device that uses heat to generate power, it takes heat from a reservoir, then does work such as moving a piston or lifting weight, and lastly releases some heat energy into a sink as shown in Figure (1-1).

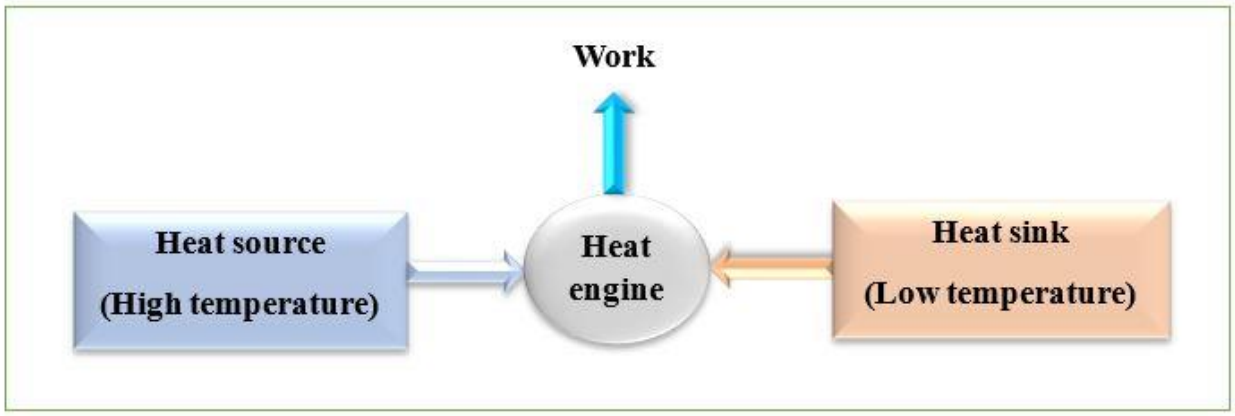

Figure 1-1: Schematic of heat engine

Steam engines, steam turbines, gas turbines, Stirling engines, internal combustion engines, and jet engines are all examples of heat engines[25]. Heat engines are mechanical devices that transform the chemical energy of fuel into internal energy and subsequently into mechanical energy on a periodic basis. In most cases, heat engines make use of gas as the working medium and exploit the expansion of gas caused by heat to do work. Theoretically, all heat engines should be able to fulfill the three requirements that are: the system should be able to absorb heat from a source of heat that is at a high temperature, the system should be able to release heat to a source of heat that is at a low temperature, and the network should be performed regularly from the outside[26].

Heat engines are classified into two main types:

- External combustion engines
- Internal combustion engines.

The Carnot cycle is a theoretical thermodynamic cycle described by the French scientist Sadi Carnot. The Carnot efficiency sets a maximum limit on the efficiency of any classical thermodynamic engine when converting heat into work, or conversely, the efficiency of a refrigeration system in generating a temperature difference via the application of work[27], [28]. The Carnot cycle illustrates the most

efficient heat engine feasible, comprising two isothermal and two adiabatic cycles. It is the most efficient heat engine possible under the constraints of physics.

According to the second rule of thermodynamics, it is impossible to remove heat from a hot reservoir and utilize all of it to accomplish work; some must be exhausted in a cool reservoir. In other words, no process can be "100%" efficient since energy is always wasted someplace. The Carnot cycle defines the highest limit of what is achievable, defining what the most efficient engine might look like[29]. The Carnot cycle is considered to be the ideal cycle due to its complete reversibility, which results in the best achievable efficiency for this specific cycle[30].

The reversible Carnot cycle has four different processes[31][32] as shown in Figure (1-2):

Process 1-2 involves an isothermal expansion at the temperature of a hot source. During this process, heat is transported from the source to the working fluid, and external work is performed. This stage supplies heat uniformly while the work done is proportional to the logarithm of the volume expansion.

Process 2-3 includes an adiabatic expansion of the working fluid towards a lower temperature heat sink. During this process, more external work is performed, using the heat content of the gases. However, no heat is transferred into or out of the piston chamber.

Process 3-4 is an isothermal recompression process at the lower temperature of the heat sink. In this stage, work is performed on the working fluid and heat is transferred from the working fluid to the cold sink.

Process 4-1 is an adiabatic compression where more work is performed on the working fluid as it is warmed to the initial temperature of the hot source.

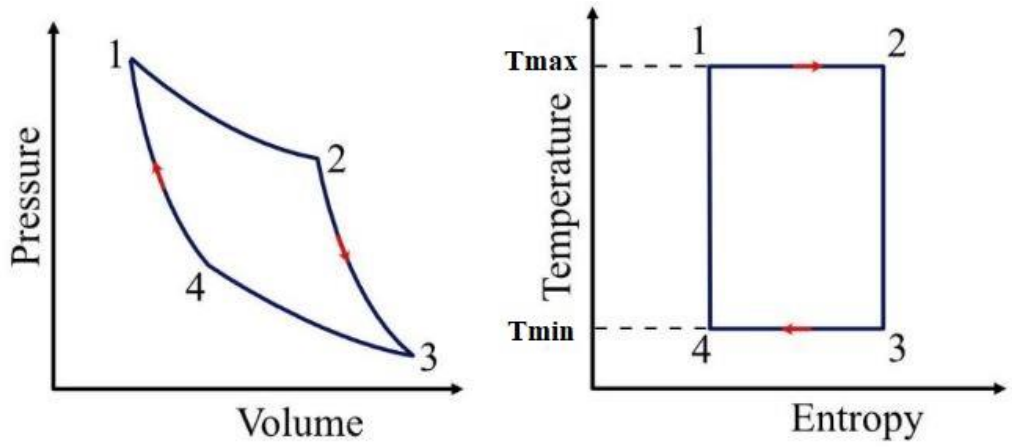

Figure 1-2: Carnot Cycle P-V diagram and T-S diagram

The thermal efficiency for this cycle is:

$$\eta = 1 - \frac{Tmin}{Tmax} \tag{1-1}$$

1.3. History of Stirling engine

The origins of the Stirling engine can be dated back to 1807, when Sir George Cayley (1773 – 1857) released detailed plans and a description of a device he referred to as the "caloric machine" in England. The invention remained at the conceptual stage and was never brought into existence. However, this concept inspired several engineers to pursue and enhance it[33][34].

By the early nineteenth century, the industrial revolution had achieved its heights in terms of progress. During this period, there were significant breakthroughs and quantifiable advances in the fields of science and technology. Mechanical engines have played an essential part in driving the success of various industries, including mining and manufacturing, by powering their operations. The emergence of one notable engine during this period was the Stirling engine, which was initially patented by Robert Stirling in the year 1816[35]. The closed cycle air engine and the economizer heat exchanger (regenerator) were both introduced in this patent, which provided a description of both original technologies.

It enjoyed significant commercial prosperity until the early 1900s, some 80 years before the diesel engine was invented. During this period, the Stirling engine was created as a safer substitute for steam engines, which were subject to explosions due to uncontrolled pressure buildup and crude engineering, resulting in poor quality. This engine possesses the capacity to attain a remarkable level of efficiency while releasing substantially fewer exhaust emissions compared to an internal combustion engine[36]. External combustion engines provide an advantage over internal combustion engines due to their ability to effectively use a diverse range of renewable energy and fuel sources[37].

The Stirling engine is closed and regenerative mechanical device that operates on thermodynamic cycle[38][39], including the cyclic expansion and compression of working fluids at different temperatures. The absence of valves results in the complete regulation of the working fluid flow through adjustments in internal volume. There is a general transfer of heat energy into work or vice versa[40][41].

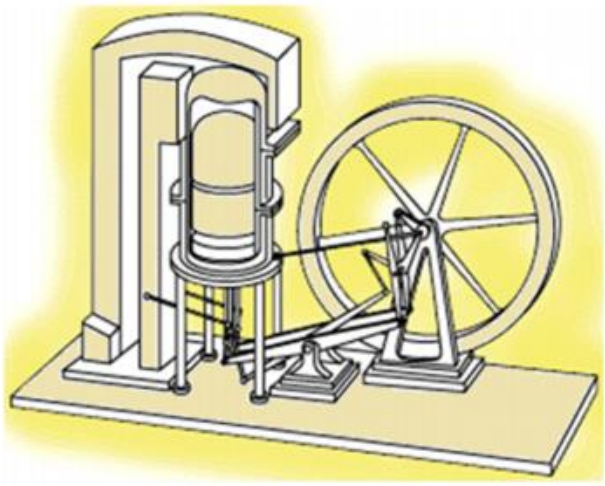

Figure 1-3: Stirling engine 1816[1]

Recently, there has been a growing interest among researchers and commercial companies in the development of the Stirling engine for many reasons. Several factors contribute to its appeal, such as its straightforward design, ability to use multiple types of fuel, small size, minimal noise, exceptional heat efficiency, and

dependable performance[42]. Furthermore, it has varied uses in heating and cooling systems, combined heat and power systems, nuclear and solar power production, heat pumps, low temperature difference engines, as well as automobile, marine, and aircraft engines[43]. The Stirling engine market was valued at USD 871.2 Million in 2022 and is projected to reach USD 1752.6 Million by 2032 (Figure 1-4), with a compound annual growth rate (CAGR) of 7.3%. The market has shown significant expansion in recent years because to the many technological advancements in the energy industry, which have driven its acceptance across different sectors.

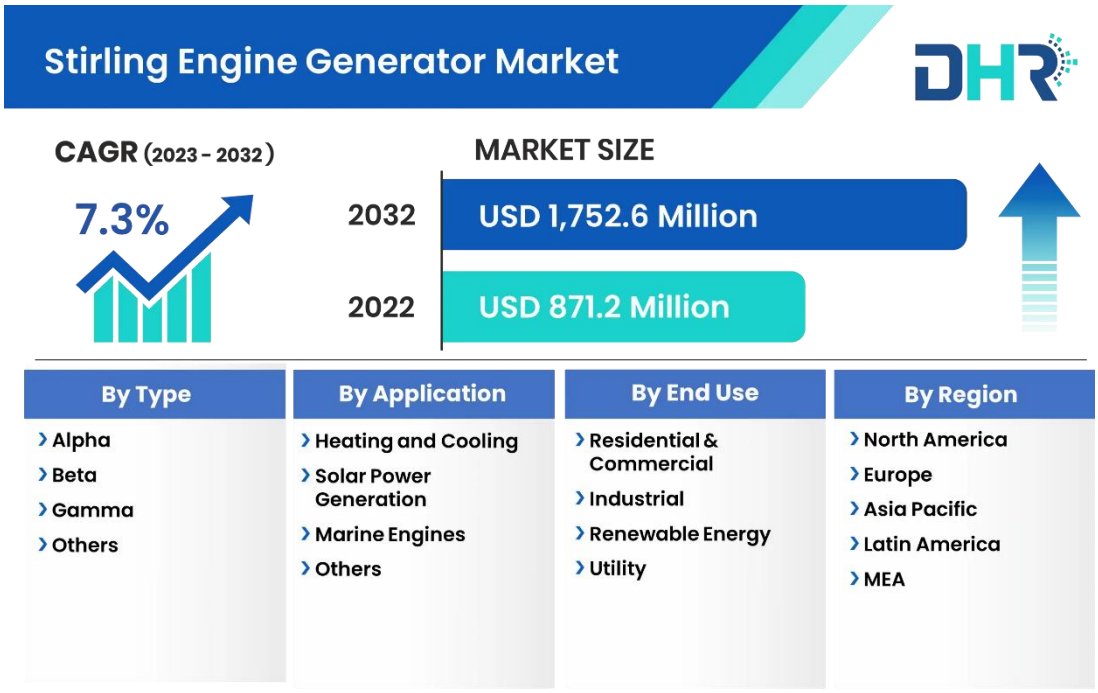

Figure 1-4: Stirling engine market[2]

The market is classified into residential, commercial, industrial, renewable energy, and utilities depending on its end use, as illustrated in Figure (1-5). Hence, the issues concerning energy revolve around optimizing the use of environmentally friendly sources while simultaneously enhancing the efficiency of engines. Robert Stirling's idea has the potential to be the essential component he envisioned: the engine of the future.

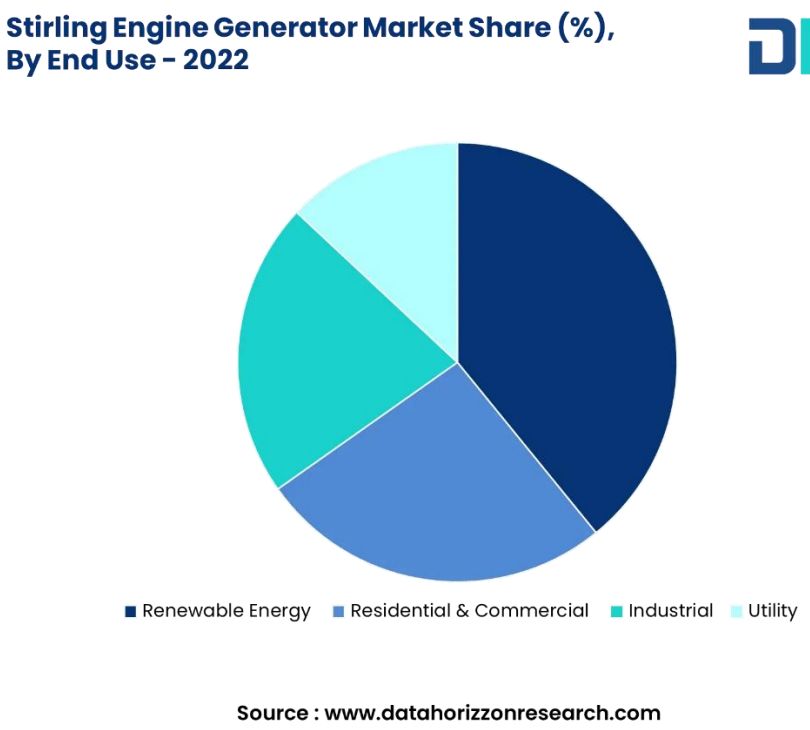

Figure 1-5: Stirling engine market by application

Table (1-1) outlines significant events and advancements in the history of Stirling engines, highlighting key developments from their invention in the 19th century to contemporary research and applications in the 21st century.

Table 1-1: Key developments in the history of Stirling engines

Year	Development
1816	Robert Stirling patents the first practical Stirling engine design.
1827	Robert Stirling and his brother James construct a working model of the Stirling engine.
1830	Stirling engines are commercially produced and used in various applications, including pumping water.
1930	Philips introduces the "Philips Stirling Engine" for applications such as electricity generation and refrigeration.
1950	NASA explores Stirling engines for space power systems due to their reliability and efficiency.

1970	Sunpower Inc. develops high-temperature Stirling engines for space missions and terrestrial applications.
1980	Stirling engine research receives renewed interest due to energy efficiency and environmental concerns.
1990	Honda introduces the "Honda ENEPO" micro-Combined Heat and Power (CHP) system based on Stirling engine technology.
2000	Development of micro-Stirling engines for portable power generation and waste heat recovery applications.
2010	Research focuses on advanced materials, control systems, and optimization techniques for Stirling engines.
2020	Continued exploration of Stirling engines for renewable energy integration, distributed power generation, and space exploration missions.

1.4. Operating principle and thermodynamic cycle

The Stirling engine operates on the principle that the pressure of a gas within a sealed container will rise when heated and drop when cooled. The engine is engineered to undergo a series of sequential processes. Initially, the gas contained within its cylinders is compressed, followed by heating to elevate its pressure. Subsequently, the gas is expanded to generate power, then cooled to reduce its pressure. Finally, the gas is compressed again to initiate the cycle once more. The gas generates more power during its expansion phase than it absorbs during compression because to its higher average temperature and pressure. This additional power is the engine's practical output[44], [45].

The Stirling engine operates as a closed-cycle system[46], where the same gas is repeatedly utilized. The only input to the system is high temperature heat, whereas the only outputs from the system are low temperature (waste) heat and mechanical

power[47]. The fundamental principle of the Stirling cycle (Figure 1-6) is similar to that of the Otto and Diesel processes, involving the expansion of hot gas and the compression of cold gas. The work required for compression is lower than the work generated during expansion through these methods; this is how the machine converts heat into work.

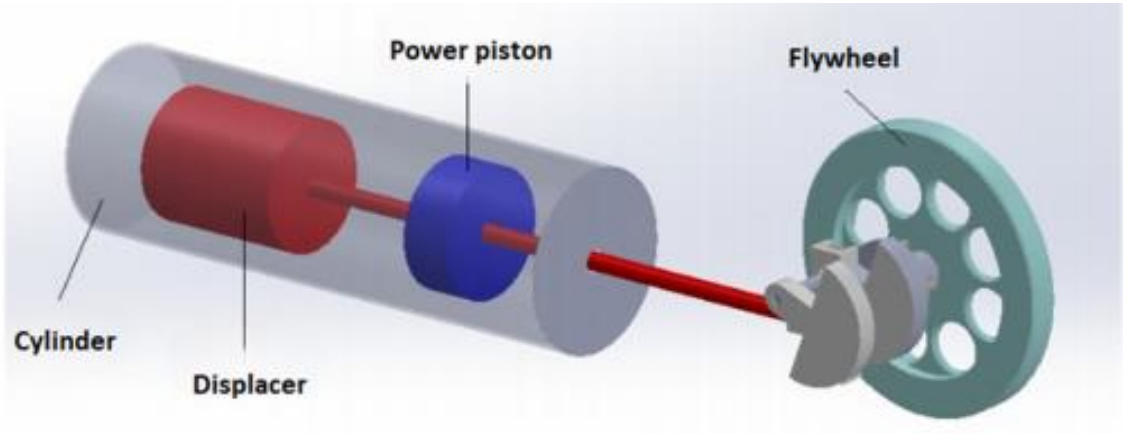

Figure 1-6: Stirling engine (beta type)

The engine cycle can be seen on the PV and TS diagram, as illustrated in Figures (1-7. and 1-8), The ideal cycle has four distinct processes, including two isothermal processes and two isochoric processes, which work together to produce a closed cycle. The system work and heat can be either added to or removed from it. In order to streamline the transition between the system and work, it is imperative to incorporate a flywheel into the design. The flywheel functions by accumulating energy during the operational phase and subsequently releasing it back into the system during the inactive phase. The thermodynamic cycle consists of four processes[48][49][50]:

Process 1–2 is an isothermal compression process. In this process, the compression piston advances towards the regenerator while the expansion piston remains stationary. The working fluid undergoes compression within the compression region, resulting in an increase in pressure from P1 to P2. The temperature remains constant as a result of the transfer of heat from a colder area to its surroundings. The

work performed on the working fluid is equivalent in magnitude to the amount of heat that is expelled from the cycle. The internal energy remains constant while the entropy decreases. The process of isothermal compression of the working fluid involves the transfer of heat from the working fluid to an external dump.

$$p2 = \frac{p1\ V1}{V2} \tag{1-2}$$

$$T1 = T2 = Tmin$$

$$Heat\ transfer\ (Q) = Work\ done\ (W)$$

$$Q = Wc = p1V1 \ln\left(\frac{V2}{V1}\right) = MRT1 \ln\left(\frac{V2}{V1}\right) \tag{1-3}$$

$$Entropy\ change\ \Delta S = R \ln\left(\frac{V2}{V1}\right) \tag{1-4}$$

Process 2-3 refers to a regenerative transfer process that occurs at a constant volume. During this stage, both pistons move in together, with the compression piston moving towards the regenerator and the expansion piston moving away from the regenerator. This ensures that the volume between the pistons remains constant. The working fluid is transported from the compression volume to the expansion volume via a regenerator made of porous media. The temperature of the working fluid rose from Tmin to Tmax as a result of heat transfer from the regenerator matrix to the working fluid. The progressive rise in temperature of the working fluid as it flows through the regenerator results in an increase in pressure. There is no waste of energy and the entropy and internal energy of the working fluid rise.

$$p3 = \frac{p2\ T3}{T2} \tag{1-5}$$

$$V3 = V2$$

$$Heat\ transfer\ (Q) = Cv\ (T3 - T2) \tag{1-6}$$

$$W = 0$$

$$Entropy\ change\ \Delta S = Cv \ln\left(\frac{T3}{T2}\right) \quad (1\text{-}7)$$

Process 3–4 refers to an isothermal expansion process. During the expansion process 3-4, the expansion piston moves away from the regenerator towards the outer dead piston, while the compression piston remains stationary at the inner dead point next to the regenerator. During the expansion process, the pressure lowers as the volume increases. The temperature is kept constant by supplying heat to the system from an external source at the maximum temperature, Tmax. The working fluid exerts work on the piston, which is equivalent in magnitude to the amount of heat delivered. The internal energy remains constant, while the entropy of the working fluid increases.

$$p4 = \frac{p3\ V3}{V4} \quad (1\text{-}8)$$

$$T4 = T3 = Tmax$$

$$Q = W = p3\ V3 \ln\frac{V4}{V3} = M\ R\ T3 \ln\frac{V4}{V3} \quad (1\text{-}9)$$

Process 4–1 constant volume regenerative transfer process, both pistons move at the same time to transfer the working fluid from the expansion area to the compression space through a regenerator. The volume remains constant during this process. As the working fluid passes through the regenerator, heat is transferred from the working fluid to the regenerator matrix, causing the working fluid's temperature to decrease to Tmin. Zero work is performed, resulting in a reduction in both the internal energy and entropy of the working fluid.

$$p1 = \frac{p4\ T4}{T1} \quad (1\text{-}10)$$

$$V1 = V4$$

$$Q = Cv\ (T1 - T4) \quad (1\text{-}11)$$

$$\Delta S = Cv\ ln\frac{T1}{T4} \quad (1\text{-}12)$$

The efficiency of the ideal Stirling cycle[51], as determined by the equation provided, agrees with that of the Carnot cycle, which represents the highest possible efficiency in thermodynamics. Theoretically, the thermodynamic cycle may be designed to be identical to the Carnot cycle, which reduces the loss of energy[52]. The useful product in the ideal Stirling engine cycle is the difference between the heat intake and the heat output. Hence, the efficiency of the ideal Stirling engine is[53]:

$$\eta Stirling = \eta Carnot = \frac{Qin-Qout}{Qin} = 1 - \frac{Qout}{Qin} = 1 - \frac{Tmin}{Tmax} \quad (1\text{-}13)$$

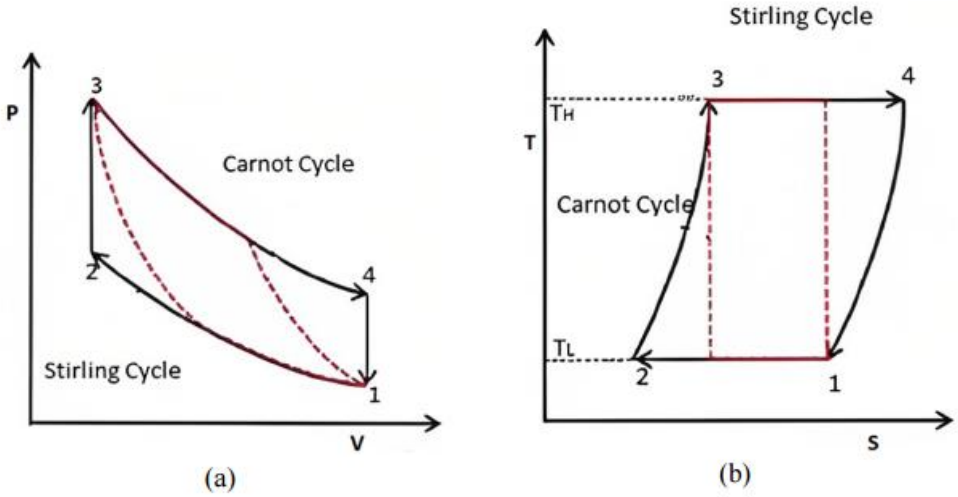

Figure 1-7: (a) PV diagram, (b) TS diagram of Stirling cycle vs. Carnot cycle[3]

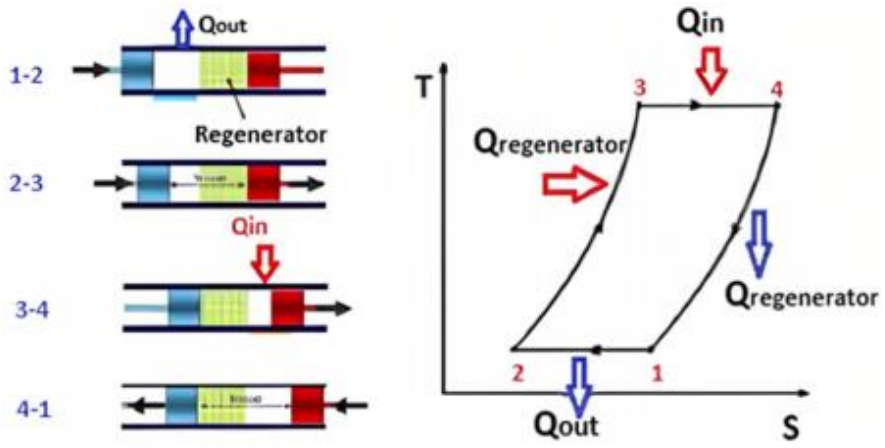

Figure 1-8: Ideal Stirling cycle[4]

Table (1-2) summarizes the operation processes of Stirling engine.

Table 1-2: Operation stages of Stirling engines

Stage	Description
Heating	The Stirling engine begins its operation with a heating phase. Heat is supplied to the hot end of the engine, usually an external heat source. The working fluid inside the engine absorbs heat, raising its temperature.
Expansion	As the working fluid heats up, it expands, causing the piston to move away from the hot end of the engine. This expansion phase converts thermal energy into mechanical work.
Cooling	After the expansion phase, the working fluid moves to the cold part of the engine. Heat is transferred from the working fluid either through a heat exchanger or through direct contact with the heat sink.
Compression	As the working fluid cools, it contracts, causing the piston to move back toward the hot end of the engine. This compression phase removes remaining heat from the working fluid.
Power Output	The movement of the piston during the compression phase generates mechanical power. This power can be used to drive a mechanical load such as a generator, pump or other equipment.
Regeneration	Some Stirling engine designs use a regenerator to improve efficiency. The regenerator stores heat during the expansion phase and releases it during the compression phase, reducing heat loss to the environment.

1.5. Classification of Stirling Engines

Over the years, numerous Stirling engine designs have been created (Figures 1-9 and 1-10), all of which incorporate the fundamental thermodynamic principle. The Stirling engine designs can be categorized based on their mechanical configurations. For example, they can have kinematic or free-piston arrangements[54].

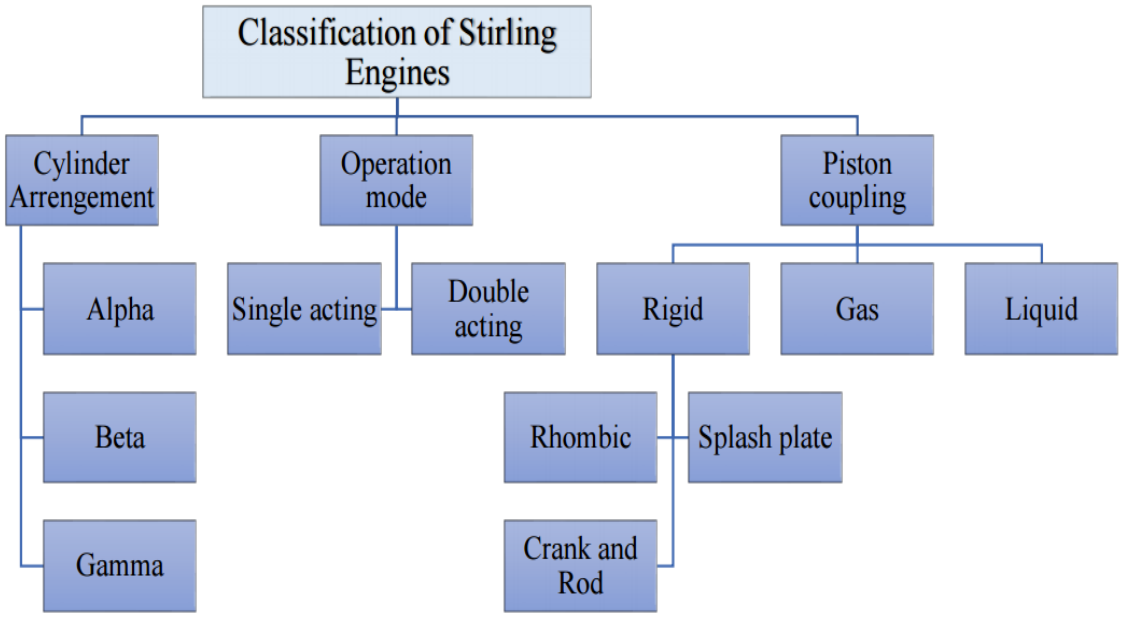

Figure 1-9: Classification of Stirling engine[5]

Kinematic engines are equipped with a crankshaft and a mechanical linkage to the operational piston. The generation of electricity involves the use of a revolving synchronous, permanent magnet, or induction generator. Mechanical linkages impose constraints on the amplitude of power piston movement. Mechanical linkages can impose limitations on the amplitude and phasing of the displacer, which is a distinctive component of Stirling engines. Free-piston engines commonly produce electrical power by utilizing a linear alternator, which is created by the back-and-forth movement of the working piston within a magnetic field. The displacer and piston generally operate as a coordinated spring-mass-damper system in reaction to pressure differences. Free-piston engines possess mechanical simplicity yet exhibit dynamic

and thermodynamic complexity. In power generation applications, electricity is transmitted through a linear alternator that is directly connected to the power piston. In cooling applications, the working piston is operated by an integrated linear motor[55], [56].

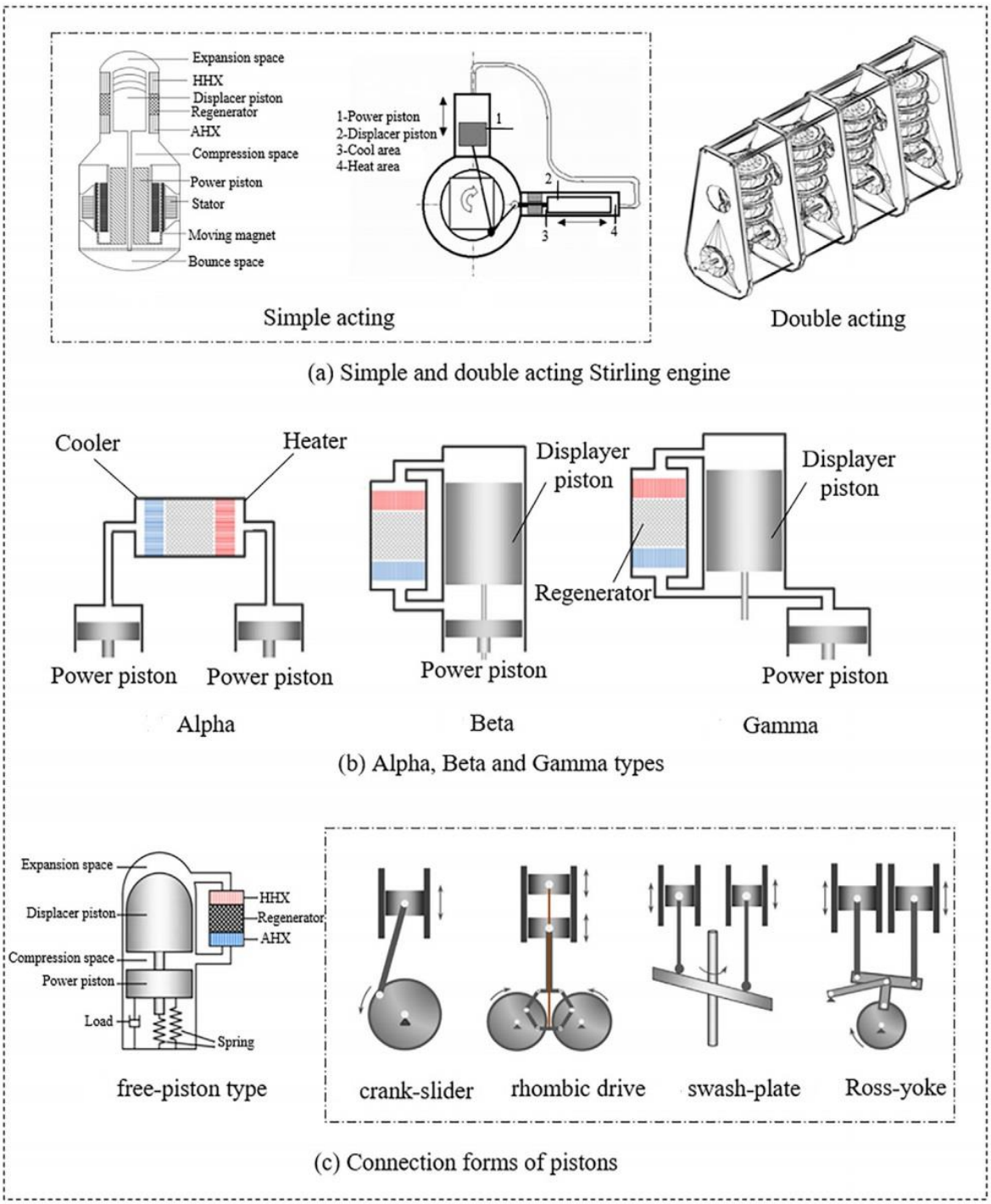

Figure 1-10: Various categorization techniques for Stirling engines[6]

The mechanical arrangements of Stirling engines are typically categorized into three main groups referred to as the Alpha, Beta, and Gamma configurations[57][58][59].

1.5.1. Alpha type

The Alpha engine consists of two pistons located in separate cylinders, which are connected in a sequential manner through a cooler, heater, and regenerator. The Alpha engine is a Stirling engine configuration that requires both pistons to be sealed in order to contain the working fluid. The Alpha engine can be integrated with a densely packed multiple cylinder configuration, resulting in a high specific power output that is well-suited for motorized engines. There exists an arrangement where many cylinders are present. The cylinders are interconnected, thus the compression space of one cylinder is connected to the expansion space of the adjacent cylinder via a passage. A regenerator, cooler, and heater that are interconnected in a series. A swash plate is responsible for driving the Pistons exhibiting sinusoidal reciprocating action. The pistons that are next to one other have a phase difference of 90 degrees.

1.5.2. Beta type

Beta engines utilize a piston-displacer arrangement. The engine's architecture is configured such that both the piston and displacer are situated within a single cylinder. The compression space is formed by the area covered by the upper side of the power piston and the lower side of the displacer. To maintain the necessary phase angle, the displacer and piston must not physically touch each other. Instead, they are connected to the crankshaft by separate connections.

1.5.3. Gamma type

Gamma engines utilize a piston-displacer layout, similar to Beta engines, where the piston and displacer are located in separate cylinders. The compression chamber of Gamma engines is partitioned into two cylinders with an interconnected transfer connection. The heater, regenerator, and cooler are connected in series within

the channel that runs from the compression cylinder to the displacer cylinder. This configuration offers the advantages of a straightforward crank mechanism.

The three engines, Alpha, Beta, and Gamma[60], [61], will exhibit distinct characteristics, as shown in Table (1-3)[62].

Table 1-3: Structure and operational features of Stirling engine types

Alpha type	Beta type	Gamma type
There are two cylinders present in the system	There is just one cylinder in this engine	There are two distinct cylinders
The heat receiver, also known as the heater, and the cooler are situated on separate cylinders	The heater and cooler are both connected to one cylinder	The heater and cooler are situated on separate cylinders
The compression ratio is large	The compression ratio is less compared to the Alpha type	The compression ratio is lower compared to the Alpha type
Both pistons have sealed rods	Only one piston must be sealed, while the other piston runs smoothly without friction in the cylinder	It is necessary to seal just one piston, while the second piston runs smoothly without any friction in the cylinder
The working piston operates at high temperatures	The pistons operate at low temperatures.	The pistons operate efficiently even at low temperatures

1.6. Performance parameters

The Stirling engine is primarily composed of two spaces with varying volumes and temperatures, which are linked by a duct. The spaces are filled with the working fluid, and the duct is equipped with devices for adding heat (heater), abstracting heat (cooler), or storing heat (regenerator). The efficiency of the Stirling engine is influenced by the engine geometric and physical characteristics, as well as the gas

properties of the working fluid. Other factors that affect performance include the efficiency and porosity of the regenerator, the dead volume and swept volume of the engine, the temperature of the heat sources, and losses due to pressure drops and shuttle movements. Figure (1-11) is a summary of the fundamental parameters that affect the performance of a Stirling engine[63].

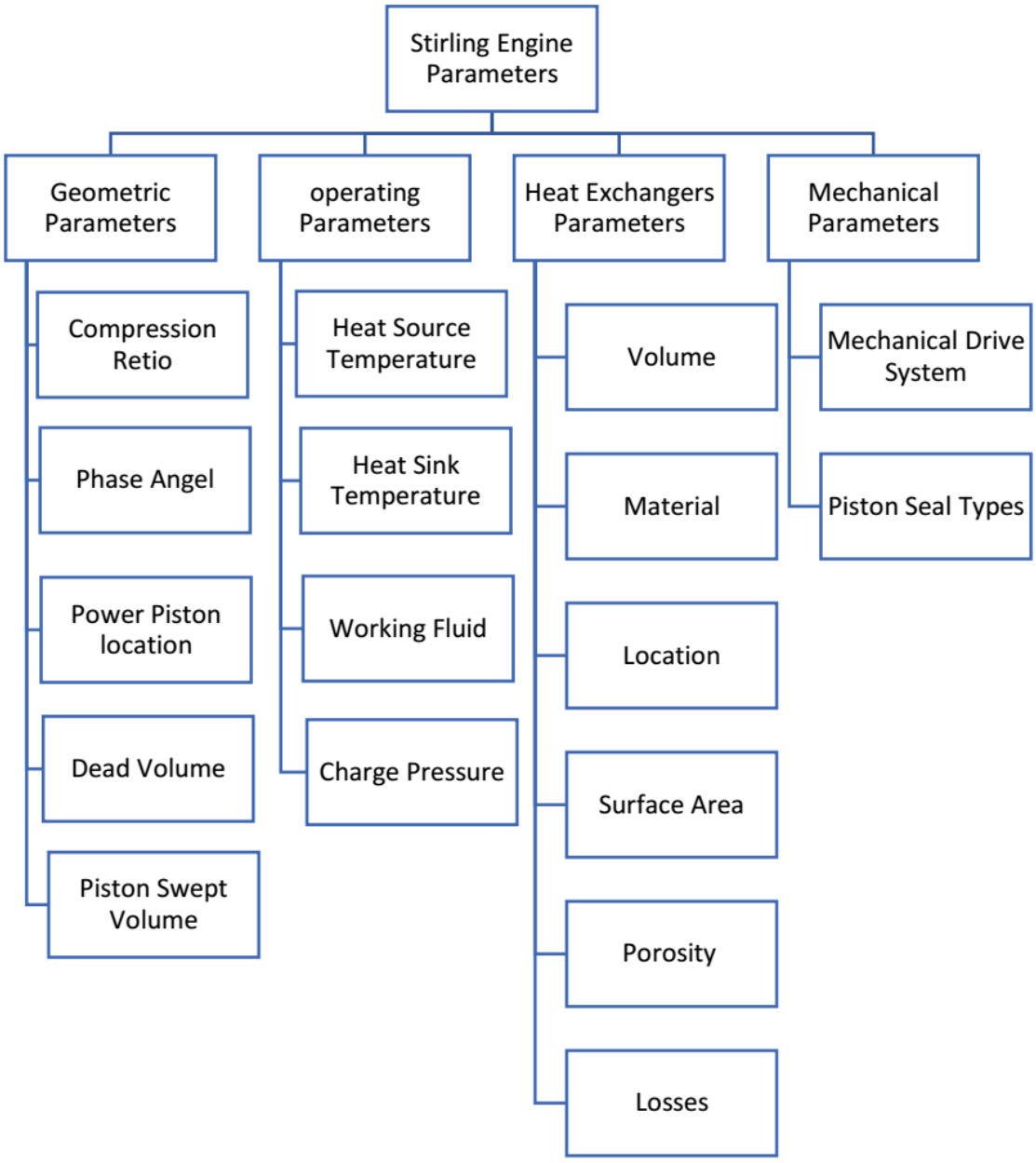

Figure 1-11: The main performance parameters of Stirling engine

1.6.1. Heat source and sink temperature

Stirling engines are a specific category of external combustion engines that have the capability to utilize many heat sources, including solar power, biofuels, nuclear energy, and more[64]. Therefore, the engine can be powered by energy sources with temperatures ranging from 200 to 500° C. or a source with a temperature ranging from 550 °C or higher[65]. Temperature increases will lead to an increase in expansion work. The rise in high temperature has a greater impact on the net work than the total input heat, resulting in an increase in thermal efficiency. When comparing the impacts of high temperatures to low temperatures, it is observed that an increase in cold temperature has the opposite impact on total input heat, net work, and thermal efficiency. While an increase in cold temperature leads to a decrease in the total input heat, which is desirable, it also reduces the net work, which is undesirable.

1.6.2. Charge pressure

Raising the mean pressure in a Stirling engine will enhance both the power output and power density, similar to its effects in an internal combustion engine and a microturbine. Efficiency exhibits an upward trend with pressure until it reaches a maximum value, beyond which pressure ceases to have an impact. Conversely, an elevation in pressure results in a corresponding rise in material stress, requiring an increase in wall thickness and compounding issues related to containing the working fluid. Although all these parameters are crucial to consider during the design process of a Stirling engine, there does not seem to be a noticeable preference for either high-pressure or low-pressure engines.

1.6.3. Phase angle

The phase angle can be easily understood as it simply indicates the extent to which the displacer and power pistons are not synchronized. The phase angle relates to the periodic synchronization between the displacer and the pistons' motion.

The phase angle has a direct impact on the engine's efficiency since it governs the amount of heat transmitted between the hot and cold ends of the engine, as well as the work performed by the pistons[66]. Practically, this means that the two pistons are at different points in their strokes at any given moment. It has been observed that when the phase angle increases, there is a decrease in both the amount of heat input and the net work produced. However, the cycle efficiency remained unchanged. By increasing the phase angle, there is a beneficial effect in decreasing the amount of heat input needed, but this comes at the expense of diminishing the net work production. Hence, it is crucial to employ an ideal phase angle while developing a Stirling engine. The phase angle may be obtained by calculating the difference of crank angle between displacer and power piston the top dead center position[30]. The optimal phase angle is 90 degrees, and the maximum work occurs at this phase angle. However, there is a distinction between the performance of the engine at 80◦ and 90◦[67].

1.6.4. Rotation speed

High-speed Stirling engines offer better power density (watts of output power per cubic meter of engine volume, weight, or engine displacement) and less torque-related difficulties. Despite the prevalence of high-speed Stirling engines, some engineers have chosen to create engines with a low piston frequency. Stirling Advantage selected a low-speed engine equipped with a hydraulic drive system to facilitate free-piston operation and avoid the issues linked to high torque, such as excessive lateral stresses on the piston bearings. Similar to internal combustion engines, Stirling engines with low-speed or low-piston-frequency characteristics exhibit extended lifespan and increased torque[54].

1.6.5. Dead volume

The unswept volume of the working space, known as 'dead space', refers to the portion that is not affected by the pistons' movement. Consequently, the gas in this

area cannot fully expand or compress, resulting in some of the gas being trapped in these areas. This encompasses the clearance areas within the cylinder, as well as the empty volumes of the regenerator, heater, cooler, and pipework. In contrast to the theoretical cycle, actual engines may possess dead volume that accounts for as much as 50% of the total gas volume. This dead volume consequently decreases the power output of the engine[68].

1.6.6. Working fluid

Heat engine or heat pump working fluid is a gas or liquid that mainly transfers thermal energy (temperature change) into mechanical energy (or vice versa) via phase change and or heat of compression and expansion. Working fluids for Stirling engines should possess high thermal conductivity, high heat capacity, and low viscosity in order to optimize their physical and thermal qualities. Working fluids that possess high thermal conductivity have the ability to produce a substantial temperature difference with little heat input. The selection of working fluids with low viscosity is also aimed at minimizing pumping losses[69]. Stirling machines exhibit unstable gas flow inside the heater and cooler, as the gas oscillates between the expansion and compression regions [70].

Air, helium, hydrogen, nitrogen, and vapor are suitable compressible fluids that may be used as working fluids in the Stirling engine. Typically, hydrogen and helium are used due to their superior heat transport capacities compared to other fluids. Hydrogen has great thermal conductivity and low viscosity, enabling the engine to operate at higher speeds compared to other gases. However, its flammability poses a safety risk, making it unsuitable for handling. Helium is an unreactive gas that poses less risk while handling, yet it is rather costly. Furthermore, enhancing the efficiency of the Stirling engine may be achieved by either mixing ambient air with bigger expansion working fluids (gases) or substituting it entirely with such fluids. Martini provides a definition for the capacity of a working fluid in terms of specific heat,

thermal conductivity, and density. This definition may be considered a reliable approximation for early analysis of the working fluid.

$$Capacity\ factor = \frac{Thermal\ condactivity}{specific\ heat * density} \quad (1\text{-}14)$$

Table (1-4) shows the steps of the working fluid operation in Stirling engine.

Table 1-4: Working fluid cycle

Step	Description
Compression	The gas is compressed, decreasing its volume and increasing its pressure.
Heating	The compressed gas is heated, increasing the temperature and pressure.
Expansion	The heated gas expands, pushing a piston or other mechanism, doing work in the system.
Cooling	The expanded gas cools, reducing temperature and pressure.

1.6.6.1. Compound working fluids

Traditional Stirling engines use a gas as the working fluid. However, it is possible to enhance the specific output by using a two-phase, two-component working fluid. This approach has additional benefits such as improved heat transfer and reduced issues with sealing. The compound working fluid comprises a gaseous carrier and a component that is initially in liquid form during the cold compression stage and transitions into a vapor phase during the regeneration process in the expansion space. This transformation of one element results in a decrease in the amount of work required for compression throughout the cycle. Additionally, it effectively raises the ratio of volume compression, leading to an increase in pressure ratio. The net cycle work is consequently increased[71].

The investigation of compound working fluids in Stirling engines was carried out in a preliminary way by Walker and Agbi (1974)[72]. They predicted that a compound working fluid would consist of two components: the gaseous carrier and the phase transition component. During the process of transitioning from the cold space to the hot space, the phase change component went through a phase change, transforming from a liquid to a vapor.

When using a gaseous working fluid, the engine cycle may be divided into several phases. The beginning of the cycle is defined as the compression process. The high-temperature pressurized gas combination is introduced into the regenerator, transferring thermal energy to the matrix material of the regenerator. The condensable fluid undergoes a phase transition from vapor to liquid at the colder end of the regenerator. During the expansion stroke, the displacer moves away from the cold end, causing suction and an associated reduction in pressure due to the expanding volume of the expansion gap. The concentrated liquid is entrained by the carrier gas and introduced into the expansion chamber. The condensable fluid performs a reverse phase transition in the presence of the carrier gas until it reaches the saturation condition, depending on its composition[73].

Throughout the whole of the system, the total pressure is supposed to be instantly constant. This pressure is calculated by combining the partial pressures of the two components (gas and vapor) in the expansion and compression spaces.

$$p = pge + pve = pgc + pvc \tag{1-15}$$

Adding liquid to the working fluid can improve heat transfer inside the engine. Liquids have higher thermal conductivity and heat capacity than gases, allowing them to absorb and dissipate heat more efficiently. The presence of liquid in the working fluid improves the cooling process in the engine. As the working fluid expands and cools during the cooling phase of the cycle, the fluid component can absorb more heat, resulting in lower temperatures and better temperature control.

Combined cycle refers to the integration of two separate cycles into a single system, enabling the conversion of heat energy into mechanical work.

The Rankine cycle is a theoretical thermodynamic cycle that explains how specific heat engines, like steam turbines or reciprocating steam engines, can extract mechanical work from a fluid as it transfers heat between a heat source and a heat sink. The combination of Stirling and Rankine cycles in an engine could potentially offer some unique advantages. Stirling engines are known for their high efficiency and quiet operation, while Rankine cycles are commonly used in steam engines due to their ability to utilize a wide range of heat sources, in this work, the engine operates in two cycles - the Stirling cycle (gas expansion during heating) and the Rankine cycle (evaporation during heating and condensation during cooling).

The thermal efficiency of the Stirling cycle is:

$$\eta Stirling = \frac{Wnet,Stirling}{Qin} \tag{1-16}$$

The thermal efficiency of the Rankine cycle is:

$$\eta Rankine = \frac{Wnet,Rankine}{Qin} \tag{1-17}$$

Also, the combined efficiency is:

$$\eta combined = \frac{Wnet,combined}{Qin,Stirling+Qin,Rankine} \tag{1-18}$$

The net work of the combined cycle is equal to the total amount of work done by both the Stirling and Rankine cycles.

$$Wnet, combined = Wnet, Stirling + Wnet, Rankine \tag{1-19}$$

Substitute in eq. (1-18)

$$\eta combined = \frac{Wnet,Stirling+Wnet,Rankine}{Qin,Stirling+Qin,Rankine} \tag{1-20}$$

$$\eta combined = \frac{(\eta Stirling * Qin) + (\eta Rankine * Qin)}{Qin,Stirling + Qin,Rankine} \quad (1\text{-}21)$$

Now simplify:

$$\eta combined = \frac{\eta Stirling * Qin}{Qin,Stirling + Qin,Rankine} + \frac{\eta Rankine * Qin}{Qin,Stirling + Qin,Rankine} \quad (1\text{-}22)$$

$$\eta combined = \eta Stirling * \frac{Qin}{Qin,Stirling + Qin,Rankine} + \eta Rankine * \frac{Qin}{Qin,Stirling + Qin,Rankine} \quad (1\text{-}23)$$

Notice that $\frac{Qin}{Qin,Stirling + Qin,Rankine}$ and $\frac{Qin}{Qin,Stirling + Qin,Rankine}$ represents the fraction of the total heat input attributed to the Stirling cycle, and Rankine cycle.

Since the total heat input is distributed between the Stirling and Rankine cycles, these fractions sum to 1. Therefore, the expression becomes:

$$\eta combined = \eta Stirling * 1 + \eta Rankine * 1 \quad (1\text{-}24)$$

As a result, we are able to draw the conclusion that the total efficiency of the combined Stirling-Rankine cycle is equal to the sum of the Stirling efficiency and the Rankine efficiency:

$$\eta combined = \eta Stirling + \eta Rankine \quad (1\text{-}25)$$

In a scenario where only gas is used as the working fluid without involving any additives, and therefore no Rankine cycle is present, the overall efficiency of the system would be equivalent to the efficiency of the Stirling cycle:

$$\eta combined = \eta Stirling \quad (1\text{-}26)$$

1.7. Stirling engine components

In closed cycle operation, the Stirling engine requires heat to be transferred from a heat source to the working fluid via heat exchangers[74], and ultimately to a heat sink. This is an essential aspect of the engine functioning. The key parts of Stirling engine are as follows[75][76]:

- Heat source
- Heater
- Regenerator
- Cooler
- Displacer
- Power piston
- Crankshaft
- Flywheel

1.7.1. Heat source

The term "heat source" refers to a thermal energy reservoir that is maintained at a high temperature and is capable of contributing heat without lowering its temperature. An extensive variety of heat sources may be included into the Stirling engine due to the fact that heat is provided to the outside of the engine. There are a variety of applications for Stirling engines that make use of heat sources that are not as widespread, and these applications have the potential to be used in the future. Stirling engines are able to operate efficiently and quietly, and they can make use of almost any source of heat external to the Stirling engine is where the source of heat energy is created. They can receive heat from a wide range of various sources, such as waste heat, combustion fuels, solar heat energy, bioenergy, geothermal energy, and nuclear energy[77].

1.7.2. Heat exchangers in Stirling engine

Heat exchangers play a crucial role in the Stirling engine. The Stirling engine system may have three to four heat exchangers. Heat exchangers play a vital part in the operation of a Stirling engine system. An optimal heat exchanger design achieves a harmonious equilibrium between fluid flow resistance and heat transfer properties. Heat exchangers that have a large frontal open area and a short axial length, together with an optimized hydraulic diameter, are considered acceptable designs[78]. The components shown in Figure (1-12) consist of heater, cooler, and regenerator[79].

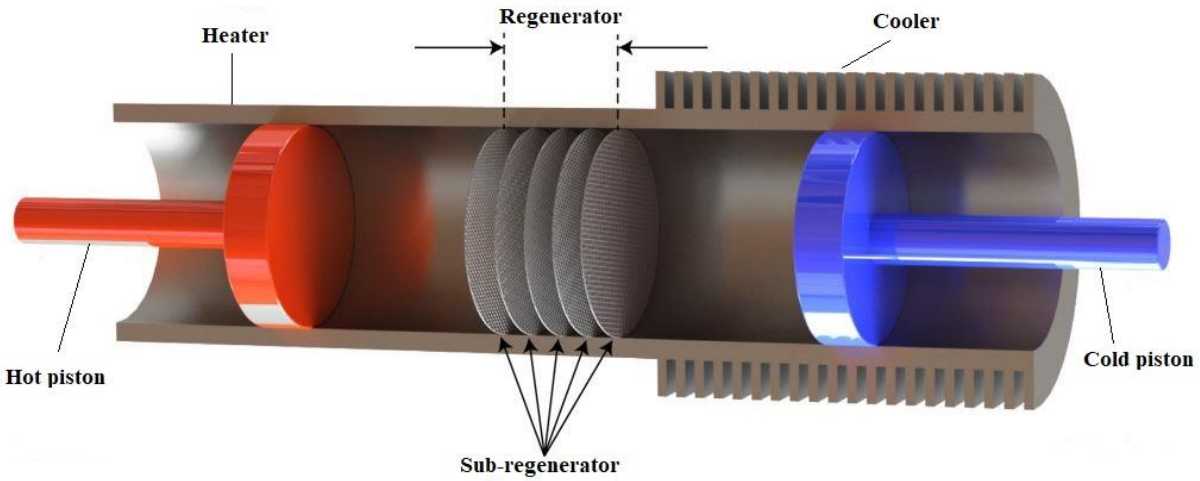

Figure 1-12: Heat exchangers used in Stirling engines[7]

1.7.2.1 Heater

The primary function of the heater in a Stirling engine is to transfer thermal energy from a high-temperature external environment to the working fluid, while simultaneously directing the flow of this fluid inside the engine. It is consistently located near the exit of the expansion chamber, but it is sometimes integrated into the heating chamber[80]. There are three heat transmission processes involved in the heating, each of which is dependent on the design of the element[73]:

Convection and radiation facilitate the passage of heat from the heater environment to the walls of the heater tube or flaps. This is crucial in the design process of heaters.

Conduction transfers heat from the outside surface of the tube to the interior surface. To ensure efficient heat conduction, heaters are often made of metallic materials, especially temperature-resistant steel that contains a significant proportion of nickel. Occasionally, ceramic grafts are used, particularly in areas with high temperatures. The wall thickness must achieve an optimal equilibrium between efficient heat conductivity and durability under high temperatures, considering the fluctuating interior pressure.

Convection is the process of heat transmission from the inner wall of the cylinder to the working fluid. The fluid undergoes compression and exhibits a high speed, hence enhancing the efficiency of heat transmission.

1.7.2.2 Regenerator

The regenerator is an essential component of a Stirling engine. Stirling engine has regenerator, which functions as both an extra heat exchanger and heat storage device. The position of the regenerator is situated between the heat exchangers for the thermal source and the sink. In the instance that the working fluid is leaving the expansion area, it first passes through the thermal source heat exchanger, then passes through regenerator, and finally proceeded to pass through the thermal sink heat exchanger. At the same time as the working fluid is moving through the regenerator, it is transferring heat to the regenerator[81][82]. This pre-cool the working fluid before it moves through the thermal sink heat exchanger, which is referred to as hot blow. Following the transmission of heat, the regenerator is used to keep the stored heat. After that, a cold blow takes place, and the working fluid leaves the compression area. It then makes its way back via the thermal sink heat exchanger, and finally it goes through the regenerator. In order to pre-heat the working fluid

before it passes through the thermal source heat exchanger, the heat that was stored in the regenerator is transferred back into the working fluid and then transferred back into the working fluid.

The procedure is carried out repeatedly during each cycle of the engine[83], [84]. The regenerator serving as the primary component for energy conservation, plays a crucial function, and variations in the inner heat transfer coefficient may have a greater impact on overall efficiency compared to friction losses[85]. Typically, a regenerator must possess an efficiency over 90% to minimize any significant decrease in the performance of the Stirling engine[86].

1.7.2.3 Cooler

In Stirling engine, the cooler is responsible for removing heat from the working fluid and transferring it to a cooler external environment, while simultaneously propelling the fluid through the engine's internal components. The structure consists of the compression chamber and, in many cases, an external heat exchanger. The Stirling cycle may be cooled using either air or water, like an Internal Combustion Engine. In order to lower the temperature of the working fluid in the engine, the cooling system will need to manage a cooling load that is almost twice as large as the cooling load of a typical internal combustion engine, given that the coolant[73].

1.7.3. Displacer

The displacer is a specialized piston used specifically in beta and gamma type Stirling engines, which results in the engine undergoing alternating expansion and contraction in order to operate properly. The primary role of the displacer in a Stirling engine is to oscillate the working fluid between a hot expansion area and a cold compression area, using a sequence of heat exchangers to achieve this separation. The displacer does not alter the engine volume and is designed to separate the compression and expansion chambers while promoting the exchange of mass between them. The displacer must be able to withstand the pressure variations that are

fundamental to the Stirling cycle, while also being lightweight in order to reduce inertial forces[87].

1.7.4. Power piston

The component that is responsible for the engine ultimate power production is known as the power piston. This stiff surface is subjected to expansion and contraction by the working fluid, which results in the creation of linear oscillating motion with each cycle. Electrical power is generated whenever this motion is connected to a generator in either a mechanical or magnetic way[88].

1.7.5. Heat sink

Due to the fact that Stirling engines are external combustion engines and simply need a consistent temperature differential for operation, a wide range of heating and cooling combinations may be used. The heat sink is the location where waste heat is discharged, so completing the cycle through which the engine operates.

1.7.6. Crankshaft

In order to transfer the mechanical work from the piston to the flywheel, the crankshaft is the transferring mechanism. It is the rotating motion that is the ultimate output produced from the flywheel, and it is the reciprocating motion of the piston that is turned into rotational motion. When using an alpha Stirling engine, the crankshaft is connected to the crank pins, which allow the pistons from both the cold cylinder and the hot cylinder to be connected to the crankshaft.

1.7.7. Flywheel

During the time that the displacer piston is moving, the power piston is also moving, which results in the transformation of the thermal energy that is being absorbed by the air into mechanical motion. Furthermore, the flywheel is responsible for storing this mechanical energy, which enables the flow of mechanical power to occur in both directions inside the engine. Even though it is responsible for rotating

the engine, the flywheel also serves the purpose of storing mechanical energy in order to maintain the engine equilibrium and ensure that it continues to work well. Energy is formed while the engine is operating. By storing the mechanical power, the flywheel is able to maintain a state of equilibrium.

1.8 Stirling engine with renewable energy

Integrating the Stirling engine with renewable energy sources requires connecting the engine to systems that provide a stable heat supply. Here are the various methods for incorporating Stirling engines into renewable energy systems:

Solar concentrator integration[89] involves focusing sunlight onto a receiver in concentrated solar power (CSP) systems to produce heat. This heat can be used to directly operate the Stirling engine. Concentrated sunlight heats the working fluid of Stirling engine, causing it to expand and produce mechanical energy, which can be converted into electricity using a generator.

Biomass boilers use organic resources such as wood pellets, agricultural waste or biofuels to generate heat. The heat can be used in Stirling engine, where the working fluid is heated by a biomass-fueled boiler, allowing the engine to produce electricity or perform mechanical operations.

Geothermal energy uses the heat of the earth crust. A geothermal heat source can directly heat the working fluid of a Stirling engine. This integration requires a mechanism to transfer heat from the geothermal source to the Stirling engine heat exchanger.

Stirling engines can be used in industrial plants or power plants to recover waste heat. The excess heat generated by these operations can be used to heat the working fluid of Stirling engine, allowing it to produce more electricity without requiring more fuel.

Biogas combustion involves burning biogas, which is produced from organic waste through anaerobic digestion, to produce heat. The heat can be used to operate Stirling engine, which converts thermal energy into mechanical energy and then into electricity.

Hybrid systems that combine multiple renewable energy sources with Stirling engine can provide more reliable and stable power generation. An example of a hybrid system could combine solar panels with a biomass boiler to provide heat to Stirling engine, ensuring trouble-free operation regardless of weather conditions.

Stirling engines can be used with energy storage technologies such as batteries or thermal energy storage to store excess energy produced during peak hours for future use when renewable energy sources are not available.

1.9 Stirling engine applications

The uses of the Stirling engine may be categorized into three primary groups:

- Mechanical propulsion
- Heating and cooling
- Power generation systems

Stirling engine has the capacity to provide almost limitless energy over an extended duration, while producing low pollutants and requiring minimum exertion. Consequently, several extensive applications that want power that remains constant might use Stirling engine technology to fulfil their power requirements. Stirling engines provide a means for producing power in a compact system to operate various equipment such as electric generators and centrifugal pumps[90].

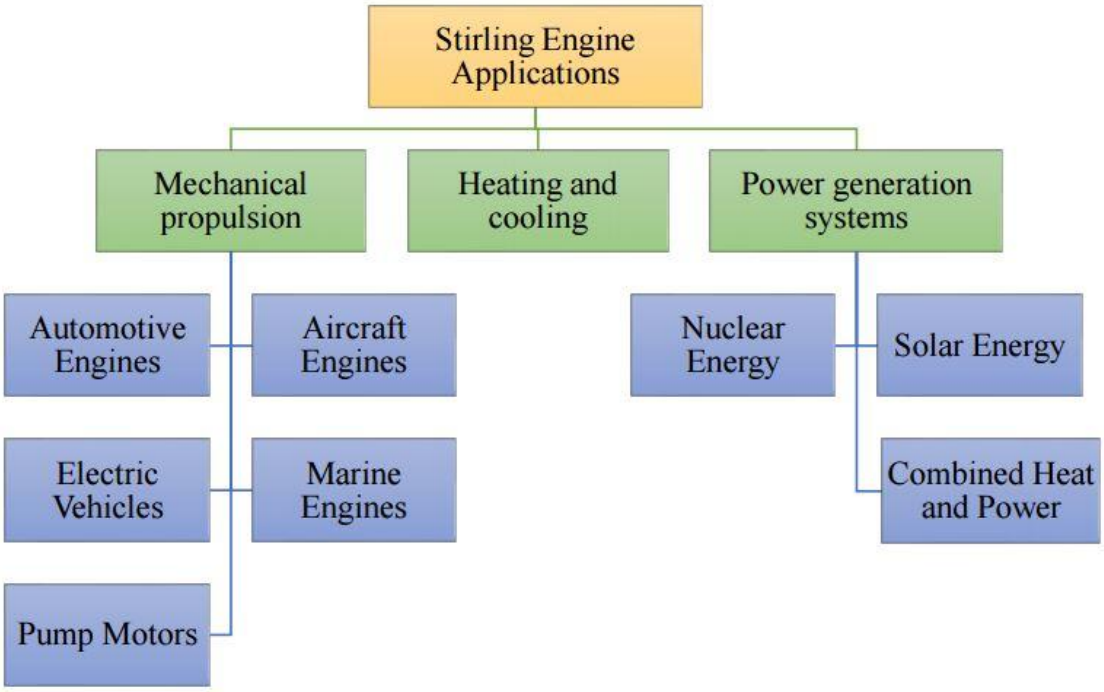

Figure 1-13: Stirling engine applications

1.9.1. Solar Stirling engine

Solar energy is a significant renewable energy source that may be used as an additional source of energy for heat engines. Solar thermal technology enables power production over a wide range of scales, from small to large power plants. It enables the reduction of reliance on fossil fuels and the mitigation of hazardous emissions in the environment. Concentrated solar power is often regarded as the most efficient and environmentally friendly technique for harnessing solar energy, compared to other solar energy technologies[91].

Solar energy is often regarded as the primary renewable energy source due to its abundant availability and ease of harnessing[92]. Solar thermal power systems, also known as concentrating solar power systems, use the heat produced by focusing and absorbing the sun energy to drive a heat engine/generator to produce electricity[93].

There are four different types of Concentrated Solar Power (CSP) technology:

- Parabolic Trough
- Solar Power Tower
- Parabolic Solar dish systems
- linear Fresnel reflectors

The Stirling engine is regarded as a significant device for converting renewable energy into mechanical energy or electricity. Stirling engines have had a revival, mostly due to their potential in solar power production. The Stirling engine may be powered by solar radiation. Dish Stirling the Concentrated Solar Power System is a significant method for efficiently turning solar energy into electricity.

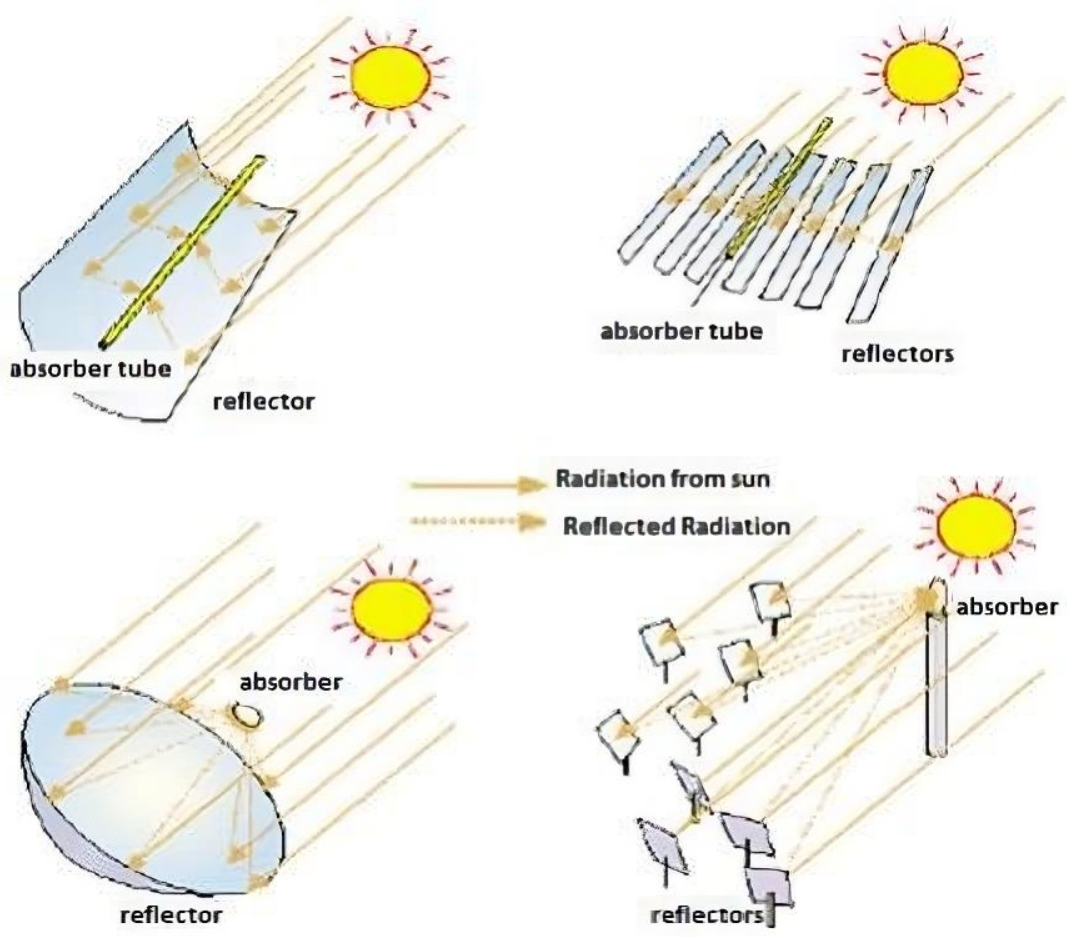

Figure 1-14: Concentrated solar power technologies[8]

Dish Stirling systems[94] belong to the category of concentrated solar energy technologies. Concentrated Solar Power Technology involves harnessing solar thermal energy by focusing it via the use of mirrors or lenses. This technique aims to harness the thermal energy emitted by the sun in order to generate electricity or provide space heating for household and industrial applications[95]. Dish-Stirling concentrated solar power system is an essential possibility for converting solar energy into electricity at high efficiency[96]. Recently, there has been an increase in the popularity of Stirling engines, mostly due to their potential in generating solar electric power[97]. The main elements of the parabolic dish-Stirling system are a concentrator, receiver, Stirling engine, and generator, as seen in Figure (1-15). Parabolic dish concentrators typically include reflecting mirrors that are accompanied by a receiver[98].

The Stirling engine and generator form the core of the power conversion unit. The concentrator is used to concentrate the sunlight into the receiver cavity. The receiver facilitates the conversion of thermal energy into working gas by transferring heat. The Stirling engine subsequently transforms thermal energy into mechanical power by the expansion of the working gas inside the cylinder. Ultimately, the Stirling engine's linear movement is transformed into rotational motion, triggering the activation of the generator to generate energy[99], [100][101]. The most common applications of solar Stirling engine systems are[102]:

- Micro-cogeneration system
- Hybridization and storage
- Solar Stirling electric power generation system
- Off-grid electrification
- Solar Stirling power plants
- Potable water production
- Water pumping

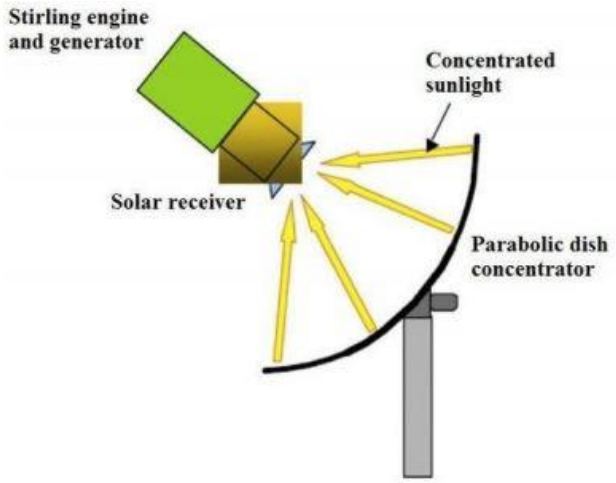

Figure 1-15: Solar dish Stirling system[9]

Table (1-5) illustrates the diverse range of applications for Stirling engines, showcasing their versatility, efficiency, and suitability for various industries and environments.

Table 1-5: Various applications of Stirling engines

Application	Description
Electricity Generation	Stirling engines can be used to generate electricity, either as standalone power generators or as part of combined heat and power (CHP) systems. They can run on various heat sources, including biomass, solar energy, and waste heat from industrial processes.
Combined Heat and Power (CHP) Systems	Stirling engines are well-suited for CHP systems, where they simultaneously produce electricity and utilize waste heat for heating or cooling purposes. These systems are used in residential, commercial, and industrial settings to improve energy efficiency and reduce overall energy costs.

Solar Power Systems	Stirling engines can be integrated into solar power systems to convert solar energy into electricity. Concentrated solar power (CSP) plants use mirrors or lenses to focus sunlight onto a receiver, heating the working fluid inside the Stirling engine and driving the power generation process.
Remote Power Generation	Stirling engines are used in remote areas where grid connection is impractical or unavailable. They provide reliable power for telecommunications equipment, remote monitoring stations, off-grid cabins, and military operations. Their low maintenance requirements make them suitable for long-term deployment in remote locations.
Marine Propulsion	Stirling engines can be employed as propulsion systems for boats and ships. Their quiet operation, high efficiency, and compatibility with alternative fuels make them attractive for marine applications, including yachts, ferries, and research vessels.
Waste Heat Recovery	Stirling engines can recover waste heat from industrial processes, engines, and exhaust gases, converting it into useful mechanical or electrical power. This improves overall energy efficiency and reduces greenhouse gas emissions in industrial operations such as manufacturing and power generation.
Space Power Systems	Stirling engines are used in space missions for power generation, particularly in deep space exploration where solar energy is limited. They provide a reliable and efficient power source for spacecraft, satellites, and planetary rovers operating in extreme environments.
Refrigeration and Air	Stirling engines can drive refrigeration and air conditioning

Conditioning	systems, utilizing their ability to provide cooling through the expansion of gases. They offer an alternative to conventional vapor-compression systems, with potential advantages in efficiency, reliability, and environmental impact.
Water Pumping	Stirling engines can power water pumps for irrigation, agricultural operations, and remote water supply systems. Their versatility and ability to run on various heat sources make them suitable for off-grid water pumping applications in rural areas and developing countries.

1.9.2 Stirling cryocooler

The Stirling cryocooler works by using a reverse Stirling cycle to generate refrigeration via the utilization of work[103]. Machines that operate on the Stirling Cycle possess the maximum theoretical efficiency achievable for any realistic thermodynamic system. The Stirling cycle cryocooler is a cryocooler that operates at a constant volume. Usually, helium gas is used as the working fluid[104]. The reverse Stirling cryocooler, also known as a cryo-condenser, cryo-refrigerator, or cryogenerator, is extensively used in research institutions, animal husbandry units, and space cryogenics for the purpose of nitrogen gas liquefaction. The cryogenerator has the capability to generate temperatures as low as 20-30K[105]. As previously mentioned, the Stirling cryocooler operates on an inverted Stirling cycle. The cycle consists of four heat transfer processes, including two isothermal processes and two isochoric processes. The different processes are outlined as follows[106][107]:

- Process 1-2: Isothermal compression inside the compression chamber. Heat is transported from the working fluid to the external sink.

- Process 2-3 involves constant volume regenerative cooling. Heat is transported from the working fluid to the regenerative matrix. Decreasing the temperature while keeping the volume constant results in a decrease in pressure.
- Process 3-4: Expansion that occurs at a constant temperature in the selected expansion area. The working fluid absorbs heat from an external source.
- Process 4-1: Regenerative heating at a constant volume. The regenerative matrix absorbs heat from the working fluid.

Figure (1-16) illustrates a segment of the Stirling cryocooler, highlighting the main components[106].

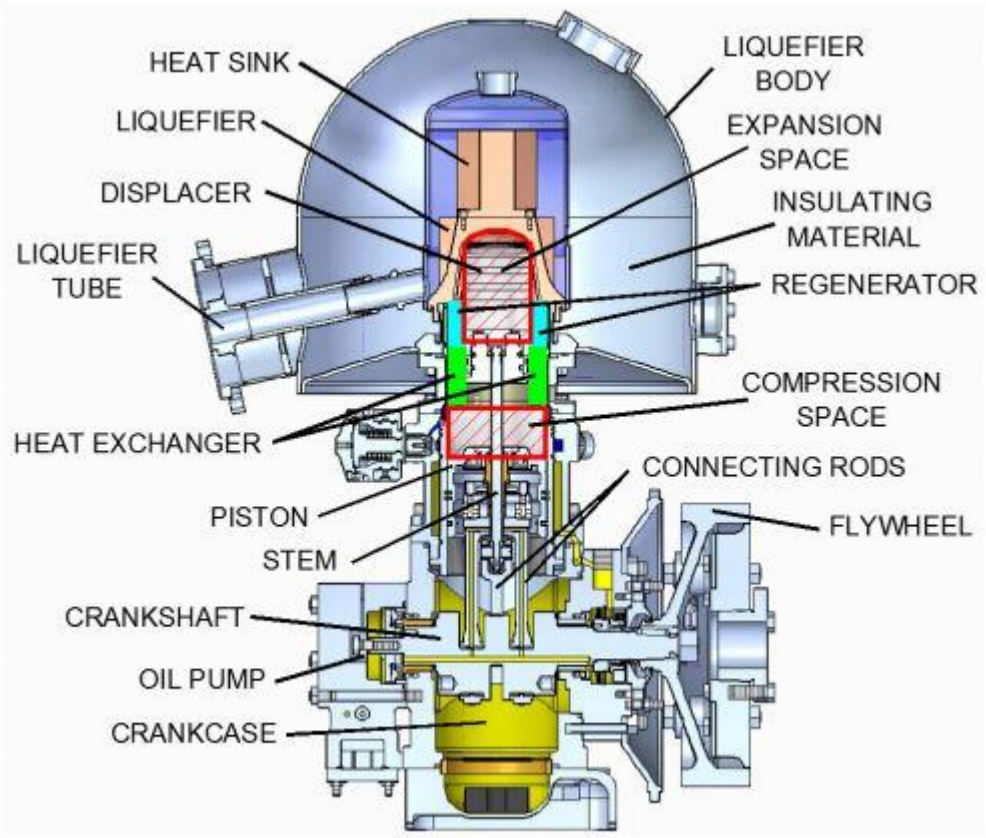

Figure 1-16: Main parts of the Stirling cryocooler.

Table (1-6) provides a comprehensive overview of Stirling engines, covering their operation, components, efficiency, fuel options, applications, advantages, disadvantages, variants, recent developments, and environmental impact.

Table 1-6: Overview of Stirling engines

Aspect	Description
Operation principle	Stirling engine operates based on the principles of thermodynamics, utilizing cyclic compression and expansion of gas to convert thermal energy into mechanical work.
Components	The main components include a heat source, working fluid (typically air, hydrogen, or helium), regenerator, piston, and crankshaft.
Efficiency	Stirling engines can achieve high efficiencies, typically ranging from 25% to 30% for small-scale applications and up to 40% for larger systems.
Fuel Options	Stirling engines can run on various heat sources, including solar energy, biomass, natural gas, and even waste heat from other processes.
Applications	Stirling engines find applications in electricity generation, space power systems, marine propulsion, and combined heat and power (CHP) systems.
Advantages	High efficiency, Quiet operation, Low emissions, Fuel flexibility, Scalability.
Disadvantages	Relatively high initial cost, Slower response time compared to internal combustion engines, Limited power density, Complex design and maintenance requirements.

Variants	Alpha Stirling engine, Beta Stirling engine, Gamma Stirling engine, Free-piston Stirling engine, multi-cylinder configurations.
Recent Developments	Recent advancements include the development of micro-Stirling engines for small-scale applications, improved materials for higher operating temperatures, and enhanced control systems for optimal performance.
Environmental Impact	Stirling engines are known for their low environmental impact due to low emissions and the ability to utilize renewable energy sources as heat inputs.

CHAPTER 2. APPROACHES AND STRATEGIES USED TO ENHANCE THE PERFORMANCE OF STIRLING ENGINES

2.1. Introduction

The Stirling engine is a mechanism that is both practically and theoretically important. Its practical advantage lies in its simplicity, reliability, and safety, which have been recognized for a full century since its creation by Robert Stirling in 1816. In the latter part of the nineteenth century, much research has been conducted on the advancement of the Stirling engine in response to the fuel crisis, rising demand for energy, and growing environmental concerns. This research has focused on investigating various material technologies. Recently, there has been a growing interest among academics and commercial enterprises in the development of the Stirling engine for many reasons. Several reasons for its popularity include its straightforward design, ability to use several types of fuel, small size, little noise, excellent heat efficiency, and dependable performance. Furthermore, it has the potential to be used in many fields such as heating and cooling systems, combined heat and power systems, nuclear and solar power production, heat pumps, low temperature difference engines, and engines for automotive, marine, and aviation applications.

The engine functions based on a thermodynamic cycle that is both closed and reversible. Currently, Stirling cycle-based systems are commercially used for applications such as heat pumps, cryogenic refrigeration, and air liquefaction. Stirling cycles continue to be the focus of research and development attempts as a primary motivation. A wide range of researchers have studied and discussed Stirling engines performance for different types, including the alpha, beta, and gamma types, using four different analytic techniques: zeroth-order first-order, second-order, third-order, and forth- order models. The models are arranged in decreasing order based on their complexity, accuracy, and computing time; each type of analysis

incorporates a distinct approach for evaluating the engine's performance. Zero order analysis relies on an empirical correlation for predicting the power generated by an engine. Beale et al. established a relationship that derived from comprehensive experimental research on certain configurations of Stirling engines[108]. He pointed out engines operating under specific conditions with comparable ratios of temperature, swept volumes, dead volume, and phase angle. Schmidt first established the concept of first order analysis[109]. He developed a method that included using algebraic equations to analyze mass and energy conservation. This methodology enables the prediction of engine power and efficiency in situations where there is sinusoidal volume change.

Finkelstein[110] enhanced the precision of the models by advancing the ideal adiabatic analysis. The engine is simplified by dividing it into five cell units, which consist of three heat exchangers (heater, cooler, and regenerator). It is assumed that both the expansion and compression spaces are adiabatic. Numerical integration is used to solve a set of ordinary differential equations that represent the mass and energy equations for each space. This process allows us to acquire the parameters needed periodic fluctuation. Finkelstein suggested third order analysis is a nodal analysis that involves the application of the principles of mass, momentum, and energy conservation to specific places inside the engine[111]. The governing equations are solved using an implicit method, taking into account both spatial and temporal dimensions. The transitory start-up behavior was not included in the model, since it only considered the periodic solution. This technique increases the level of complexity by including various energy losses into the governing equations.

The Stirling engine operates by gas expansion and compression processes, including unstable, transient, oscillating, laminar or turbulent, compressible flow and heat transfer. The proper handling of these intricate processes, together with geometrical effects, may be achieved by using fourth-order analysis, namely computational fluid dynamics (CFD) analysis. This chapter provides an extensive

review of the previous theoretical and experimental research conducted on Stirling engines.

2.2. Literature review

This section of the chapter will examine and analyze several research and studies conducted on the performance of the Stirling engine. The objective of this review is to identify methods for enhancing and advancing the performance of the Stirling engine.

Walker[112] The dimensionless Schmidt equations were expanded to include four additional parameters: temperature ratio, dead volume ratio, swept volume ratio, and phase angle. This expansion was done to optimize the output of Stirling engines and the amount of heat raised for Stirling refrigerators. Based on comprehensive performance comparisons of both the engine and refrigeration, it is very probable that the optimal results may be attained by constructing the machine with a restricted maximum cycle pressure.

Walker [113] On the Stirling cycle cooling engine, a Schmidt analysis was done using a compound working fluid. The compound working fluid was composed of two components: one that worked as a perfect gas at all times, and the other that was present in the expansion chamber as a liquid at cooling temperatures and in the compression chamber as a liquid at compression temperatures. At near-ambient temperatures, vapor. According to preliminary study, adopting a compound working fluid might greatly increase cooling capacity while retaining the same size, weight, and cost.

[114] Expanded Filkenstein's work and introduced an adiabatic model for non-ideal heat exchangers. In the model, heat exchanger walls and gas remain isothermal, whereas gas temperatures in working areas fluctuate owing to adiabatic expansion and compression. A fourth-order Range-Kutta method was used to solve the model. In addition, the quasi-steady model was evaluated against GPU-3 engine data. Conflict between the Losses unaccounted for by the model and steady flow

correlations for heat transfer and pressure drop may cause two sets of results. Heat transfer correlations and this model computed heat exchanger heat transfer.

Senft [115] Proposed a public hypothesis on the overall mechanical effectiveness of kinematic heat engines, with a specific focus on the Stirling engine. Initially, the researcher constructed a theoretical framework for the exchange of energy between fundamental elements of reciprocating thermal engines. Furthermore, it was shown that the optimal Stirling engine had the greatest potential for mechanical efficiency among all kinematic engines, so establishing an absolute upper limit for the mechanical efficiency of all kinematic engines.

Senft [116] Implemented the Schmidt analysis to optimize a gamma-type Stirling engine with the objective of maximizing braking power, as opposed to indicated power. He argued that prior optimization efforts might result in engines that are non-functional because of significant unexplained mechanical losses. The study emphasized that there is a drop in shaft work as the swept volume ratio increases, and highlighted the negative impact of dead volume, among other results.

[117] Developed a mathematical model for a compact Stirling engine using the isothermal analysis method to enhance the engine's efficiency. This analytical model took into account a pressure loss in the regenerator, a loss in the buffer space owing to leakage of the working gas, and a mechanical loss. The first testing findings of the prototype engine indicated that, at an average engine pressure of 0.8 MPa and a speed of 1300-rpm, the engine achieved a maximum power output of 74 W.

Thombar et al.[48] Offered an elaborate outline on how to construct the Stirling engine. The careful design of the heat exchangers, proper selection of the drive mechanism, and engine configuration are crucial for the successful and efficient operation of the engine system. Stirling engines operating at relatively low temperatures with helium or air as the working fluid have the potential to be attractive engines of the future.

Hachem et al.[118] The article provides a comprehensive summary of the research conducted on Stirling technology. The performance of Stirling engines is determined by many geometric factors, including swept volumes, dead volumes, heat exchange areas, and compression ratio. Additionally, the engine's performance is influenced by numerous working circumstances, including speed, mean pressure, temperature differential, and the kind of working fluid used. It has been determined that multi-objective optimization approaches are valuable for predicting the geometry and working parameters that lead to optimum performance of the Stirling engine.

Timoumi et al. [119]Constructed a second order Stirling model to analyze the impact of geometric and physical characteristics on the performance of a Stirling engine. The model's accuracy was verified by comparing its predictions with the experimental data collected from the prototype Stirling engine GPU-3. Efficiency increased from 39% to 51%, the power observed a growth of about 20%, and there was a minor rise in the average pressure.

Snyman et al. [120]Conducted a comprehensive study and experimental validation of the analytical data for a Heinrici Stirling engine. Implemented three simulation techniques of varying complexity, including Schmidt analysis and two methods created by Berkowitz and Uriel (an ideal adiabatic analysis and a basic analysis). The simple analysis yielded the most accurate estimation of the actual engine and aligned with the project objectives of creating a Stirling engine design synthesis tool.

Martaj et al.[121] This study provides a thermodynamic analysis of a low temperature gamma-type Stirling engine in steady-state operation. The engine was divided into three isothermal control volumes, comprising the heater, cooler, and regenerator, using a zero-dimensional numerical model. Each cell's energy, mass, entropy, and exergy balance were calculated as a function of crank angle (kinematic-thermodynamic coupling). The research results demonstrated that engine components might be optimized for maximum efficiency while producing the least amount of

entropy. The results showed that increasing the dead volume of the regenerator affected the thermal and exergy efficiency of the whole engine.

Eid [122]Considered the efficiency of a beta Stirling engine equipped with a regenerative displacer, evaluating the engine based on the principles outlined in the Schmidt theory. The results indicated that the Beta engine, equipped with a regenerative displacer instead of a fixed displacer and stationary regenerator, achieved a 20% higher power output compared to the GPU-3 engine, which has a stationary regenerator and fixed displacer. Additionally, the Beta engine demonstrated an efficiency improvement of around 10%.

Shendage et al. [123]Studied the structure of beta-type Stirling engines (utilizing a rhombic drive mechanism) and investigated the enhancement of the phase angle, taking into account the impact of volume overlap between the compression and expansion areas. The obtained data demonstrated a positive correlation between the rise in eccentricity ratio and the increase in power output. Simultaneously, there is a need for an increase in the length of the connecting rod. It is worth mentioning that the change in volume of the compression space follows a sinusoidal pattern regardless of the phase difference.

Puech et al.[124] This study conducted a theoretical investigation of the thermodynamic analysis of a Stirling engine, specifically focusing on the impact of linear and sinusoidal regenerator volume changes. An isothermal model was employed to analyze the net work and the heat stored in the regenerator throughout a complete cycle. The findings revealed that the engine efficiency, when regeneration is perfect, is not influenced by the dead volume of the regenerator. However, it was observed that this dead volume significantly magnifies the effect of incomplete regeneration.

Campos et al.[125] The investigation introduced a mathematical model to simulate the functioning of Stirling engines. The numerical findings indicate the existence of an ideal engine shape that optimizes thermal efficiency.

Salazar et al.[126] Developed a compressible computational fluid dynamics (CFD) program to analyze the thermal transfer properties of a Beta type Stirling engine with a simple and straightforward design and geometry. The study determined that impact is the main method of heat transmission in the expansion and compression chambers. Additionally, it observed that the temperature distribution throughout the engine is very unequal at any given moment. Furthermore, the complexities of heat transfer rate fluctuations beyond the basic variations predicted by the second-order model.

Ferral et al.[127] Considered significant variables influencing the thermodynamic efficiency of Stirling engines include the choice of working fluids, the presence of dead volume, the engine's design, and the arrangement of pistons. The study determined that working fluids should possess a high specific heat capacity, low viscosity, and low density. It was shown that helium is the most efficient working fluid at high pressures and temperatures. The gamma configuration has been shown to be the most efficient design for a Stirling engine, with an efficiency of 30% to 32%.

Cinar et al.[128] Studied the impact of hot source temperature on the operational efficiency of a beta-type Stirling engine. The experimental findings demonstrated a positive correlation between the hot source temperature and the engine speed, engine torque, and power output. Additionally, the maximum temperature of the cycle also exhibited an increase. The test engine achieved a peak power output of 5.98 W at a rotational speed of 208 rpm, while operating at a hot-source temperature of 1000 °C.

Mishra et al.[129]Analyzed the impact of several factors on the Stirling cycle, including pressure, temperature, volume, mass flow, and heat and energy transfer across all stages of the cycle. The results indicate that the reduced efficiency of the actual Stirling engine is attributed to several imperfections, including imperfect

regeneration, non-uniform heat transfer, gas leakage, and substantial friction caused by the fluid passing through the heat exchangers.

M. Ni et al.[130] Developed and enhanced a prototype Stirling engine experimental setup to accurately forecast power generation, thermal efficiency, and other performance characteristics. The results demonstrated that the heat flux issuing from the heating element escalated, resulting in an enormous difference in temperature for heat transfer between the hot and cold ends, when the pressure and speed were augmented. The mean gas pressure enhancement led to a rise in pressure differential, as well as improvements in indicated power, cycle efficiency, shaft power, and electric power.

Suyitno et al.[131] Conducted an investigation on the impact of various working fluids on the operational efficiency of a Stirling engine. The Stirling engine of the gamma type may be operated using several working fluids, such as air, an air-ethanol combination, or ZnO nanoparticles. The working fluid used in the engine was a mixture of air and ethanol, with volume ratios of 1%, 5%, and 10%. Additionally, nano-fluids were used with volume ratios of 0.1%, 0.25%, and 0.5%. The engine performed best when the volume ratio of the air-ethanol mixture was 5%. At this ratio, the engine achieved a torque of 0.29 Nm, power of 10.6 W, and efficiency of 3.9%. Engine performance is enhanced by the use of nano fluids containing ZnO nanoparticles.

Yang et al.[132] The classical simple thermodynamic model has been enhanced by including the local pressure loss and improving the second-order adiabatic model. This enhanced model is known as the Incorporated Pressure Drop-modified Simple Model (IPD-MSM). In addition, examined the thermodynamic characteristics of hydrogen, helium, and a combination of helium and xenon in the Stirling cycle. The results indicated that the helium-xenon mixture had the greatest power output and thermal efficiency when the mole percentage of xenon was about 2%. This is because

the inclusion of xenon resulted in a decrease in non-ideal heat transfer loss, which balanced the increase in pressure loss.

Hachem et al.[133] Investigated on how operational and geometric characteristics affect the performance of a four-cylinder Stirling engine. Analyzed numerically to determine the impact of gas quality on performance and efficiency. Explored the effects of four gases: helium, neon, argon, and nitrogen. The results clearly demonstrate that the selection of filling gas for the regenerator is influenced by its form factor. Among the four gases examined, helium yields the maximum power output. However, it was noted that the lowest output power was produced when argon was employed.

Hosseinzade and Sayyaadi [134] Presented an innovative thermal model that takes into account the impact of the finite speed of the piston, pressure throttling in heat exchangers and regenerator, and mechanical friction of the piston. This model aims to calculate the pressure drops in the regenerator and heat exchangers, as well as to propose a new correlation for estimating the effectiveness of the regenerator based on the transfer unit (NTU) correction.

Rahmati et al.[135] Explored the process of designing the Stirling engine for many configurations, including alpha, beta, gamma, and alpha with rose-yoke layouts. The findings indicate that by adjusting the geometric characteristics (such as the length of the links and the radius of the pistons) of the Stirling engine mechanism, the work may be enhanced by an increase of 9 to 14 times. It is important to note that these adjustments do not consider any changes in the thermodynamic parameters.

Laazaar et al.[136] This research examined the process of selecting the most suitable Stirling engine design for a certain power source. It developed a non-ideal adiabatic model using MATLAB. The results showed the Alpha configuration's capacity to effectively operate under significant temperature differences, which aligns with its suitability for waste heat recovery in industrial areas characterized by elevated gas temperatures. When tested under identical operating situations, Beta and

gamma types demonstrated greater suitability for low and medium temperature changes, such as those seen in biomass and solar energy applications.

Abuelyamen et al.[137] Conducted a quantitative analysis of the power generation and energy efficiency of three Stirling engine types (alpha, beta, gamma) using computational fluid dynamics (CFD) simulation. None of the three kinds of Stirling engines include a regenerator. The temperature range of the Stirling engine was investigated, with operating limits set at 300 K and 800 K, while using air as the working fluid. The study also considered the internal radiant heat transfer inside the engine. The results indicated that the gamma type Stirling engine has the maximum power production and thermal efficiency.

Gheith et al.[138] Carried out experimental research on a gamma Stirling engine to examine the impact of several operational factors, including starting charge pressure, engine speed, cooling water flowrate, and temperature gradient. The results showed that the engine's braking power exhibited an increase in correlation with the starting charge pressure, cooling water flow, and engine rotational speed. Furthermore, the temperature profiles derived from these measurements revealed that the flow of the working fluid in the regenerator is not symmetrical. This asymmetry leads to a significant radial temperature fluctuation, which has the potential to impact the overall performance of the Stirling engine.

Scollo et al.[139] Developed and created a model of a dual cylinder alpha type Stirling engine. This mechanical model is connected to a thermodynamic model, enabling an examination and comparison of the theoretical and experimental performance of the engine. This integrated approach provides a comprehensive knowledge of the whole process. The thermal circuit was enhanced to decrease losses, minimize dead volumes, and optimize heat transmission to the working fluid.

Féniès et al.[140] This model of the Stirling engine has been improved to include the effects of non-linear pressure drops, gas inertia, and heat exchange with external heat sources. The analysis focused on the effect of many parameters,

including the dead volume in the chambers, the oscillating mass, and the functioning of the exchangers. In order to develop a new engine, it is feasible to decrease the dead volume inside the chamber to enhance the resonance frequency of the mechanical component. This may be achieved by either lowering the rigidity of the springs or increasing the mass of the mechanical components.

R. Li et al.[141] Considered research on irreversible processes in solar-powered Gamma Stirling engines to investigate the influence of losses on mechanical power and performance. The losses taken into account include the effects of viscous friction, imperfections in the regenerator, hysteresis, leakage in the clearing seal, the displacer shuttle, the limited speed of the piston, and heat conduction. The comparison between simulation results and experimental data, together with the energy and exergy analysis, revealed that the two primary sources of dissipation in this engine are regenerator imperfection and clearance leakage.

Ahmadi et al.[142] A finite-time thermodynamic evaluation and analytical study of a Stirling heat engine was presented. The power output of the engine was maximized in two optimization situations (engine hot temperature and temperature ratio). The results revealed that in the second optimization scenario, where two design parameters were considered, the magnitude of thermal efficiency and maximized power were greater than in the first scenario, where only the engine hot temperature was considered as a design variable.

Chahartaghi et al.[143] A detailed thermodynamic study (energy and exergy studies) of a Beta Stirling engine was performed under various operating conditions, including two working gases of helium and hydrogen. The results showed that as engine speed increased, friction and heat losses increased, and exergy efficiency reached its peak with shorter regenerator lengths. Furthermore, when average engine pressure rises, a bigger regenerator may be employed owing to reduced friction and heat losses. Furthermore, because of its low viscosity and high specific heat, hydrogen has a better exergetic efficiency with a longer regenerator length.

Ranieri et al.[144] Developed a model to do an isothermal investigation of an Alpha-type Stirling engine with a phase angle offset of 90° to highlight the influence of sinusoidal motion on thermal efficiency relative to the ideal cycle. Because running with sinusoidal motion reduces the greatest attainable efficiency, Stirling engines operating with sinusoidal motion should be compared using maximum efficiency for the sinusoidal cycle rather than Carnot efficiency.

Egas et al.[145] Considering Stirling engine configuration, according to the results of this research, Ross yoke alpha machines are better suitable for high temperature differential applications, such as high concentration ratio solar energy, nuclear energy, and high temperature geothermal energy. Beta machines with rhombic drives and Alpha machines with crank-valve drives are better suited for medium to high temperature differential applications using petrol or liquefied petroleum gas. Only Gamma machines are appropriate for low and ultra-low temperature differential applications. Crankshaft powered Beta machines are better suited for medium to low temperature differential applications.

Rogdakis et al.[146] Using Computational Fluid Dynamics, a three-dimensional Beta-type Stirling engine was developed. The simulation focused on the gas cycle, and the regenerator was investigated as a porous medium with heat exchange between the gas and the generator matrix. The simulation results were evaluated against a third-order one-dimensional model. The simulation's efficiency is comparable to the efficiency of a genuine Stirling engine.

Rutczyk et al.[147] Considered the topic of analyzing the internal heat transfer between the heat exchanging surfaces and the working fluid. The adoption of a surface gas model also aided in assessing factors such as viscosity and thermal conductivity of the gas (which is ambient air), which are required for the computation of heat transfer coefficients. The research revealed that the behavior of the Stirling engine is substantially connected to heat transmission in the cylinders.

Buliński et al.[148] Conducted a Computational Fluid Dynamics (CFD) analysis on the Alpha Stirling engine. The purpose of the analysis was to examine how the regenerator affects the performance of the cold Stirling engine under different operating conditions. The analysis took into account all forms of heat transmission, including conduction, convection, and radiation. The modelling findings demonstrated that the use of the regenerator led to an increase in the particular engine work at elevated engine speeds, resulting in an improvement in engine efficiency.

Hachem et al.[149] Examined the impact of several operational factors, such as load pressure, rotating speed, hot source temperature, and cooling water flow, on the efficiency and effectiveness of Gamma Stirling engines. The experimental findings indicate that the ideal rotational velocity of the Stirling engine is dependent upon the temperature of the hot end and the pressure of the load. Furthermore, enhancing the initial charge pressure results in an increase in the mass of the working fluid, which improves the braking power of the Stirling engine.

Raghavendra et al.[150] Created a mathematical model to analyze the performance of a Beta Stirling engine equipped with a rhombic drive mechanism. The results demonstrated that the engine's performance is influenced by the dimensions of the displacer length and crank length. Specifically, altering the engine's compression ratio had a significant impact on the work done in both the expansion and compression chambers. Higher compression ratios led to an increase in the work performed in these chambers.

Joseph et al.[151] Developed and experimented with a compact prototype of a gamma Stirling engine, use a spirit lamp flame as the primary heat source and air as the working fluid. The engine was seen to operate between the range of 500 to 2000 RPM. The engine was started by an initial cranking action, leading to a subsequent low speed. As the temperature on the hot side rises, the temperature differential likewise increases, resulting in an increase in speed.

Erol et al.[152] A rhombic mechanism beta Stirling engine was created and produced, considering the influence of factors such as the mass of the working fluid, pressure, heating, and coolant temperature. Conducted experiments with various gases, such as helium, air, nitrogen, carbon dioxide, and argon. The performance of Stirling engines was significantly affected by the thermal conductivity and density of the working fluid.

Romanelli et al.[153] Conducted research on the behavior and energy transfer of Stirling engines operating with temperature differentials below 100°C. Demonstrated quantitatively that the optimal conditions for achieving maximum shaft work and power occur when all the gas is originally located in the cold zone. In contrast, the minimal amount of effort and power required is achieved when the majority of the gas is originally located in the hot zone.

Dobre et al.[154] This work aims to demonstrate the applicability of two models, namely finite physical dimension thermodynamics and Schmidt model with incomplete regeneration. The numerical model enables the assessment of energy processes based on the crankshaft angle (kinematic-thermodynamic coupling).

Cheng et al.[155] Created a prototype beta Stirling engine that functions at a moderate temperature for heating purposes, with a rhombic driving mechanism. The results indicated that the compression ratio exhibited a rise as the diameter rose.

Ipci [156] Utilized a three-dimensional computational fluid dynamics (CFD) model to accurately simulate the physical actions occurring in a 100 W beta Stirling engine. The engine achieved its maximum rated power of 87.2 W at 1350 rpm and a charged pressure of 10 bar. The efficiency was measured to be 41.9%. Additionally, the power increased from 30.3 to 111.5 W, and thermal efficiency increased from 13.3 to 42.3% when the heating temperature was raised from 673 to 1173 K.

Masser [157] This research performed a thermodynamic examination of a gamma Stirling engine driven by a Scotch-Yoke mechanism, which demonstrated an increase in engine power and thermal efficiency when compared to the crank drive

mechanism. The numerical analysis revealed that the engine achieved its highest power output of 1105 W while operating at an engine speed of 800 rpm and with a gas mass of 0.3 g. This was achieved under the condition of a heat transfer coefficient of 1200 W/m²K.

Alfarawi [158] Investigated the impact of distinct loss mechanisms on the optimized Piston Motion for an Alpha-Type Stirling Engine. The optimization of piston movement demonstrated a significant increase in average power production, around 50%. This improvement may be attributed to the enhanced pressure fluctuations within the system resulting from the optimized piston movement. Investigated the performance comparison of a beta type Stirling engine operated by rhombic and crank mechanisms based on non-ideal adiabatic model. The results indicated that the rhombic drive mechanism yields a 32% increase in power and provides a 20% improvement in efficiency compared to a crank mechanism during regular operation.

Ipci [156] Created a comprehensive model that combines thermodynamics and dynamics to describe a novel kind of Stirling engine called the gamma free piston Stirling engine. This engine is composed of two displacers and a power cylinder, and it operates using hydrogen as the working fluid. It is determined that a decrease in cycle work happens due to a drop in the compression ratio and operation frequency of the engine. The upper limit for the hot end temperature is 1100 K, and the highest expected power is 1.6 kW.

Mansuriya et al.[159] Explored the multi-objective optimization of the Stirling engine by using the thermodynamic finite-speed model and utilizing methane gas as the working fluid. The optimization results demonstrated that changes in power output and total pressure drop may occur within the two-dimensional optimization space.

Mukhtar et al.[160] Performed thermodynamic study on a suggested Stirling engine using a gamma-configuration slider-crank mechanism. The research used the

modified Schmidt ideal adiabatic model, with air employed as the working fluid and a phase angle of 90°. The engine performance improved by increasing the temperature difference between the expansion and compression chambers.

Topgül et al [161] Considered the impact of connecting the power and displacer cylinders of a gamma-type Stirling engine at the hot-end and cold-end, using helium as the working fluid at various charge pressures. The results indicated that engine torque and power output initially reached their peak and subsequently decreased due to insufficient heat transfer to the working fluid. This was caused by the rise in working gas mass resulting from increased pressure. Furthermore, the engine power increased at higher charge pressures when employing methods that supplemented the quantity of heat introduced to the working gas.

Murti et al.[162] Proposed a quantitative design for a liquid-piston with several cylinders. The Stirling engine operates using air and water as its operating fluids. The design included using a mass spring model to identify the engine's geometric characteristics, using thermoacoustic theory to estimate the regenerator's pore sizes, and employing a basic heat transfer model to pick the heat exchanger geometries. The research results demonstrated that the developed alternator successfully attained the desired electric power output.

Kumaravelu et al.[163] This research conducted a numerical analysis of a three-dimensional cylinder model of a Stirling engine with a beta-type configuration. The objective was to examine the effect of several types of fins (circular, pin, and rectangular) on the efficiency of the Stirling engine. The Computational Fluid Mechanics (CFD) approach was used for this investigation. The result led to a rise in the rate of heat transfer, effectiveness, and power output of the engine. Bataineh et al.[164] Enhanced theoretical and numerical thermodynamic model developed for a Beta type Stirling engine coupled with a rhombic driving mechanism. The results indicate that the existing theoretical model remains accurate at high speeds. However, the power loss resulting from the inertia effect increases in a quadratic manner with

engine speed. Additionally, the regenerator faces the most significant heat losses, which negatively impacts the engine's performance.

Katooli et al.[165] Applied artificial neural networks to analyze several factors and operational variables that impact the cooling flow and efficiency of a gamma-type Stirling engine. The created model predicts the output characteristics of a Stirling engine using sample data obtained from a MATLAB code (Nlog code). The results were aligned with the experimental data, exhibiting an average difference of less than 1% for the cooling capacity and an average difference of less than 8% for the coefficient of performance.

Cao et al.[166] Carried out an analysis using a three-dimensional finite element model to investigate the impact of the parallel displacement of the piston rod in a Stirling engine and its influence on the sealing performance under various operating situations. The results indicated that the displacement of the piston rod contributes to wear, leading to a higher risk of seal damage under heavier loads. The contact pressure remains unaffected by seal wear when the piston rod is displaced. Additionally, the opposite side of the crank is more susceptible to leakage. On the other hand, the cap-seal demonstrates excellent sealing capability under high pressures and low pre-compression ratios.

Yu et al.[167] Performed a structural analysis of a circular microchannel regenerator. Results indicated that the rate of exergy loss reaches its lowest point when the channel diameter is around 0.5 mm, given the specified parameter values. The minimal total exergy destruction rate is significantly affected by all factors examined. The regenerator's inner radius, total volume, and porosity, as well as the engine speed, also have a noticeable influence on the ideal structure of the regenerator.

Ali Abro et al.[168] Conducted an empirical investigation to assess the efficiency of a Solar Dish Stirling engine (gamma type). The system included a parabolic dish, solar reflectors, fan blades, a flywheel, and a dynamo (alternator) with

the capacity to produce around 100 watts of power. The empirical investigation revealed that the Sterling engine had an overall efficiency of around 70.96%, disregarding any losses.

Babikir et al.[169] Studied the efficiency of the Dish/Stirling power generating system by using a mathematical model that used two different working fluids, namely hydrogen and helium. Conclusively determined that hydrogen is the optimal fluid for efficiently transferring energy at elevated temperatures to operate the Stirling engine. The solar concentrator's outer surface experiences a rise in temperature due to the Direct Normal Irradiance (DNI). This leads to thermal and optical losses inside the concentrator and the receiving cavity, which are influenced by the characteristics of the materials employed.

Vahidi et al. [170] Performed research on solar dish/Stirling engine systems, analyzing their performance in various operating situations and climatic zones. Specifically, investigated the impact of dynamic factors such as radiant flux and ambient temperature, and verified the results via experimental measurements. The results showed that the lowest limit for solar flux required to initiate engine functionality is 480 W/m^2. The overall solar energy received by the dish amounted to 40.4 GJ, with 6.5 GJ being transformed into electricity.

Zhang et al.[171] Provided improvement of a solar system using a Stirling engine array, analyzed several sources of energy loss, evaluated irreversibility, and investigated the impact of various parameters on the efficiency of Stirling engine arrangements and configurations. The results suggested that the flow arrangement, whether co-current or counter-current, had little influence on the performance of the engine array. The disparities in thermal efficiency and power output across various flow orders are at most 0.39% and 0.70%, respectively.

Zayed et al.[172] The Solar Dish/Stirling System was developed and created, with a thorough analysis of characteristics including concentrator diameter, receiver temperature, direct solar radiation, wind speed, and ambient temperature. The results

demonstrated that the Solar Dish/Stirling System, when equipped with concentrators ranging in diameter from 10 to 17.5 m, showed the ability to generate substantial electrical capacity ranging from 18.6 to 58.1 kW, and the total efficiency has a range of fluctuation between 23.7% and 24.25%.

İncili et al.[173] Developed and produced an innovative micro-combined heat and power production system comprising of solar panels, a Beta-type Stirling engine, and a coal-fired boiler for domestic heating and electricity supply. The collected data indicated that the average daily power generation from the Stirling engine and PV system was 3.126 kWh. The Stirling engine and coal boiler together generated an average daily heat output of 985.97 kWh. The system exhibited average thermal efficiencies of 31.78% and 30.78% with and without the Stirling engine, respectively. The Stirling engine had an average Carnot efficiency of 30.2%.

Musmar [174] Presented assessment of the operational substance used in a solar dish The Stirling engine's thermal efficiency, energy efficiency, and the rate of entropy creation are assessed for the optimal output power. Numerical results demonstrated that the swept volume ratio is unaffected by the selection of the working fluid. Engine power is directly proportional to the heater temperature, heat input, and regenerator heat transfer. The choice of working fluid greatly influences engine power, with helium or hydrogen resulting in higher power output compared to air.

2.3. Review summery

Considering the excellent environmental performance of the Stirling engine in comparison to that of other kinds of engines, a substantial amount of research efforts is now being concentrated on figuring out how to improve this specific engine. In this chapter, we investigated, evaluated, and reviewed previous research and studies that were performed on the performance of the Stirling engine of different kinds. As a result, we are able to summarize and establish the following conclusions:

- Most studies and research have concentrated on the kinematic Stirling engine type, which includes alpha, beta, and gamma types. Additionally, the first and second order models, which include isothermal, ideal, and non-ideal adiabatic models, have been taken into consideration. This is due to the fact that these models provide a more accurate prediction of the performance of the Stirling engine.
- Numerous studies have been conducted to investigate the impact of the primary elements on the performance of the Stirling engine. These parameters include the influence of hot source and cold sink temperatures, charge pressure, dead and swept volumes, compression ratio, working fluid, engine speed, phase angle, heat exchangers effectiveness.
- It has been proved that Stirling engines are capable of operating on every potential fuel source, including liquid, gas, or solid, across a broad variety of temperatures. Additionally, the engine is able to use numerous heat sources, including solar, geothermal, and waste heat.
- As far as the configuration of the Stirling engine is concerned, the Gamma configuration has been shown to be the most effective form of Stirling engine in comparison to the Alpha and Beta configurations. This is because the Gamma configuration can deliver the maximum power output and thermal efficiency. Additionally, it was discovered that beta and gamma kinds are better suited for low and medium temperature changes, such as those occurring in solar energy and biomass.
- The physical and thermal characteristics of working fluids for Stirling engines include high thermal conductivity, high heat capacity, low viscosity, and low density. This is since fluids with high thermal conductivity are able to create a large temperature differential with a relatively little amount of heat input. Air, helium, and hydrogen are the three most numerous types of fluids.

- The speed of the engine, the torque of the engine, and the power output of the Stirling engine all grow alongside the temperature of the hot source. Therefore, it is necessary to take into consideration the various kinds of materials and alloys throughout the design process. This is due of the high temperatures and thermal stresses that are present. Additionally, increasing the average pressure in the Stirling engine will result in an increase in the amount of power generated.
- When it comes to regenerator, cold, and hot spaces, dead volumes are taken into consideration. It is estimated that the dead volume of many Stirling engines is between 40 and 50 percent of the entire volume. These dead volumes result in a lower pressure level and a drop in overall efficiency.
- One of the most important geometric parameters that influences the performance of Stirling engine is the phase angle. It is consequently necessary for the phase angle to have a value that is ideal, which is around 90 degrees in theory.
- It is possible to effectively manage the amount of power that is produced by a Stirling engine by adjusting the stroke length of either one of the pistons or both displacer elements. When the stroke length is decreased, the swept volume is also decreased, which leads to a lower pressure ratio. This results in a decrease in the power output of the engine.
- One of the functions of the regenerator is to recycle the heat that is generated inside the engine, rather than releasing it into the environment. Because of this, both overall efficiency and power output are improved. Because part of the heat is stored in the regenerator for use in the subsequent cycle, the amount of heat that is wasted is reduced with the operation of regenerator.

CHAPTER 3. THERMODYNAMIC MODELS AND ANALYSIS OF STIRLING ENGINE

3.1. Introduction

Modelling operations play a vital role in predicting engine performance over a wide range of design and operating elements and scenarios. Modelling is recognized as a beneficial technique for identifying essential control factors without the need for costly research and testing, or due to the impossibility of obtaining direct measurements for all flow characteristics and quality. Although the Stirling engine seems to have a straightforward conceptual structure, it really has a complicated mathematical analysis. It is difficult to understand even idealized versions of the engine in terms of simple and closed equations, which is one of the primary reasons for the widespread negativity and lack of information that exists in modern times.

There are many different models that may be used to make predictions about the thermodynamic cycle of Stirling engine. The complexity and assumptions of these thermodynamic models are different, and they are categorized according to their order (zeroth, first, second, third, and fourth orders), with a higher order number indicating a higher level of complexity[175]. As shown in Figure (3-1), various methods of analysis are categorized into various classifications. This chapter discusses the thermodynamic approach models of first and second-order analysis to evaluate the Stirling engine performance, the study involves three models: isothermal, ideal adiabatic, and non-ideal adiabatic.

- The study of the ideal isotherm assumes that all heat exchangers are ideal and that all heat transfer activities take place in expansion and compression zones, respectively.
- In an ideal adiabatic analysis, the heat exchangers are assumed to be ideal, while the expansion and compression spaces are assumed to be

adiabatic. Heat exchangers are designed to facilitate the transfer of work and regulate the transmission of heat.

- Regardless of whether a simple analysis or a non-ideal analysis is conducted, heat exchangers are regarded to be non-ideal. This means that there is a pressure loss associated with the flow of working fluids inside heat exchangers.

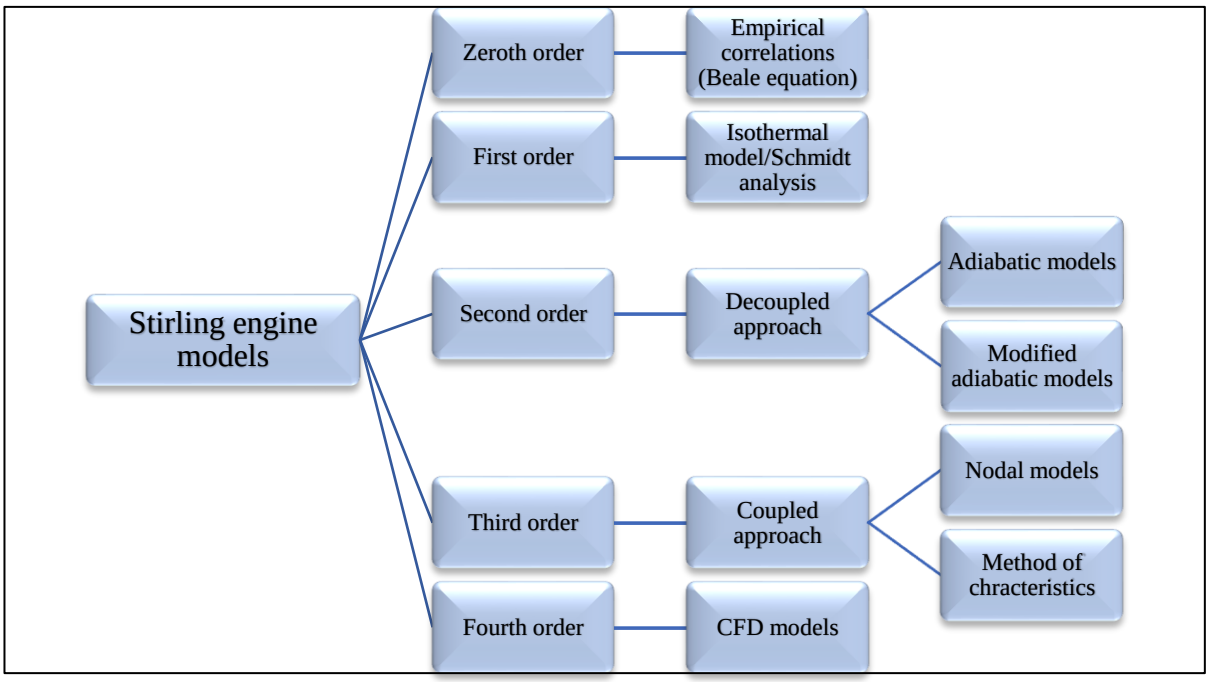

Figure 3-1: Various classifications for the analysis of Stirling engines [176]

3.2. Thermodynamic models and analysis

3.2.1. Zeroth order analysis

Zero order models estimate the power output by evaluating empirical correlations that are based on the total size of the engine. Beale introduced a correlation that calculates the power generated by the engine. Senft further expanded on this technique and obtained the generalized Beale number. These approaches forecast power outputs, but they are only applicable to engines that meet certain geometrical and operating requirements[177], [178], [179]. In order to determine the

power generated by an engine, the Beale number, pressure, swept volume, and frequency are assigned assumed values. The Beale number is often used for predicting the initial design of a Stirling engine, since it quantifies the efficiency of the Stirling engines[180]. The power is then computed by multiplying these parameters together, as shown below:

$$P = Bn.p.Vsc.freq \quad (3\text{-}1)$$

3.2.2. First order analysis

This technique is employed to forecast the efficiency of the Stirling engine. It involves utilizing either the Schmidt equation or the generalized Beale number, as derived by Senft in an analysis that assumes no energy losses, to compute the power output. From the ideal power output, a straightforward correction factor is applied to determine the brake power output[177].

Schmidt first established the concept of first order analysis. He devised a method that included using algebraic equations to analyze mass and energy conservation. This method enables the prediction of engine power and efficiency in situations where there is sinusoidal volume change[181]. The Schmidt hypothesis is founded on the premise of isothermal compression and expansion of working areas. This study is greatly simplified and does not take into account heat transfer or internal pumping losses. Typically, the power and efficiency projected using Schmidt analysis are over estimated, surpassing the actual values by a margin of at least 30%. Nevertheless, doing a preliminary examination at the first-order level might serve as an effective first step in examining engine performance at a fundamental level[109], [182]. There has been a significant amount of use of the Schmidt theory, which is an isothermal calculation approach, in the design phase of Stirling engine[183].

3.2.2.1. Schmidt analysis

Schmidt formulated a theory that showed sinusoidal variations in the volume of workspace in alternating engines. The theory asserts that the crucial elements for compression and expansion are the isotherm assumptions and impeccable regeneration. Hence, it is obvious that the cycle remains highly idealized, but much more realistic than the ideal Stirling engine[184]. The Schmidt theory is one of the isothermal calculation methodologies used for Stirling engines. This method is fundamental and very advantageous for constructing Stirling engines. This concept is based on the isothermal expansion and compression of an ideal gas[72][185]. The most important assumption of an isothermal analysis is that the working fluid in the expansion area and the heater is at a constant high temperature, while it is at a constant low temperature in the compression space and the cooler. This isothermal method enables us to represent pressure as a function of variation in volume. It also allows for the investigation of the influence of the kind of kinematic mechanism on the generated power[186].

Schmidt study is based on the following principal assumptions[73]:

- Any processes may be reversed.
- Regeneration is a perfect operation.
- The ideal gas law is applied to the working fluid: pV = MRT.
- The mass of air in the system stays constant; there is no system leakage.
- Changes in volume in the workspace are sinusoidal.
- The heat exchanger has no temperature gradient.
- The piston and cylinder wall temperatures are constant.
- The engine speed remains constant.
- Continuity terms are established.
- There are no flow losses and hence no pressure losses.
- There is no operating gas leakage.

- Isothermal temperature in the heater and expansion space.
- The compression space is isothermal, and the temperature is colder.
- The temperature in the dead zone, and hence the regenerator space, remains constant.

The analysis starts by assuming that the total mass of working fluid inside the engine remains constant. Also, assuming constant pressure throughout the engine and constant temperature in the compression space, cooler, and expansion space, as well as the heater.

$$Mtotal = Me + Mh + Mr + Mk + Mc \quad (3\text{-}2)$$

$$Te = Th$$

$$Tc = Tk$$

The compression and expansion spaces are isothermal, as shown in Figure (3.2), in accordance with the hypothesis offered by Schmidt.

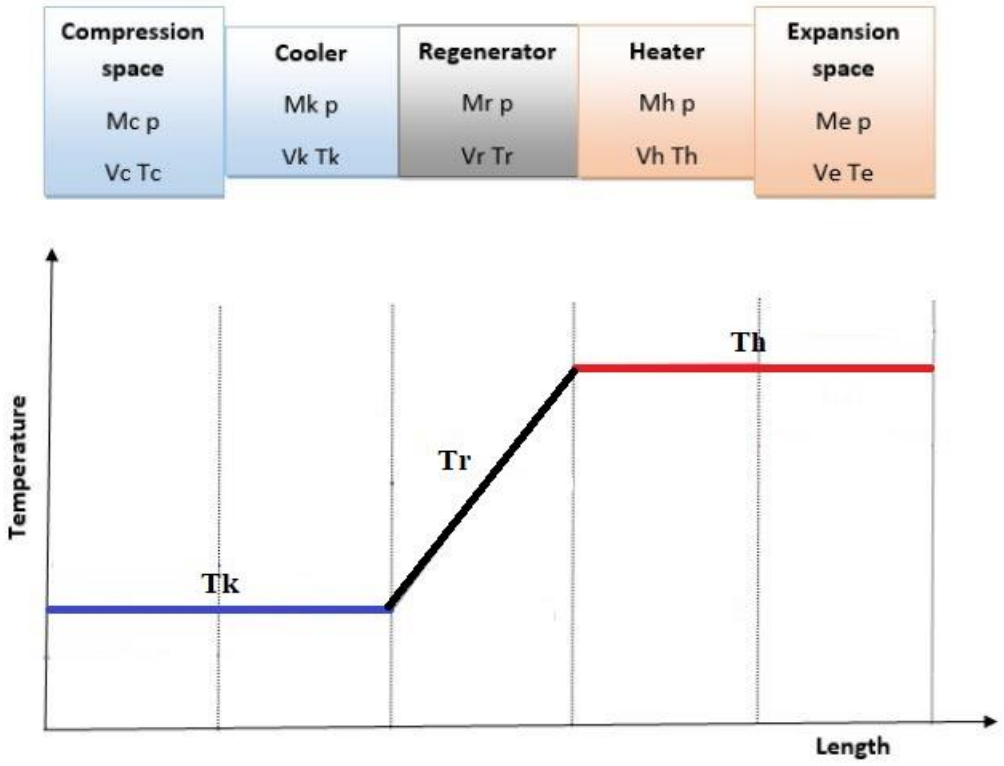

Figure 3-2: Ideal isothermal analysis temperature distribution

Utilizing the ideal gas equation, we can calculate the total mass by considering the charge pressure, gas constant, volumes, and temperatures of each component as follows[187]:

$$pV = MRT \tag{3-3}$$

$$M = \frac{PV}{RT} = \frac{PVe}{RTe} + \frac{PVh}{RTh} + \frac{PVr}{RTr} + \frac{PVk}{RTk} + \frac{PVc}{RTc} \tag{3-4}$$

The pressure of the cycle may be represented as[188]:

$$p = \frac{MR}{\frac{Ve}{Te}+\frac{Vh}{Th}+\frac{Vr}{Tr}+\frac{Vk}{Tk}+\frac{Vc}{Tc}} \tag{3-5}$$

Given the following expression, the instantaneous total volume is represented as [189]:

$$V = Ve + Vh + Vr + Vk + Vc \tag{3-6}$$

The effective temperature of the regenerator gas is calculated by taking the average of the temperatures achieved during expansion and compression[190]:

$$Tr = \frac{Te-Tc}{\ln\frac{Te}{Tc}} \tag{3-7}$$

The temperature, swept volume, and dead volume ratios are determined by using the following equations[191]:

$$Rt = \frac{Tc}{Te} \tag{3-8}$$

$$Rs = \frac{Vsc}{Vse} \tag{3-9}$$

$$Rde = \frac{Vde}{Vse} \tag{3-10}$$

$$Rdc = \frac{Vdc}{Vse} \tag{3-11}$$

$$Rr = \frac{Vr}{Vse} \tag{3-12}$$

In accordance with the assumption made by Schmidt that volumes move in a sinusoidal way, it is possible to determine the expansion and compression volumes by using the expansion, compression swept, and dead volumes, as well as the crank angle and phase angle for each type of Stirling engine[192]:

For alpha types

$$Ve = \frac{Vse}{2}(1 - \cos\theta) + Vde \quad (3\text{-}13)$$

$$Vc = \frac{Vsc}{2}(1 - \cos(\theta - \alpha)) + Vdc \quad (3\text{-}14)$$

For beta types

$$Ve = \frac{Vse}{2}(1 - \cos\theta) + Vde \quad (3\text{-}15)$$

$$Vc = \frac{Vsc}{2}(1 - \cos(\theta - \alpha)) + \frac{Vse}{2}(1 + \cos\theta) + Vdc - Vb \quad (3\text{-}16)$$

In the beta type, the displacer and power piston are located in the same cylinder. When the strokes of both pistons overlap, efficient functioning is achieved. The volume of overlap is[193]:

$$Vb = \frac{Vse+Vsc}{2} - \sqrt{\frac{Vse^2+Vsc^2}{4} - \frac{Vse\ Vsc\cos\alpha}{2}} \quad (3\text{-}17)$$

For gamma types

$$Ve = \frac{Vse}{2}(1 - \cos\theta) + Vde \quad (3\text{-}18)$$

$$Vc = \frac{Vsc}{2}(1 - \cos(\theta - \alpha)) + \frac{Vse}{2}(1 + \cos\theta) + Vdc \quad (3\text{-}19)$$

The following formula can be used to calculate the mean pressure:

$$pmean = \frac{1}{2\pi}\int_0^{2\pi} pd\theta = \frac{MR}{s\sqrt{1-b^2}} \quad (3\text{-}20)$$

$$Where, s = Rt + 2RtRde + \frac{4RtRr}{1+Rt} + Rs + 2Rdc + 1 \quad (3\text{-}21)$$

$$b = \sqrt{Rt^2 + 2(Rt-1)Rs\ cos\alpha + Rs^2 - 2Rt + 1} \quad (3\text{-}22)$$

The variations in the magnitudes of work in the expansion and compression regions generate the engine output on the surroundings. The total work conducted by the engine throughout a cycle is the sum of the work carried out by the compression and expansion spaces[194].

$$Wc = \oint pdVc = \int_0^{2\pi} p \frac{dVc}{d\theta} d\theta \quad (3\text{-}23)$$

$$We = \oint pdVe = \int_0^{2\pi} p \frac{dVe}{d\theta} d\theta \quad (3\text{-}24)$$

$$W = Wc + We \quad (3\text{-}25)$$

The indicated expansion and compression power are calculated based on the engine speed per one second and torque [195][196]:

$$P = W \,.\, N \quad (3\text{-}26)$$

$$P = 2\pi \frac{N\, t}{60} \quad (3\text{-}27)$$

And the thermal efficiency of the cycle is:

$$\eta = \frac{W}{We} \quad (3\text{-}28)$$

2.3.2. Second order analysis

Second-order design techniques are efficient computer algorithms that are especially valuable for optimizing the construction of a Stirling engine from scratch. Second order analyses attract attention due to their higher accuracy compared to first order analyses, while still being sufficiently rapid for design applications, unlike third order analyses. Second order design approaches include first determining the ideal power output, followed by eliminating losses caused by fluid friction and thermal shorting. Additionally, power losses are subtracted, and losses are added to either the heat input or heat rejection. The model used for forecasting the ideal power is often more intricate than the one employed for the first investigation[197].

2.3.2.1. Ideal adiabatic analysis

Urieli and Berchowitz utilized and confirmed the use of the adiabatic model in 1984[198]. The adiabatic analysis is an improved version of the Schmidt isothermal analysis, applied to both the expansion and compression regions, when no heat exchange occurs. Hence, the engine heat exchangers, located outside the engine's expansion and compression areas, serve as the only means for heat transfer into or out

of the engine[199]. In order to conduct an ideal adiabatic analysis, the components of the Stirling engine are divided into five distinct control volumes, as seen in Figure 3.3. The ideal adiabatic equations for each component are constructed based on the equations for energy and mass conservation, considering the following assumptions[200][201]:

- All operations are conducted in a state of equilibrium.
- The engine is operating with a constant rotational speed.
- The working fluid is an ideal gas.
- The engine operates via adiabatic compression and expansion spaces.
- The instantaneous pressure in the compression and expansion regions is uniform.
- The temperatures of the working fluid in the cooler and heater remain constant.
- The temperature of the working fluid in the regenerator undergoes a linear change.
- The kinetic and potential energy of gas streams are insignificant.
- Heat is exclusively delivered to the working fluid in the heater and cooler.
- The total mass of the working gas remains constant.
- The amount of heat that leaks between the compression and expansion areas and the amount of heat transferred to the environment are very little and may be considered insignificant.
- It is considered that there is no gas leakage from the engine to the outside.

The spaces for expansion and compression, as well as the heater, regenerator, and cooler, are represented by symbols (e, h, r, k, c). Additionally, there are four interfaces represented by symbols (he, rh, kr, ck), which correspond to the heater-expansion space, regenerator-heater, cooler-regenerator, and compression space-cooler, respectively. To get the set of differential and algebraic equations, the main

approach is to apply the energy and state equations to each individual cell, considering them as control volumes. This is the first phase of the process. By using the continuity condition, it becomes possible to construct interconnected equations that are applicable to the whole system.

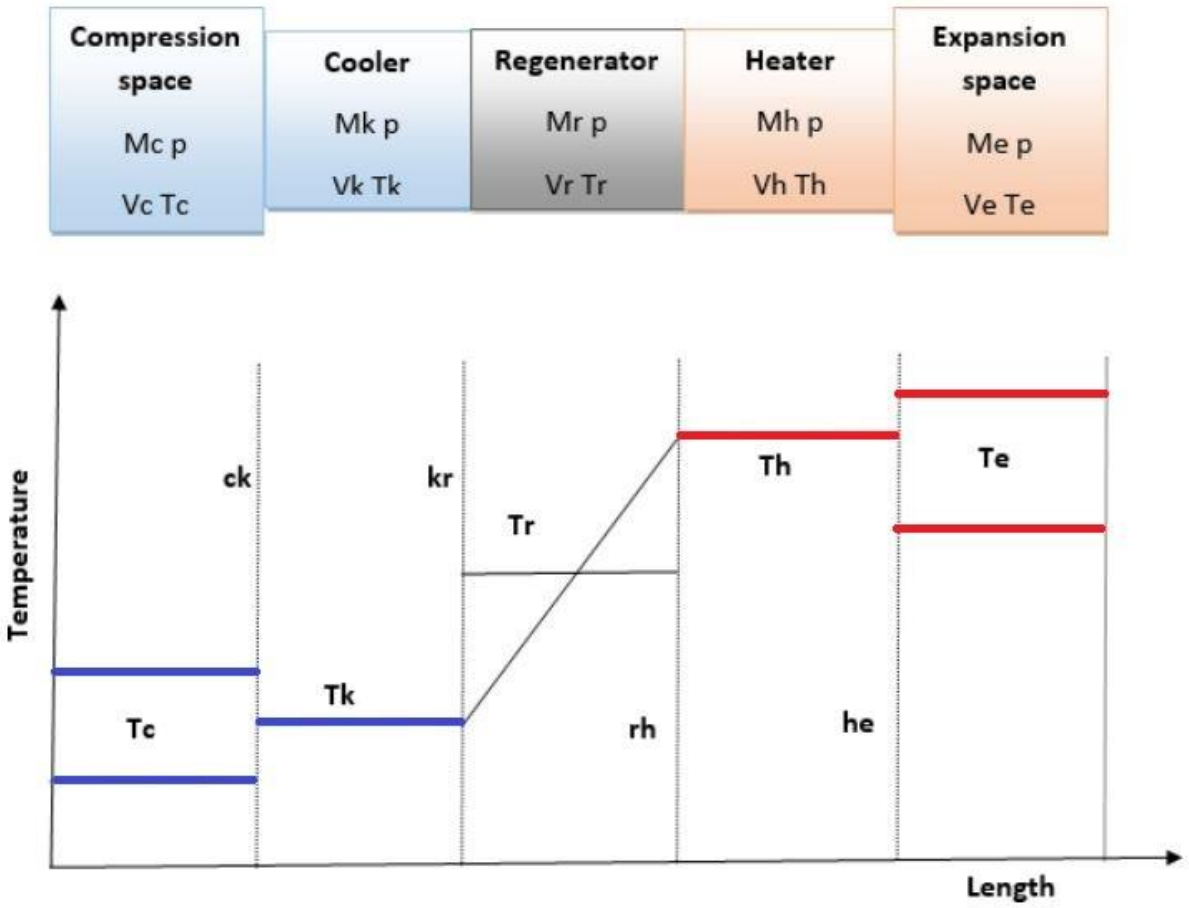

Figure 3-3: Engine control volumes and temperature profile in ideal adiabatic model

The key governing equations were derived by combining the equation for the ideal gas state with the mass and energy conservation equations in each component. To get the set of differential and algebraic equations, the method involves applying the energy and state equations to each individual cell, treating them as control volumes. The obtained equations are interconnected by applying the continuity equation across the whole system. The temperature is dependent upon the direction of flow[202][203].

$if\ Mck > 0\ then\ Tck = Tc\ else\ Tck = Tk$

$if\ Mhe > 0\ then\ The = Th\ else\ The = Te$

By applying the assumption that the temperature of the regenerator varies linearly between the hot and cold sides, the temperature may be computed by using the logarithmic mean temperature difference in the following manner[204].

$$Tr = \frac{Th - Tk}{\ln\frac{Th}{Tk}} \tag{3-29}$$

According to the assumption of adiabatic analysis, the total mass of the working gas stays constant and is provided as follows[205]:

$$Mtotal = Mc + Mk + Mr + Mh + Me \tag{3-30}$$

Taking the derivative of the equation provided

$$dMc + dMk + dMr + dMh + dMe = 0 \tag{3-31}$$

We use the ideal gas equation and apply differentiation:

$$\frac{dp}{p} + \frac{dV}{V} = \frac{dM}{M} + \frac{dT}{T} \tag{3-32}$$

$$where\ R = Cp - Cv\ and\ \gamma = \frac{Cp}{Cv}$$

The differential equation governing the equation of state becomes simpler in the adiabatic model when the temperature and volume of the heat exchangers are held constant[206].

$$\frac{dp}{p} = \frac{dM}{M} \tag{3-33}$$

The mass accumulation of heater, regenerator and cooler can be calculated as:

$$dM = \frac{dp\,V}{R\,T} \tag{3-34}$$

The Compression and expansion spaces mass evaluated by applying the energy equation[207]:

$$dMc = \frac{p\ dVc + Vc\frac{dp}{\gamma}}{R\ Tck} \tag{3-35}$$

$$dMe = \frac{p\ dVe + Ve\frac{dp}{\gamma}}{R\ The} \tag{3-36}$$

The equations shown below describe the rates at which mass accumulates at engine interfaces[208]:

$$Mck = -dMc \tag{3-37}$$

$$Mkr = Mck - dMk \tag{3-38}$$

$$Mrh = Mkr - dMr \tag{3-39}$$

$$Mhe = Mrh - dMh \tag{3-40}$$

The instantaneous pressure and pressure variation are calculated as follows[209]:

$$p = \frac{M\ R}{\frac{Vc}{Tc}+\frac{Vk}{Tk}+\frac{Vr}{Tr}+\frac{Vh}{Th}+\frac{Ve}{Te}} \tag{3-41}$$

$$dp = \frac{-p\gamma\left(\frac{dVc}{Tck}+\frac{dVe}{The}\right)}{\frac{Vc}{Tck}+\frac{Ve}{The}+\gamma\left(\frac{Vk}{Tk}+\frac{Vr}{Tr}+\frac{Vh}{Th}\right)} \tag{3-42}$$

The equation for the ideal gas is used to calculate the changes in temperature in both the compression and expansion zones[210][211]:

$$dTc = Tc\ \left(\frac{dp}{p} + \frac{dVc}{Vc} + \frac{dMc}{Mc}\right) \tag{3-43}$$

$$dTe = Te\ \left(\frac{dp}{p} + \frac{dVe}{Ve} - \frac{dMe}{Me}\right) \tag{3-44}$$

The amount of heat transferred by each section may be described using the energy equation for the cooler, regenerator, and heater[212][213]:

$$dQk = \frac{Cv\ dp\ Vk}{R} - Cp\ (Tck\ Mck - Tkr\ Mkr) \tag{3-45}$$

$$dQr = \frac{Cv\ dp\ Vr}{R} - Cp\ (Tkr\ Mkr - Trh\ Mrh) \tag{3-46}$$

$$dQh = \frac{Cv\ dp\ Vh}{R} - Cp\ (Trh\ Mrh - The\ Mhe) \quad (3\text{-}47)$$

The net work is calculated based on the compression and expansion volumes

$$dWc = p\ dVc \quad (3\text{-}48)$$

$$dWe = p\ dVe \quad (3\text{-}49)$$

$$dW = dWc + dWe \quad (3\text{-}50)$$

The thermal adiabatic efficiency

$$\eta = \frac{W}{Qh} \quad (3\text{-}51)$$

2.3.2.2. Non-ideal or simple adiabatic analysis

The simple analysis enhances engine efficiency by including the transmission of heat between the regenerator's matrix and the working fluid, so expanding upon the ideal adiabatic analysis. The adiabatic analysis is conducted by considering the regenerator's efficiency and the pressure drop in the heat exchangers. The fluid temperature in the core analytical model is determined by adding real regeneration. Moreover, the effective power gain is determined by factoring in the pressure drops throughout the three heat exchangers. The simple analysis examines the effects of imperfect regeneration, inefficient heat exchangers, and energy losses due to pumping[64].

Pumping losses due to pressure drop throughout the numerous portions of the engine, including the three heat exchangers and piping sections, may contribute to the engine's power output loss in addition to the power loss caused by actual seals and a real drive mechanism. Mechanical losses are caused by frictional forces between mechanical elements, such as those between the sealing ring and the cylinder, in the shaft seal, in all rolling bearings, and in the flywheel aerodynamic resistance. These losses are generally compensated for by the actual engine's braking efficiency.

Thermal losses between the expansion area and regenerator in Stirling engines may significantly impact working gas temperatures depending on the kind of heat source. The appendix gap, which is the gas domain contained between the displacer and the housing cylinder, is highly subject to a combined form of loss caused by the displacer's movement between extreme positions and major temperatures[178], [214], [215]. Enhancing engine performance requires minimising losses, which may be achieved by determining the ideal geometrical and physical properties of the regenerator and the displacer piston[216].

The Stanton number is used to assess the effect of non-ideal regeneration using the number of transfer units method[64], [120].

$$NTU = \frac{ST}{2}\left(\frac{Awg}{Ar}\right) \tag{3-52}$$

The relationship between the Staunton number and the convective heat transfer coefficient is as follows:

$$ST = \frac{h}{\rho\, u\, Cp} \tag{3-53}$$

The Staunton number is calculated based on the values of the Reynolds and Prandtl numbers[217].

$$ST = \frac{0.46\, Re^{-0.4}}{Pr} \tag{3-54}$$

The regenerator effectiveness determines the non-ideal heat exchange in the regenerator due to imperfect regeneration. The regenerator effectiveness, on the other hand, may be determined by knowing the number of transfer units (NTU) of the regenerator[158] [218].

$$E = \frac{NTU}{NTU+1} \tag{3-55}$$

The regenerator is fundamental thermal model that analyses non-ideal regeneration by considering geometrical features, matrix packing, porosity, and the influence of various raw materials at the same time. Calculating the thermal losses

that are brought about by improvements in a regenerator may be calculated by taking into account the maximum and minimum heat exchange of the regenerator, as well as the effectiveness of the regenerator, which is as follows:

$$Qrloss = (1 - E)(Qrmax - Qrmin) * freq \quad (3\text{-}56)$$

There is a difference in temperature along the heat exchangers, which results in conductive losses, which indicates the axial heat transfer that occurs. An expression that was taken into consideration to calculate the heat transfer loss between the heater and the cooler as follows[219][220]:

$$Qcrloss = \frac{Kr\ Ar}{Lr}(Twh - Twk) \quad (3\text{-}57)$$

The equation that describes the fundamental process of convective heat transfer is expressed as:

$$Q = h\ Awg\ (Tw - Tg) \quad (3\text{-}58)$$

It is possible to calculate the convection heat transfer coefficient by using the Stanton number (St), the Prandtl number, and the Reynolds simple analogy[197][221].

$$St = \frac{f}{2Re\ Pr} = \frac{h}{\rho\ u\ Cp}$$

$$Re = \frac{\rho\ u\ d}{\mu}$$

$$h = \frac{f\ \mu\ Cp}{2d\ Pr} \quad (3\text{-}59)$$

As shown in Figure (3-4), the temperatures of the gas within the cooler and heater are not the same as the temperatures on their walls. In order to increase the accuracy of the model, it is necessary to make the appropriate adjustments. The calculation for this may be done as follows[222]:

$$Tgk = Twk - \frac{freq*(Qk-Qrloss)}{(hk\ Awgk)} \quad (3\text{-}60)$$

$$Tgh = Twh - \frac{freq*(Qh-Qrloss)}{(hh\ Awgh)} \quad (3\text{-}61)$$

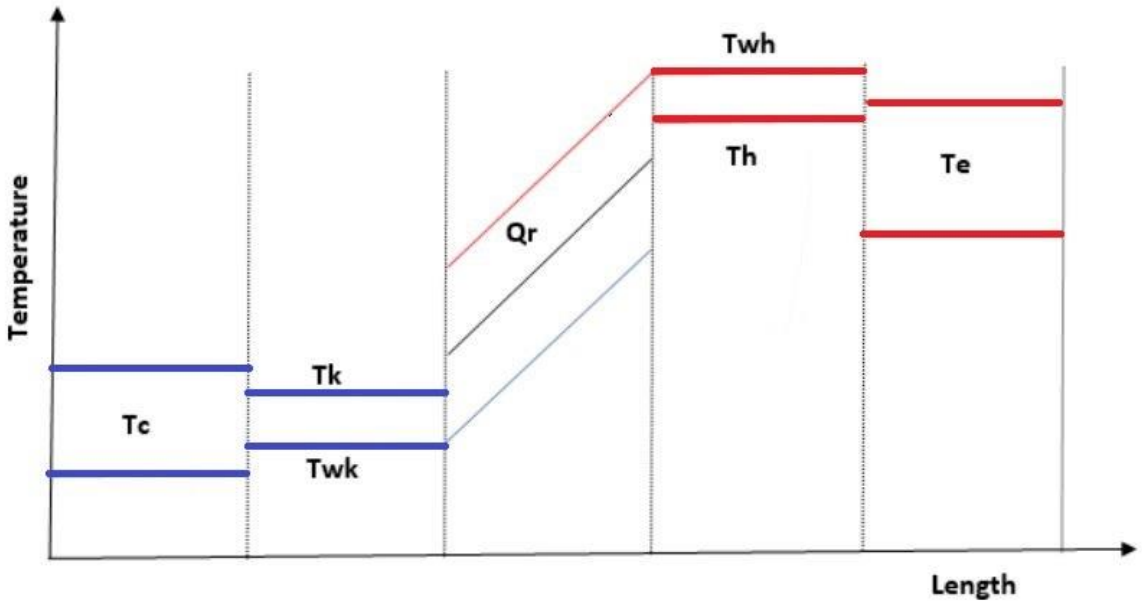

Figure 3-4: Temperature profile in simple analysis

Utilize the formula provided to determine the actual heat input of the heater as well as the heat output of the cooler:

$$Qah = (Qh * freq) + Qrloss + Qcrloss \quad (3\text{-}62)$$

$$Qak = (Qk * freq) + Qrloss + Qcrloss \quad (3\text{-}63)$$

The pressure drop for all heat exchangers may be mathematically described by an equation that conforms to the principle of momentum conservation for both positive and reversed flow. The decrease in pressure inside heat exchangers, resulting from fluid friction, leads to a reduction in power output in Stirling engines. The pressure drop in heat exchangers must be determined to quantify the power loss resulting from pressure losses. The pressure drops in heat exchangers may be determined using the following equation[223]:

$$\Delta p = -\frac{2f\mu uV}{A\,d^2} \tag{3-64}$$

As a result of the Darcy friction factor and the Reynolds number, the Reynolds friction factor may be calculated.

$$f = \frac{fD*Re}{4} \tag{3-65}$$

$$if\ Re < 2000\ , fD = \frac{64}{Re}$$

$$if\ 2000 < Re < 20000\ , fD = 0.316\ Re^{-0.25}$$

$$if\ Re > 20000\ , fD = \ 0.184\ Re^{-0.2}$$

In addition, the total pressure drops in the heat exchangers are equal to the sum of the pressure drops in the heater, the regenerator, and the cooler, as determined by algebraic calculation:

$$\Delta p = \Delta ph + \Delta pr + \Delta pk \tag{3-66}$$

Through the process of subtracting the work that was lost due to pressure drops in the heat exchanger, the actual work that the Stirling engine performed may be determined. Equations that follow provide a description of the actual work and efficiency of the Stirling engine[224]:

$$Wactual = W - dWloss \tag{3-67}$$

$$where\ dwloss = \oint \sum \Delta p\ dVe \tag{3-68}$$

$$\eta actual = \frac{Wactual}{Qah} \tag{3-69}$$

2.3.3. Third order modelling

Third order modelling is a more complex method used to evaluate the performance of Stirling engines. The principle of volume partitioning remains applicable; however, the governing equations are now expressed as partial differential equations instead of ordinary differential equations, requiring the use of advanced solution techniques. In third-order models, the operational mechanism was a unidirectional flow achieved by solving the governing equations for numerous nodes[225][226]. The process of third order design approaches starts with formulating the differential equations that articulate the principles of energy, mass, and momentum conservation. Due to their complexity, these equations cannot be solved analytically and thus need a numerical solution. The differential equations are simplified to their one-dimensional form. Subsequently, more simplifications are implemented based on the specific formulation given by the author[227].

Finkelstein [111]presented a third order approach that involves applying the principles of mass, momentum, and energy conservation at the nodal points of the engine. The governing equations are solved using an implicit method, both in space and time. The transitory start-up behavior was not accounted for since the model only considered the periodic solution. This technique increases the level of complexity by including various energy losses into the governing equations. Because the equations were too complicated for a general analytical solution, they were solved numerically using minor incremental time increments. Depending on the author, these equations were always reduced to a one-dimensional form with more simplification[72].

2.3.4. fourth order modelling

Recently, there have been advancements in the development of modern fourth order approaches or multidimensional analysis. These use computer fluid dynamic simulation algorithms. These multi-dimensional models provide comprehensive data on the flow pattern, temperature, and pressure distributions throughout the engine.

The primary constraint of these models is the need for much increased computational resources, which are both costly and limited to the intricacies of engine design.

Computational Fluid Dynamics (CFD) is used to demonstrate the fluid's flow characteristics inside certain geometries[228]. It has the ability to calculate flow losses and pressure drops accurately. Additionally, it can provide a detailed analysis of how the gas is heated and cooled. This analysis helps improve the efficiency of heat exchangers by optimizing flow conditions, pressure drops, and heat transfer. These models may be used to evaluate regenerator performance by simulating the whole engine or only the regenerator[229]. Because third order analysis is faster and, for the most part, an appropriate engineering tool, very little work has been undertaken at this level of analysis. However, in order to improve efficiency further (to understand and decrease losses), a greater knowledge of the actual flow characteristics and heat transfer throughout the engine is likely to be required[230]. The use of Computational Fluid Dynamics techniques is essential in this particular work. A computational fluid dynamics simulation was created and used to study multiphase flow. The simulation utilizes the discrete particle technique of the commercial program FLUENT, which was originally designed for pulverized coal combustion[231].

A CFD simulator typically consists of five main phases. First, a computational aided design set is used to specify the geometry under consideration. Second, the geometry is discretized using appropriate meshing tools. Third, define the issue using multi-physics and appropriate boundary conditions. Fourth, an appropriate approach for converting the governing equations, which are often sets of partial differential equations, into a set of algebraic equations utilizing the Finite Element Method or the Finite Volume Method. The last stage is to post-process the results so that they may be evaluated or compared to experimental data[176]. Table (3-1) summarizes different orders of models used in the analysis of Stirling engines, ranging from simplified conceptual models to more detailed and complex representations.

Table 3-1: Stirling engine models and analysis

Order model	Description
Zeroth Order Model	This model simplifies the analysis by assuming idealized conditions where all losses are neglected. It is typically used for preliminary conceptual design and rough estimation purposes.
First Order Model	Considers some losses and non-idealities, focusing on dominant effects. Provides a balance between accuracy and simplicity.
Second Order Model	Incorporates detailed losses like heat leakage, pressure drop, and mechanical losses. Offers greater accuracy but requires more computational resources.
Higher Order Models	Account for finer details such as transient behavior, fluid dynamics, and structural dynamics. Highly accurate but computationally intensive.
Empirical Models	Derived from experimental data rather than theoretical principles. Useful when theoretical analysis is impractical.
Analytical Models	Based on fundamental principles and equations. Offer insights into specific aspects of the engine.
Numerical Models	Use computational methods to solve complex equations and simulate engine behavior. Capable of handling intricate geometries.
Experimental Models	Derived from physical experiments, providing real-world data for validation of theoretical models.
Hybrid Models	Combine analytical, numerical, and empirical approaches. Offer a balance between accuracy and computational efficiency.

CHAPTER 4. EXPERIMENTAL SETUP AND METHODS OF INVESTIGATION

4.1. Introduction

Whenever there is a change in the temperature of a substance, the substance will either expand or contract depending on the change, and this expansion or contraction will take place simultaneously in all directions. Experimentation reveals that there are two methods for changing the state of the gas (and thus, its internal energy). The cylinder should be brought into contact with a body that is hotter than the gas. The gas will receive heat from the hotter body, which will result in an increase in the gas's internal energy. Pushing the piston down, which engages the system, is still another method that may be used for increasing the gas internal energy. These things might also occur in the other direction. Most Stirling engines employ a gaseous working fluid, but a two-phase, two-component fluid may increase heat transmission and reduce sealing issues while increasing specific output. The compound working fluid contains a gaseous carrier and a liquid component in the cold compression area that becomes vapor in the expansion space during regenerative operation. This chapter analyses the behavior of volume and pressure changes of gas chamber containing air with additive low boiling liquids such as (acetone, spirit) depending on heating temperature effect, also study this experiment with Stirling engine operating enhancements.

4.2. Volume expansion of gases and liquids

The three forms of matter all experience changes in volume when conditions of temperature and pressure are changed; however, liquids also experience similar changes. Even though liquids are not sensitive to changes in pressure, they may be sensitive to changes in temperature depending on the composition of the liquid. It is essential to have knowledge of the coefficient of volumetric expansion of a liquid in order to determine the degree to which the volume of the liquid varies as a function of

temperature. On the other hand, the change in volume of gases is not dependent on the composition of the gas since the volumes of all gases expand and contract generally in accordance with the law of the ideal gas. When a liquid is heated, the particles that make up the liquid experience an increase in their kinetic and vibrational energy. As a result of this, they can move at a broader range of motion within the limits of the forces that maintain them together as a liquid. These forces are unique to each liquid and change based on the strength of the bonds that bind molecules to each other and hold molecules together. Additionally, these forces are not shared by any other liquid. The coefficient of volumetric expansion (βv) is a scientific measurement that quantifies the amount of expansion that a particular liquid experiences in response to a change in temperature.

The volume change may be computed by using the formula:

$$\Delta V = Vo\ \beta v\ (T1 - To) \qquad (4\text{-}1)$$

Where ΔV is the volume change, Vo, To, T1 are the initial volume, initial temperature, and new temperature.

4.3. Experimental description

A diagrammatic representation of the apparatus that was used in the investigational experiment can be seen in Figure (4-1). Additionally, the properties of the numerous fluids that were put to the test in the experimental work are defined in Table (4-1) that can be found below. To investigate the relationship between the boiling temperature and the changes in volume and pressure, the experiment was carried out using a number of different combinations (air, air-acetone, and air-spirit) with different volume concentrations.

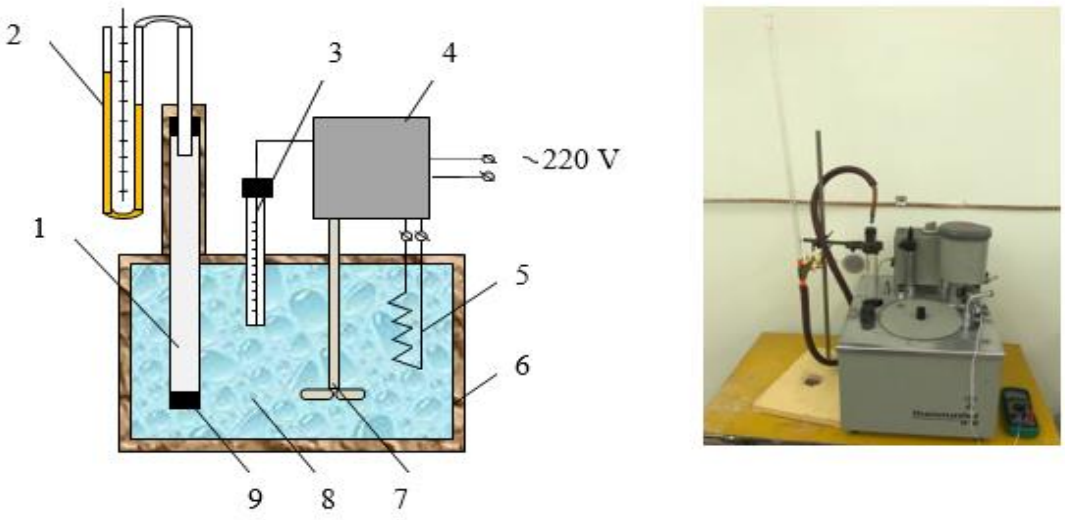

Figure 4-1: Scheme and photo of the experimental setup (1-Gas working volume, 2-U shaped pressure gauge, 3-pin thermometer,4- control unit, 5- electric heater, 6-thermal insulation, 7- stirring device, 8- thermostat liquid, 9- plug)

Figure (4-2) shows the temperature difference between the hot space and cold space during the experiment and Figure (4-3) shows the working fluids used in experiment which are low boiling liquids.

Figure 4-2: The temperature difference between hot and cold spaces

Figure 4-3: Different fluids used

Table 4-1: Fluids properties

Fluids	Molar mass (g/mole)	Density (kg/m³)	Boiling point (°C)
Acetone	58	784	56
Spirit (alcohol)	46	789	78
Benzene	78	876	80
Water	18	997	100

4.4. Gamma Stirling engine

The Gamma Stirling engines use a displacer-piston combination that is like the structure of beta engines, where the displacer and piston are located in separate cylinders. This machine utilizes two cylinders with an interconnected transfer port to divide the compression area. The cooler, heater, and regenerator are linked in series

between the displacer cylinder and compression cylinder. This configuration has the advantage of simple crank mechanism.

The details, components, schematic diagram, and operating parameters of gamma Stirling engine are presented in the Figures (4-4, 4-5, and 4-6) and Table (4.2), which is one of Bengs Modellbau (German company) products. Specifically, the displacement cylinder and the working cylinder are both cylinders that include pistons, the cooling system in this engine is air-cooled by using cooling fins. While the working cylinder is constructed out of steel, the displacement cylinder is constructed out of aluminum with a diameter of 60 mm due to the superior thermal conductivity of aluminum against steel. In addition, the cooling fins that are installed on the displacement cylinder are designed to guarantee that the machine continues to function for the longest amount of time feasible. The flywheel and the pulley are both components of the hot air engine, just as they were in the historical type.

The size of this engine has several benefits that come along with it. Since the Stirling engine has a large surface area, it is able to dissipate heat more effectively and, as a result, it can operate for longer. Additionally, as compared to smaller model Stirling engines, this large Stirling engine is capable of operating at speeds that are substantially lower. But the model can handle even high speeds without any issues. The speed of this hot air motor may be adjusted with the help of a wheel designated for that purpose. A flywheel with a diameter of 140 mm and a pulley made of our well-known cast steel quality spin on the driving shaft. There is no longer a need for the working cylinder to undergo any processing on the interior since it is composed of a hydraulic cylinder tube. The throttle screw is used to obstruct the airflow passage between the displacement cylinder and the working cylinder while in operation. This guarantees that the Stirling engine will revolve at a slower or higher speed, regardless of the flame being unchanged. Consequently, this enables control of the speed of the Stirling engine.

Figure 4-4: All parts of Gamma Stirling engine

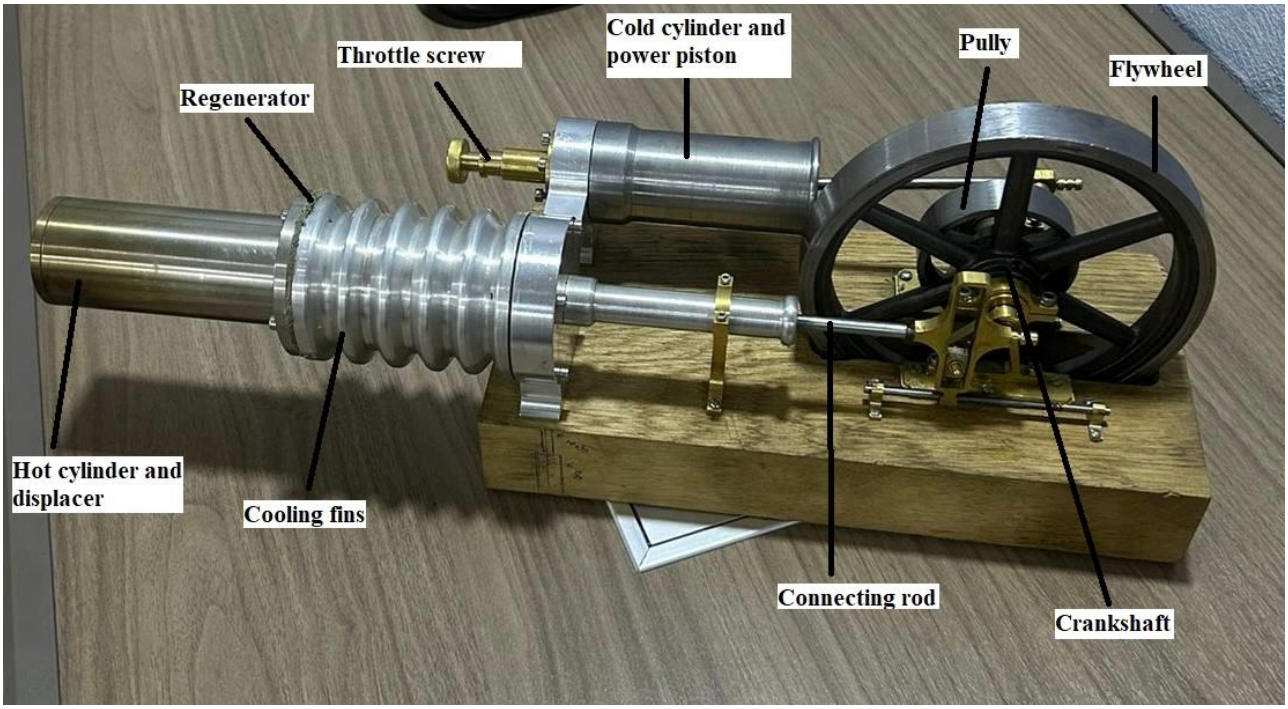

Figure 4-5: Gamma Stirling engine

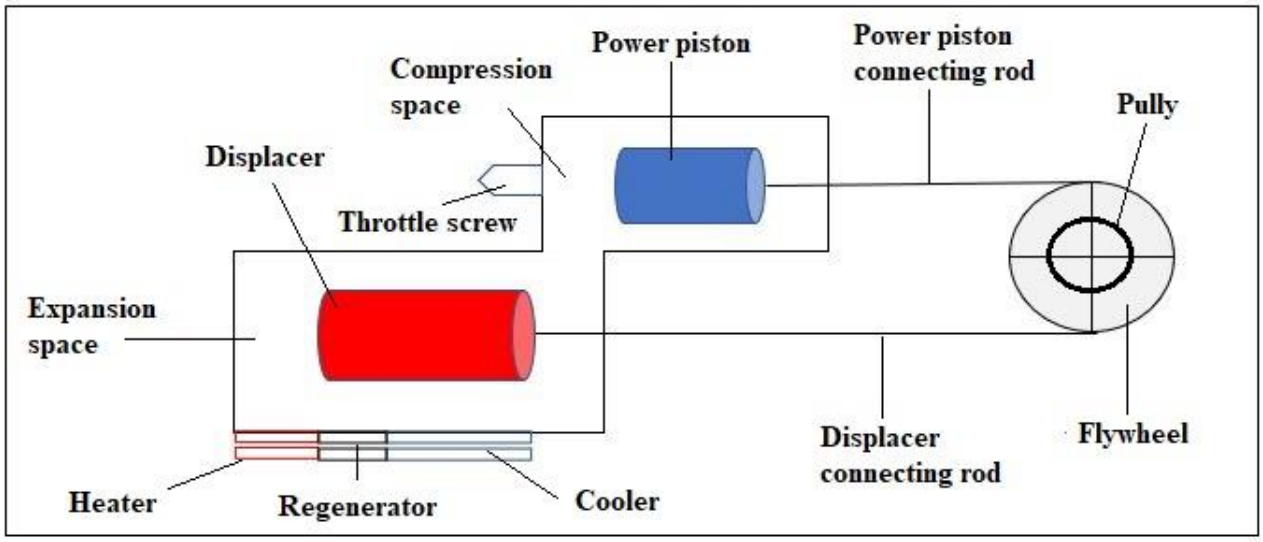

Figure 4-6: Schematic diagram of Gamma Stirling engine

Table 4-2: Stirling engine geometrical and operational parameters

Parameter	Value
Engine type	Gamma
Power piston diameter	30 mm
displacer piston diameter	35 mm
Stroke	22 mm
Flywheel diameter	140 mm
Pully diameter	56 mm
Displacement cylinder diameter	60 mm
Working cylinder diameter	40 mm
Charge pressure	1-3 bar
Cold sink temperature	288 K
Hot source temperature	700 K
Rotational speed	600 rpm
Working fluid	Air
Cooling system	Air- cooled

4.5. Measurement tools

In the context of Stirling engine experiments, measurement tools refer to instruments or devices specifically used to quantify and analyze various parameters related to the engine's operation and performance. These tools are essential for collecting accurate data that allows us to evaluate the efficiency, power output, thermal characteristics, and overall behavior of the Stirling engine. In this part, we cover the various instruments and measurement equipment that were used in this research as shown in Figure (4-7). Table (4-3) classifies the measurement tools used in Stirling engine experiments along with their respective purposes.

Table 4-3: Measurement instruments

Parameter	Measurement Tool	Purpose
Temperature	Thermocouples, Thermistors, Infrared Sensors	Measure temperatures at different points within the engine
Pressure	Pressure Transducers, Pressure Gauges	Measure the pressure of the working fluid at various stages
Speed	Tachometers, Rotational Speed Sensors	Measure the rotational speed of the engine shaft
Torque	Dynamometers, Torque Sensors	Measure the torque applied to the engine shaft
Gas Flow Rate	Flow Meters, Flow Sensors	Measure the flow rate of the working fluid
Displacement	Displacement Sensors, Linear Encoders	Measure movements of the piston and displacer
Heat Transfer	Heat Flux Sensors, Thermal Imaging Cameras	Measure heat transfer rates and temperature gradients
Data Acquisition	Data Acquisition Systems	Collect, store, and analyze data from various sensors and devices

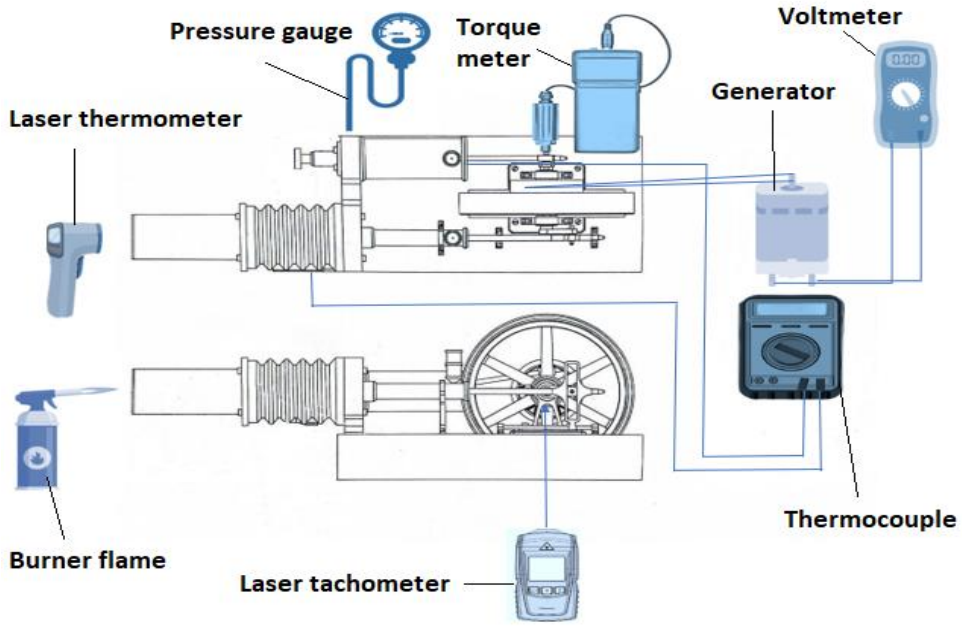

Figure 4-7: Measurement tools

- **Thermocouple type K**

A Thermocouple is a temperature sensor that consists of two different metal wires welded together at one end, known as the junction. One of the most used types of thermocouples is Type K. It works by identifying the specific locations within the Stirling engine where temperature measurements are needed. These could include the hot end where heat is supplied, the cold end where heat is rejected, the regenerator, or other critical components. Type K thermocouples are widely used due to their wide temperature range, relatively low cost, and good accuracy.

- **Laser temperature measurement**

Also known as laser thermometry is a non-contact method used to measure the temperature of an object or a surface using laser technology. This technique relies on the principle of measuring the thermal radiation emitted by the object and determining its temperature based on the characteristics of the emitted radiation.

- **Pressure Gauge**

A pressure gauge is a device used to measure the pressure of the working fluid within the engine. Pressure gauges provide important information about the operating conditions and performance of the engine, allowing to monitor and analyze various parameters such as pressure variations, compression and expansion ratios, and gas exchange processes. The pressure gauge is typically connected to the Stirling engine at specific locations where pressure measurements are desired. Common installation points include the compression and expansion spaces, the hot and cold ends.

- **Tachometer**

In Stirling engine, tachometer is a device used to measure the rotational speed of the engine shaft. The rotational speed, often measured in revolutions per minute (rpm), provides important information about the engine operating frequency and performance. The tachometer plays a vital role in monitoring the rotational speed of the shaft in the Stirling engine experiment, providing valuable data for analysis and optimization of engine performance.

- **Dynamometer**

A dynamometer is an instrument used to quantify force, torque, or power. An instance of this is when the power generated by an engine, motor, or any other rotating device may be determined by measuring both the torque and rotational speed (rpm) concurrently. One common type of dynamometer used for testing Stirling engines is an absorption dynamometer. This type of dynamometer absorbs the power output of the engine and converts it into heat or mechanical work, allowing for precise measurement of torque and rotational speed. Absorption dynamometers can come in various forms, such as hydraulic, electromagnetic, or mechanical load brakes.

In the Gamma Stirling engine experiment, a gas combustion flame is used as a heat source to provide the necessary temperature gradient for engine operation as shown in Figure (4-8).

A controlled gas supply is ignited to produce a stable gas burn flame. The flame is directed towards the hot cylinder of the Stirling engine to transmit heat to the enclosed air.

By controlling the intensity of the gas burning flame, we can regulate the rate of heat transfer to the engine and explore its effects on performance parameters. In addition, we will monitor key variables such as temperature and pressure at different points within the engine to evaluate its thermodynamic behavior.

During the start-up phase, the engine undergoes temperature stabilization as the hot and cold cylinders reach thermal equilibrium. As this balance is achieved, the efficiency of heat transfer within the engine improves, leading to a more efficient conversion of thermal energy into mechanical work. This improved efficiency results in an increase in power output and thus an increase in rotational speed.

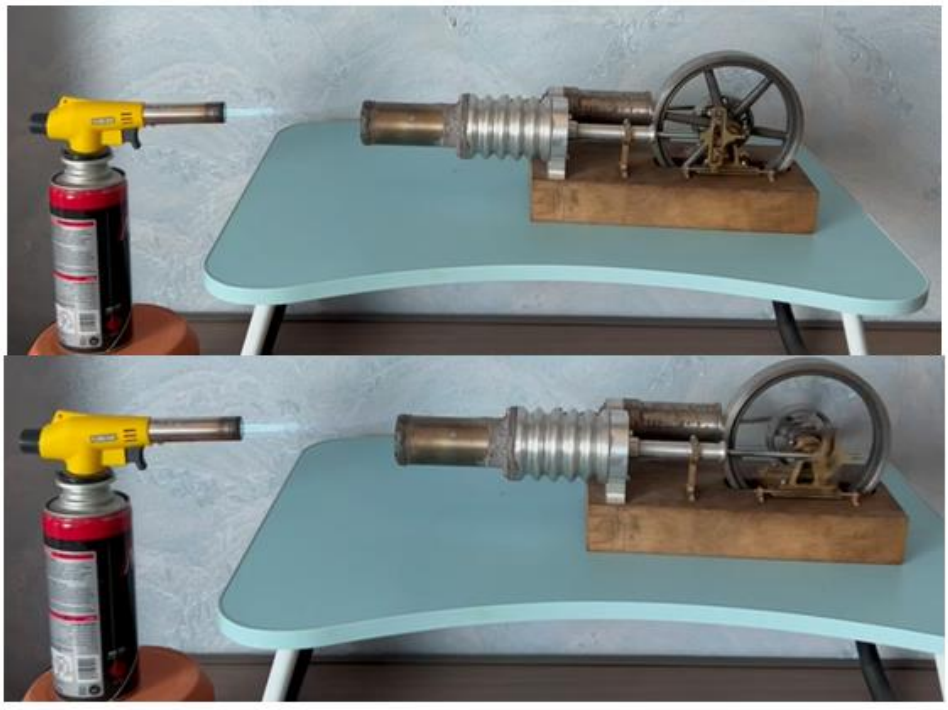

Figure 4-8: Experimental operation

When the flame heats the air in the hot cylinder, the air expands, causing the Stirling engine to cycle. This expansion drives the power piston, converting thermal energy into mechanical work. At the same time, the expanding air displaces the displacer piston, causing the working fluid to move towards the cold cylinder.

The movement of the working fluid between the hot and cold cylinders facilitates heat exchange within the engine, which is essential for maintaining the temperature gradient necessary for continuous operation (Figures 4-9, 4-10). When the hot air reaches the cold cylinder, it releases heat and contracts, completing the cycle and preparing for the next stage of expansion.

Figure 4-9: Temperature difference between hot side and cold side

Figure 4-10: Gradual rise in temperature during the heating process

Since the engine operates continuously, the rotational speed increases gradually over time. This process is the result of several factors related to the thermodynamic processes of the engine and its mechanical properties. Initially, when the engine is started, it starts at a relatively low rotational speed due to the inertia of its moving parts and the initial conditions of the working fluid as demonstrated in Figure (4-11).

Figure 4-11: Gradual rise in rotational speed during the operating

CHAPTER 5. RESULTS, ANALYSIS, AND DISCUSSIONS OF MATHEMATICAL MODELING AND EXPERIMENTAL STUDY

5.1. Introduction

In this chapter, the results that were identified via the examination of the data that was gathered for this research are presented. One of the key objectives of this study was to evaluate the impact that compound working fluid has on the performance of the Gamma Stirling machine. The analysis of the data was carried out by using both the numerical and experimental investigations, and the results are presented in a manner that is consistent with the study analysis and hypotheses that were specified.

An overview of the sample features is presented at the beginning of the study. This overview provides information on the composition and specifications of the Stirling engines that were scrutinized, as well as the characteristics of the compound working fluids that were employed in the tests. It is very necessary to have a solid understanding of these contextual aspects in order to correctly evaluate the ensuing results.

Furthermore, the chapter discusses the consequences of the results in relation to the wider framework of Stirling engine technology. The use of compound working fluids in real-world applications is carefully examined, with a focus on the possible benefits, constraints, and practical factors. To summarize, this chapter combines the main discoveries obtained from the practical examination, emphasizing their importance in improving our comprehension of Stirling engine performance enhancement methods and providing insights into the viability of using compound working fluids for sustainable energy production.

5.2. Experimental study results

This section presents a comprehensive analysis of the experimental results obtained from testing conducted on the Stirling Engine prototype. The experimental investigation allowed for precise measurement of key performance parameters, including power output. By systematically varying working fluid composition, we aimed to explore the engine behavior and uncover its operational limits.

The first research included introducing fluids (acetone and spirit) with different concentrations (1%,5%,10%,20%) into a sealed cylinder containing air, which was then subjected to heating by an electric thermostat. The purpose was to examine the impact of temperature on the volume of the system. Figures (5-1, 5-2, 5-3) present the change of volume of air and additives with heating temperature.

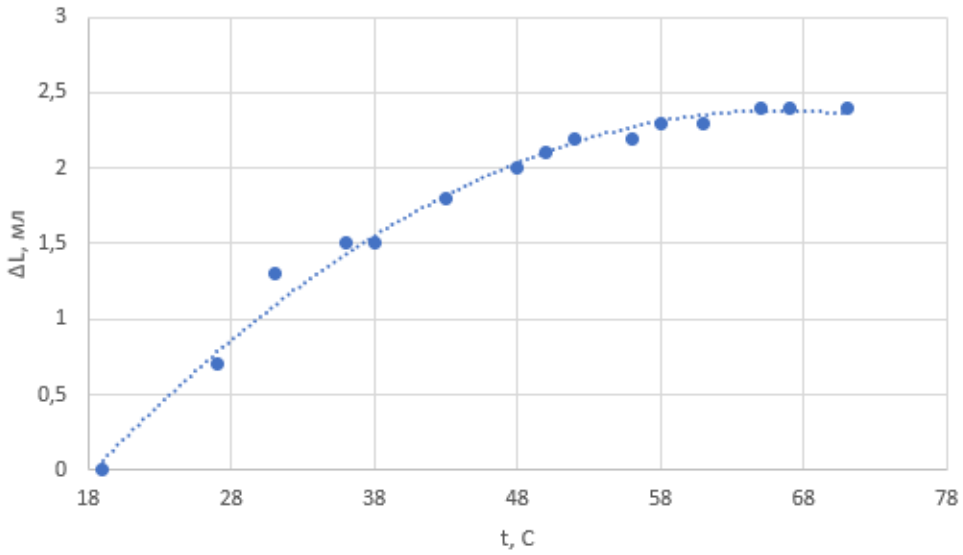

Figure 5-1: Change in volume of air

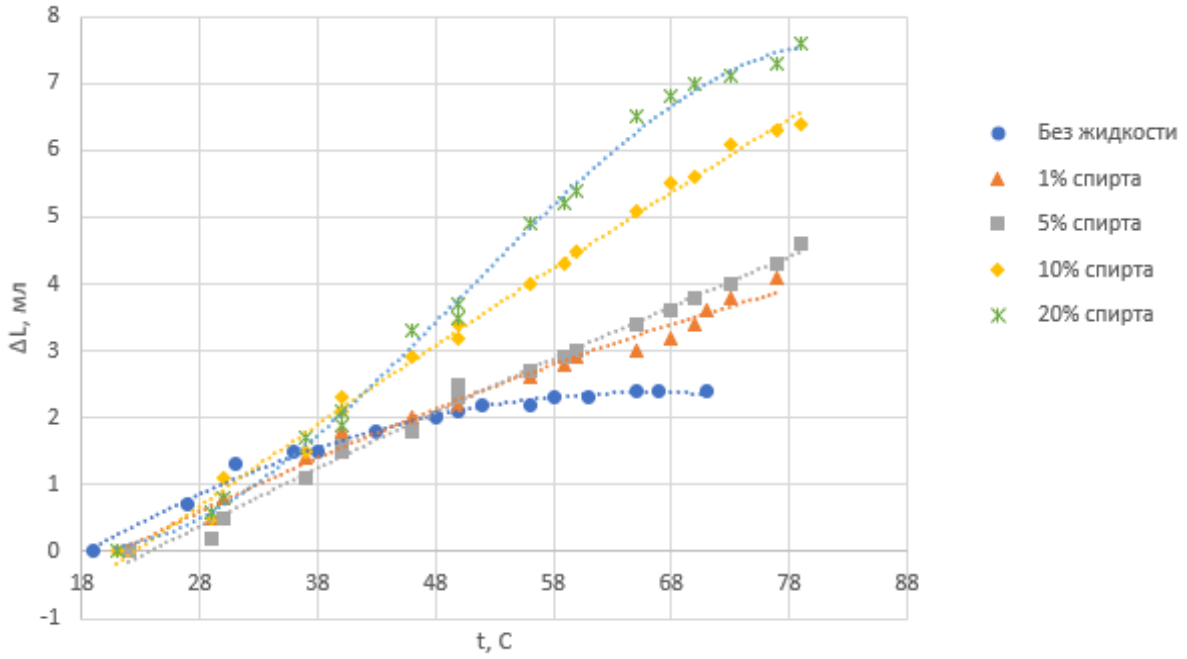

Figure 5-2: Change in volume of air-spirit mixture

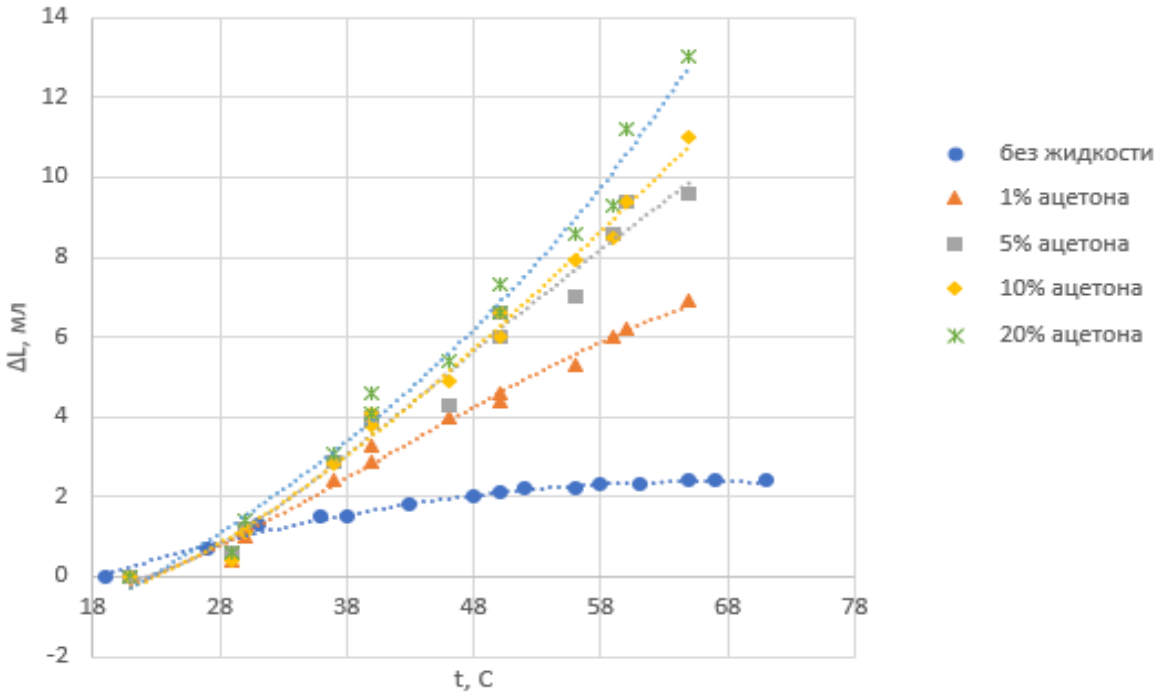

Figure 5-3: Change in volume of air-acetone mixture

The second research project was conducted to improve the efficiency and performance of the Gamma Stirling engine by optimizing its operating dynamics through the addition of fluid additives to the principal working gas, air, in the engine's chamber. This experiment comprised adding acetone and spirit at different volume ratios of 1%,5%,10% and 20% to assess their effects on engine performance and output.

This inquiry aims to explore how fluid additives can impact the thermodynamic properties and heat transport characteristics in the engine, potentially improving its overall performance metrics. Acetone and alcohol were selected for their recognized effectiveness as heat carriers and their suitability with the operational parameters of the Stirling engine. To introduce these chemicals into the air and monitor changes in the engine cyclic behavior, power production, and efficiency.

By conducting systematic experiments and analysis, we can get insights into how fluid additives affect the internal processes of heat transfer and energy conversion in the engine. Using different volume ratios enabled a thorough investigation of how the amount of acetone and spirit affects engine performance. This method allowed for determining the best additive concentrations that result in maximum enhancements in operating efficiency and power production, while also ensuring conformity with the engine's design limitations.

This research attempt is a significant advancement in understanding fluid dynamics of Stirling engines, which could improve their practical use in various applications such as power production and automobile propulsion.

5.2.1. Effect of operating parameters

The geometric and operational parameters of Stirling engine are essential factors in influencing its performance, efficiency, and operational characteristics. Optimizing these parameters is crucial for attaining the required balance between power output, efficiency, and reliability in Stirling engine applications.

5.2.1.1. Effect of hot source and cold sink temperatures

The Stirling engine operates on the principle of temperature difference between a hot source and a cold sink to generate mechanical work. Therefore, the temperature of the hot source directly affects the efficiency and performance of the Stirling engine.

The effect of heating temperature on power, and thermal efficiency in different cases is shown in Figures (5-4, 5-5, 5-6, 5-7, 5-8), which consider adding acetone, spirit, and water with concentrations of (1%, 5%, 10%, 20%) into the air.

The total work and power output of Stirling engine generally increases with an increase in the temperature of the hot source. This is because a higher temperature difference between the hot source and the cold sink leads to greater thermal expansion and contraction of the working fluid. The results that were obtained demonstrated that the performance of the Stirling engine was improved as a result of the addition of acetone and alcohol to the air that was present in the engine. In the scenario in which air was the only working fluid, the power that was produced was 8 W. However, when acetone was added, the power increased to 10 W. Additionally, the power output increased to 9.5 W 8.5 W when spirit and water were included.

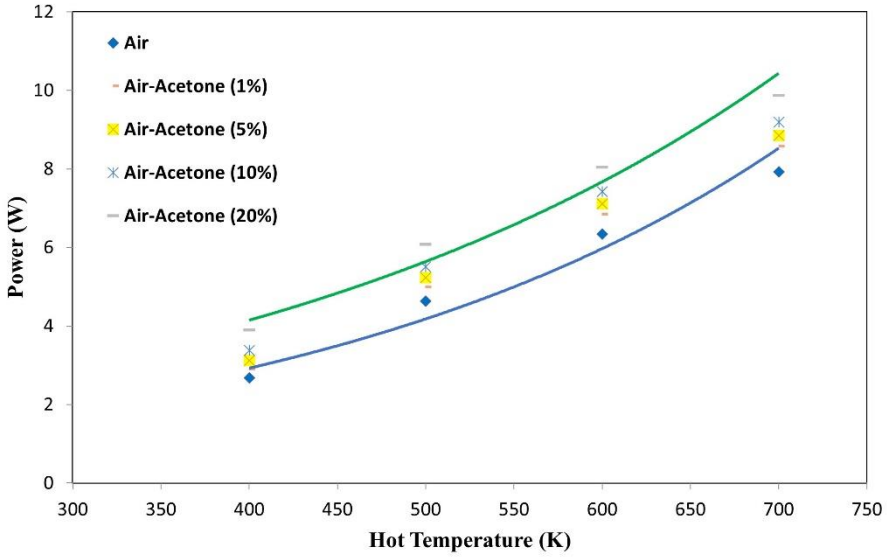

Figure 5-4: Power variation when add acetone with heating temperature effect

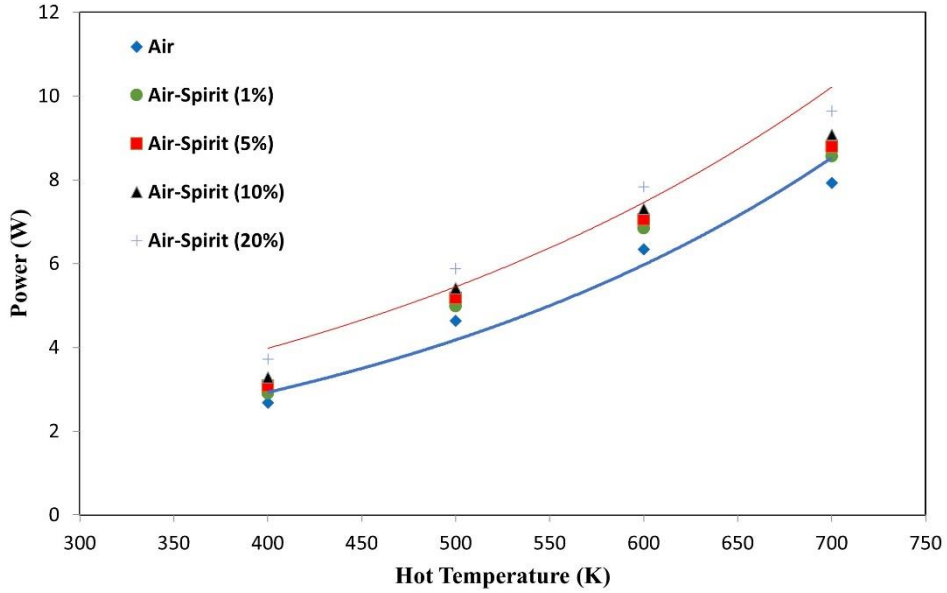

Figure 5-5: Power variation when add spirit with heating temperature effect

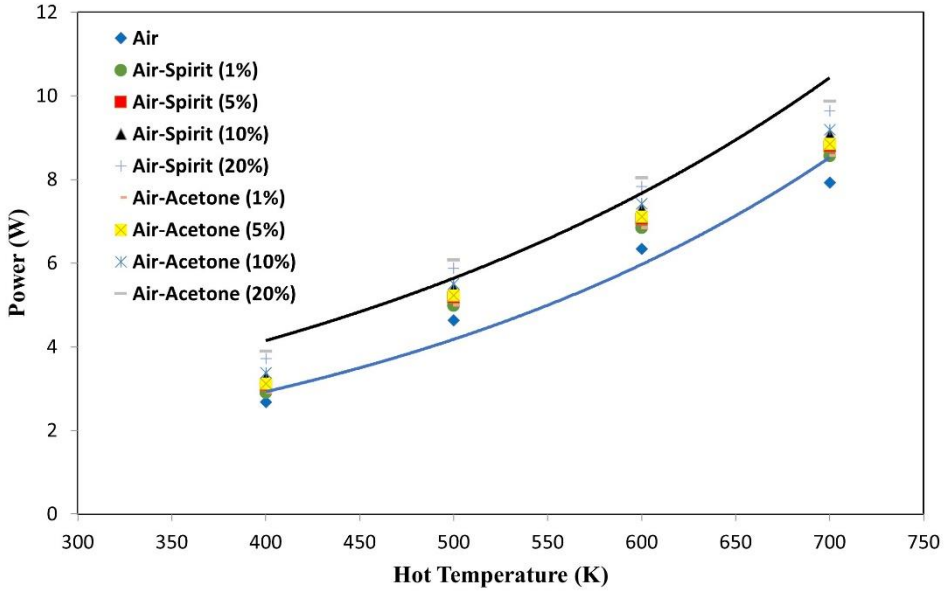

Figure 5-6: Power variation when add spirit and acetone into air with heating temperature effect

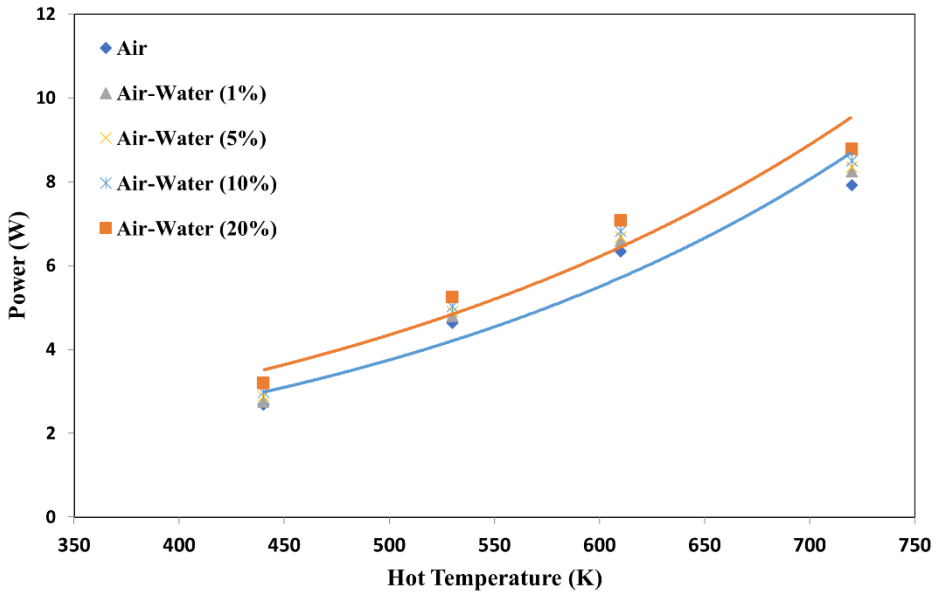

Figure 5-7: Power variation when add water with heating temperature effect

Also increased temperatures of the heat source often result in higher thermal efficiency in Stirling engines. This is since a greater temperature differential enables more effective heat transfer and the conversion of thermal energy into mechanical energy.

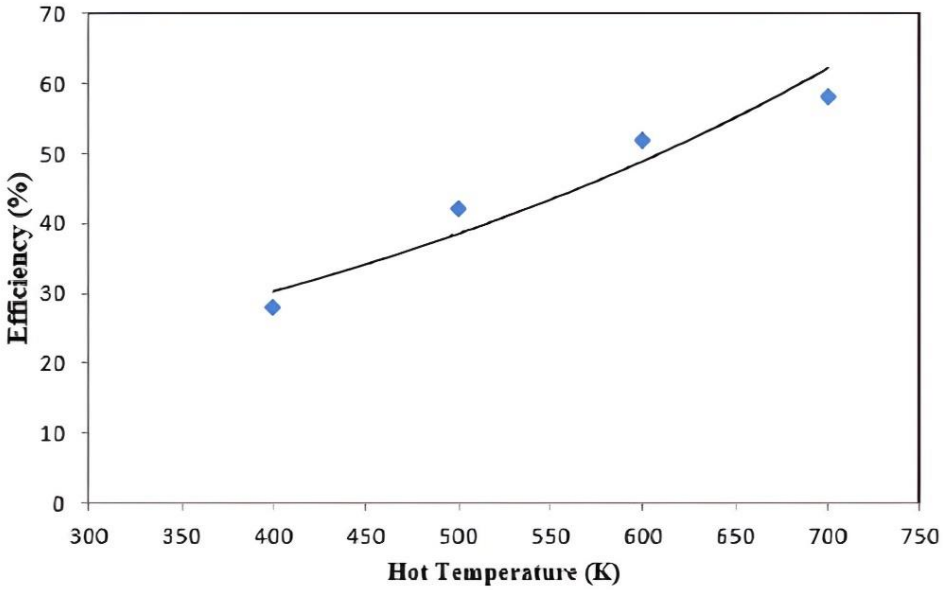

Figure 5-8: The effect of hot source temperature on efficiency

Conversely, the impact of cooler temperatures in the cold sink on power and efficiency could be observed in Figures (5-9, 5-10, 5-11, 5-12) and Figure (5-13) shows the Output power variation with hot source and cold sink temperature. The results indicated a decrease in power and efficiency as the cold temperature increases. Increasing the temperature of the cold sink reduces the temperature differential between the hot source and the cold sink, which in turn decreases the Stirling engine's ability to generate mechanical work efficiently. This leads to a reduction in work output, power, and efficiency. The temperature difference between the hot source and the cold sink is a key determinant of the engine's efficiency and power output. A larger temperature difference generally leads to higher efficiency and power output. Therefore, reducing the temperature of the cold sink while keeping the hot source temperature constant can increase the temperature difference and improve performance.

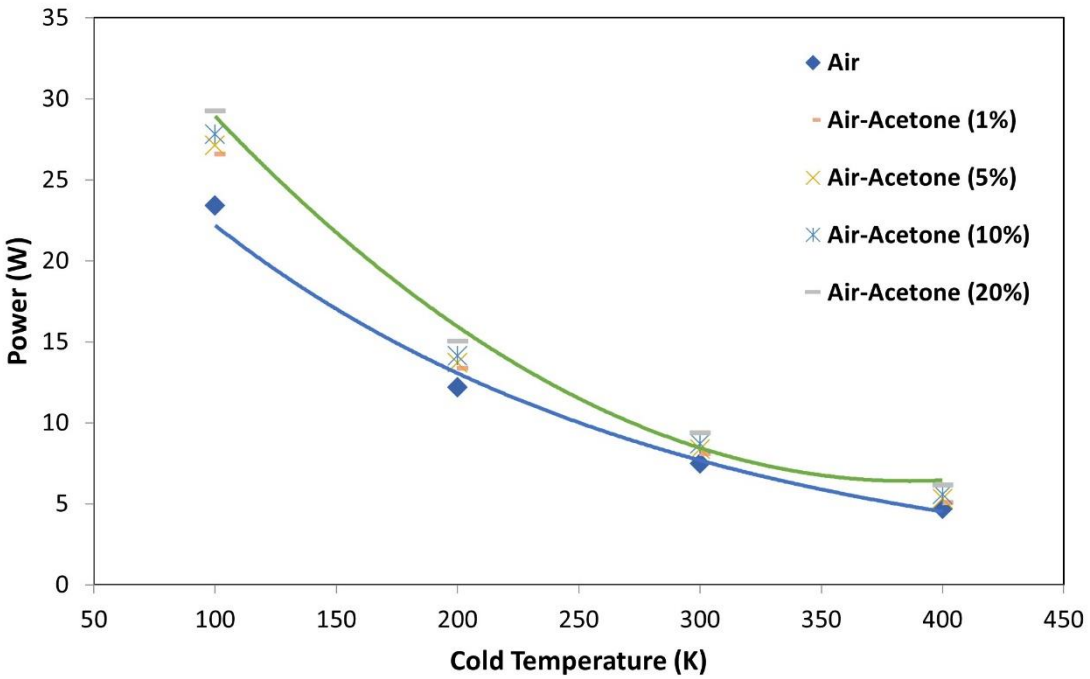

Figure 5-9: Power variation when add acetone with cold sink temperature effect

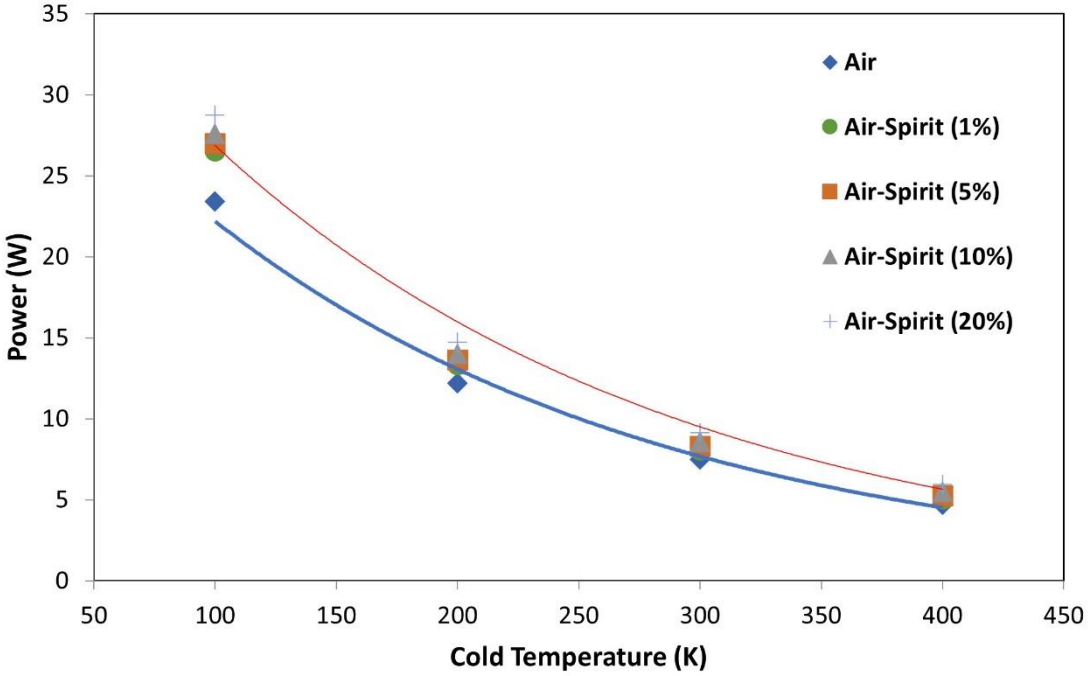

Figure 5-10: Power variation when add spirit with cold sink temperature effect

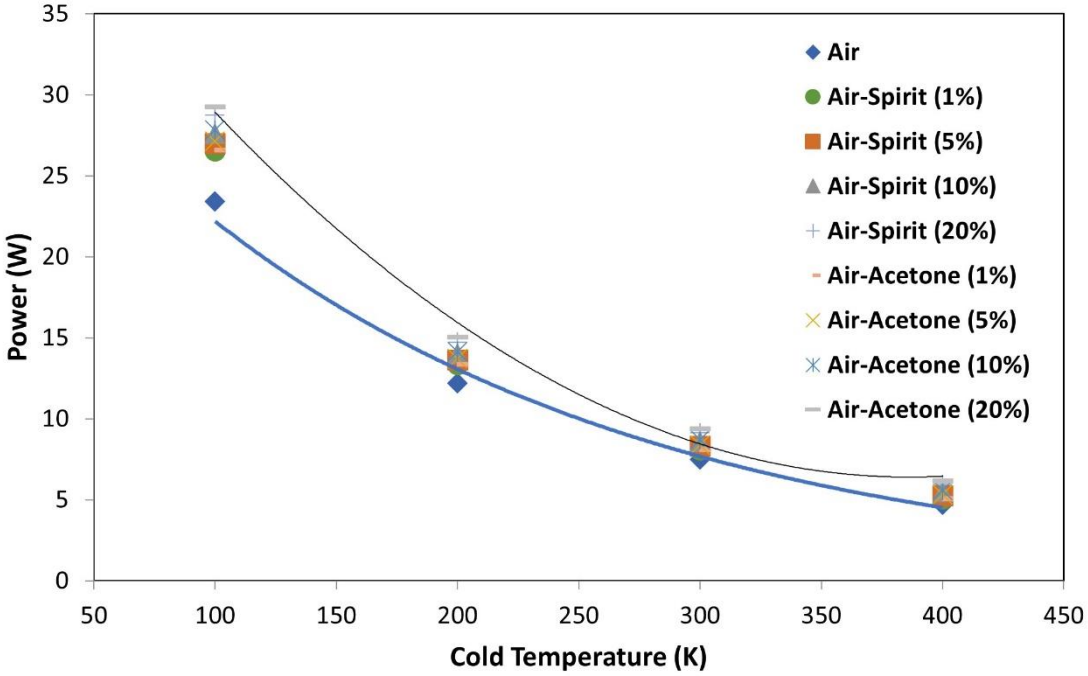

Figure 5-11: Power variation when add spirit and acetone into air with cold sink temperature effect

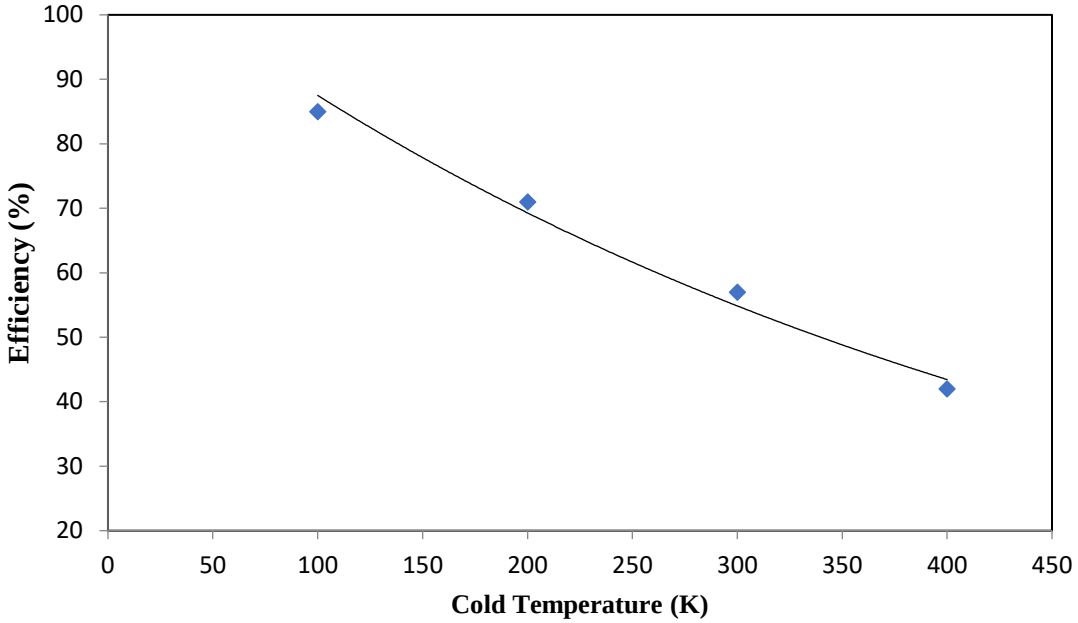

Figure 5-12: The effect of cold sink temperature on efficiency

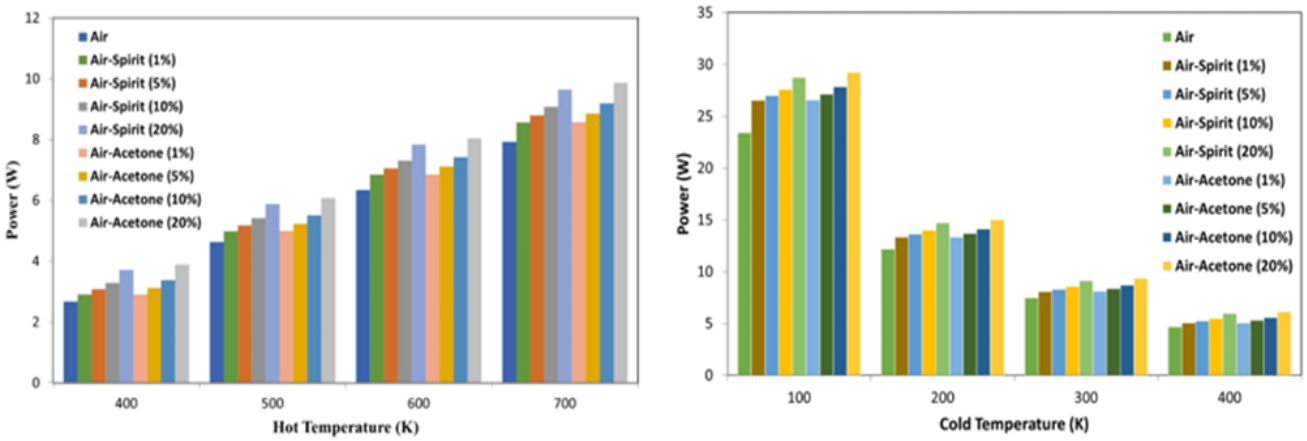

Figure 5-13: Output power variation with hot sauce and cold sink temperature

5.2.1.2. Effect of charge pressure

The charge pressure in Stirling engine, also known as the working fluid pressure, refers to the pressure inside the engine working spaces. It can significantly impact the engine performance, efficiency, and operating characteristics. The power output of the Stirling engine is directly influenced by the charge pressure. Higher charge pressures typically result in greater pressure differentials between the hot and cold sides of the engine, leading to increased mechanical work output. This is because

the expansion and contraction of the working fluid are more pronounced at higher pressures, resulting in larger forces acting on the pistons or displacers, as shown in Figures (5-14, 5-15, 5-16, 5-17).

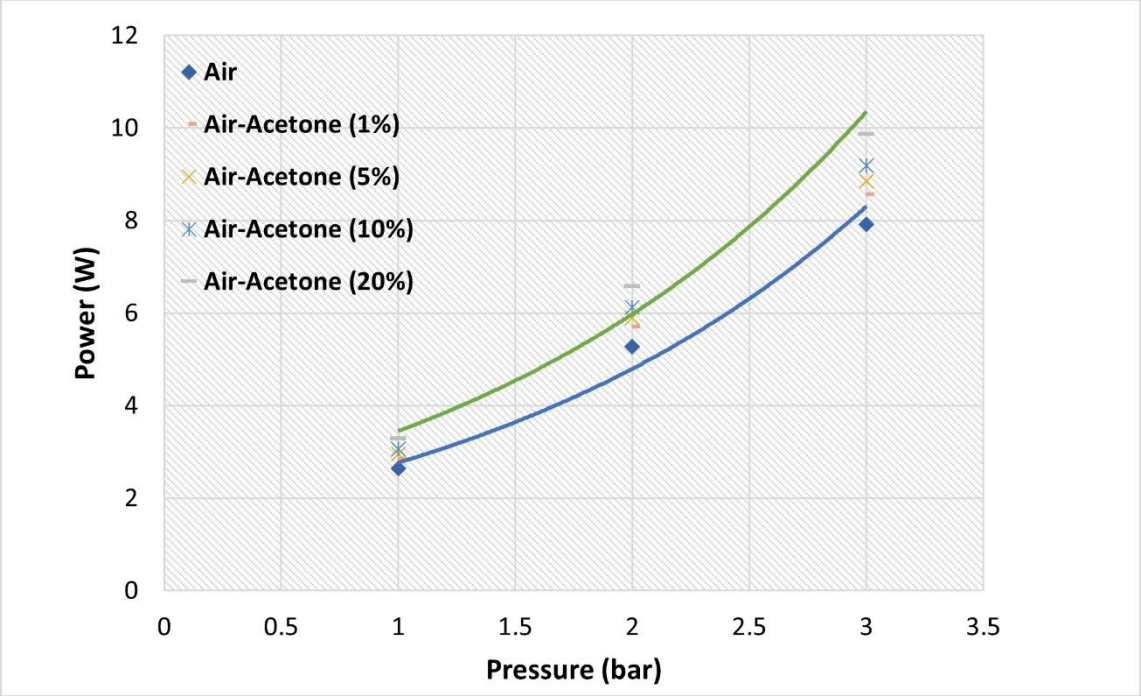

Figure 5-14: Power variation when add acetone with pressure effect

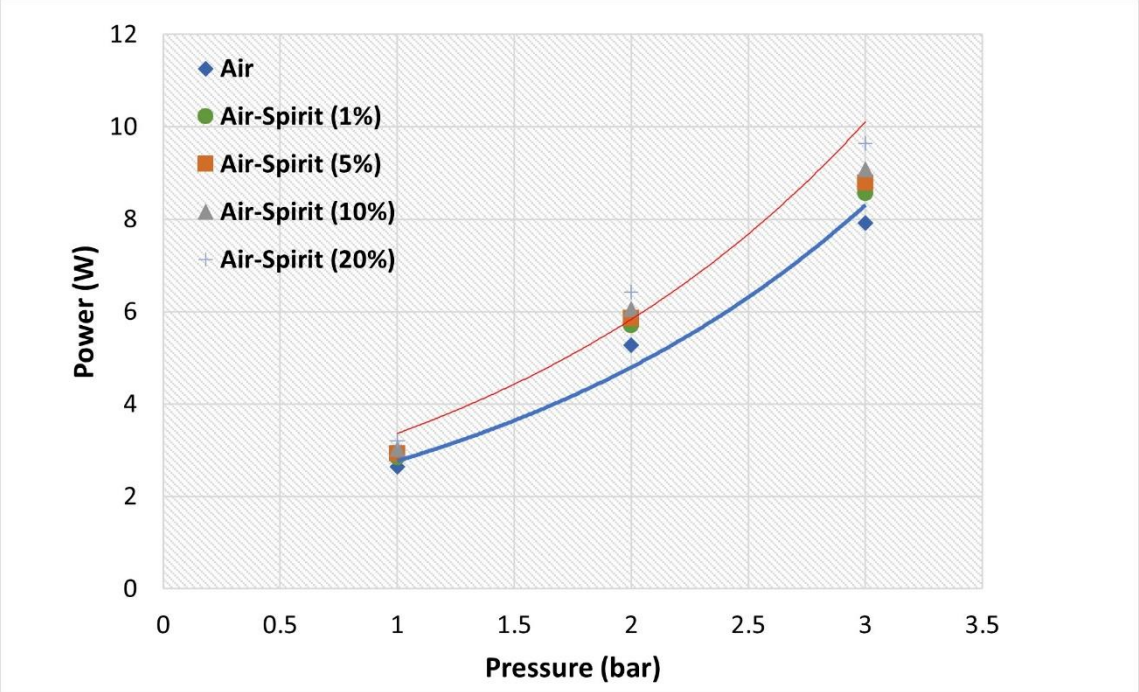

Figure 5-15: Power variation when add spirit with pressure effect

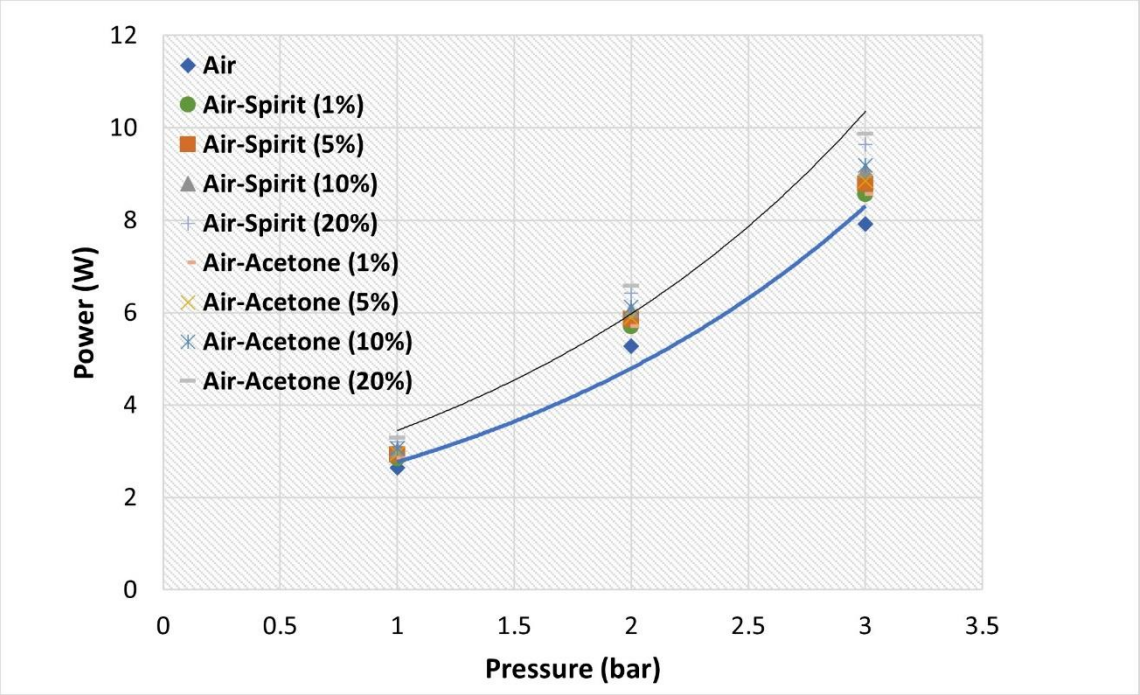

Figure 5-16: Power variation when add spirit and acetone into air with pressure effect

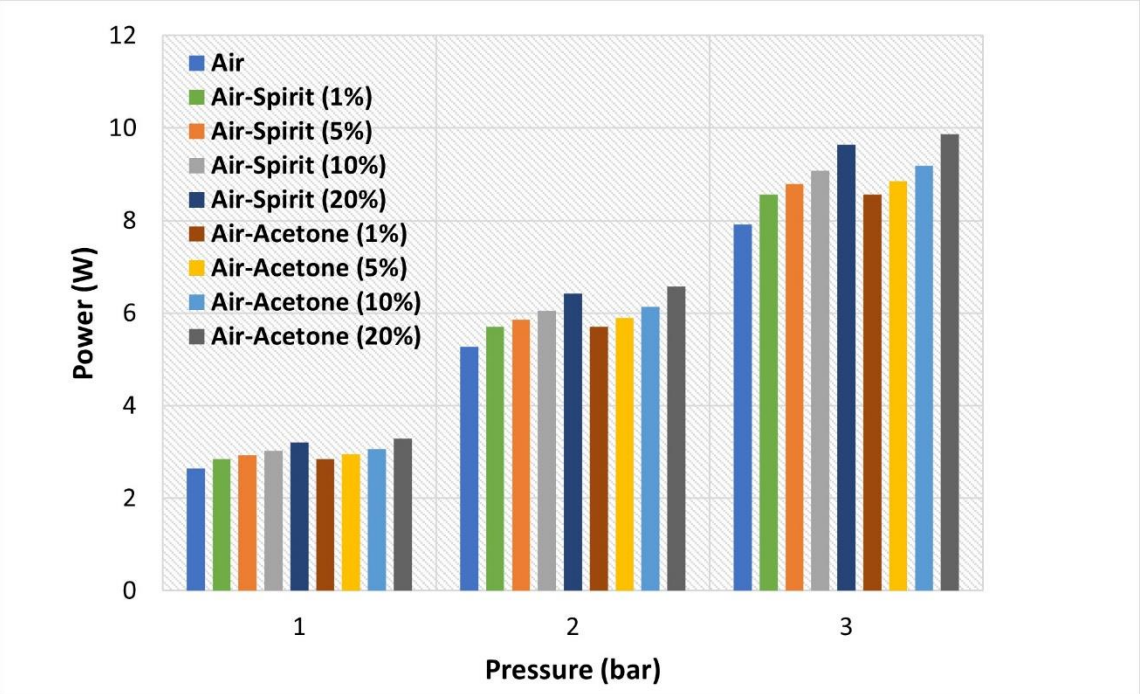

Figure 5-17: Output power variation with pressure

5.2.1.3. Effect of rotational speed

The engine speed, or rotational speed, refers to the rate at which the Stirling engine pistons or displacers move back and forth. This speed has a significant effect on the engine's power output. The power output of a Stirling engine is directly proportional to the mechanical work performed by the pistons or displacers. As the engine speed increases, the pistons or displacers move more rapidly, resulting in increased mechanical work output per unit time. This leads to higher power output from the engine as demonstrated in Figures (5-18, 5-19, 5-20, 5-21).

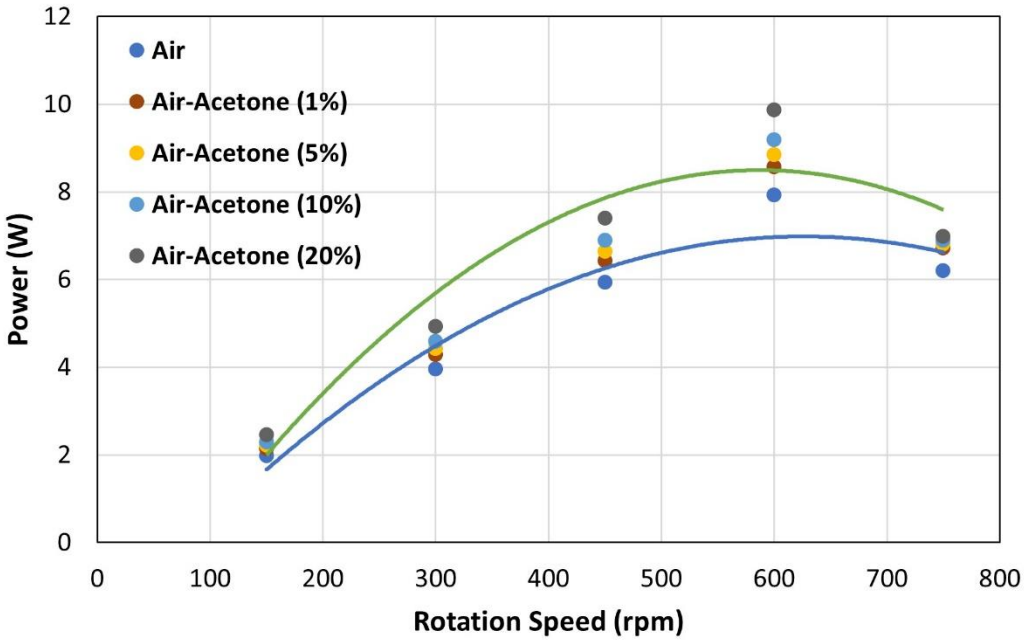

Figure 5-18: Power variation when add acetone with rotational speed effect

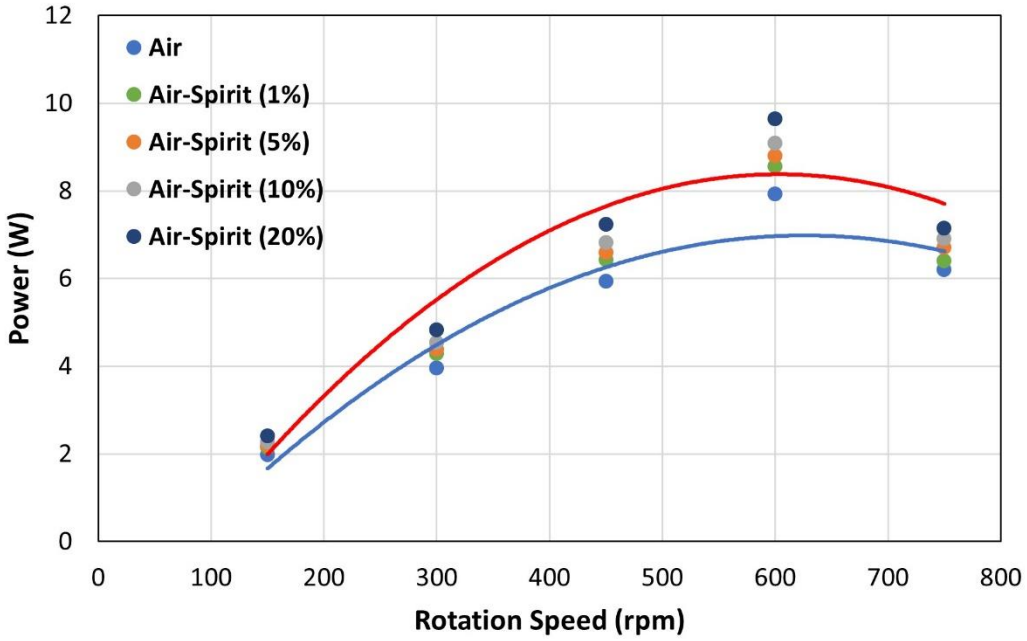

Figure 5-19: Power variation when add spirit with rotational speed effect

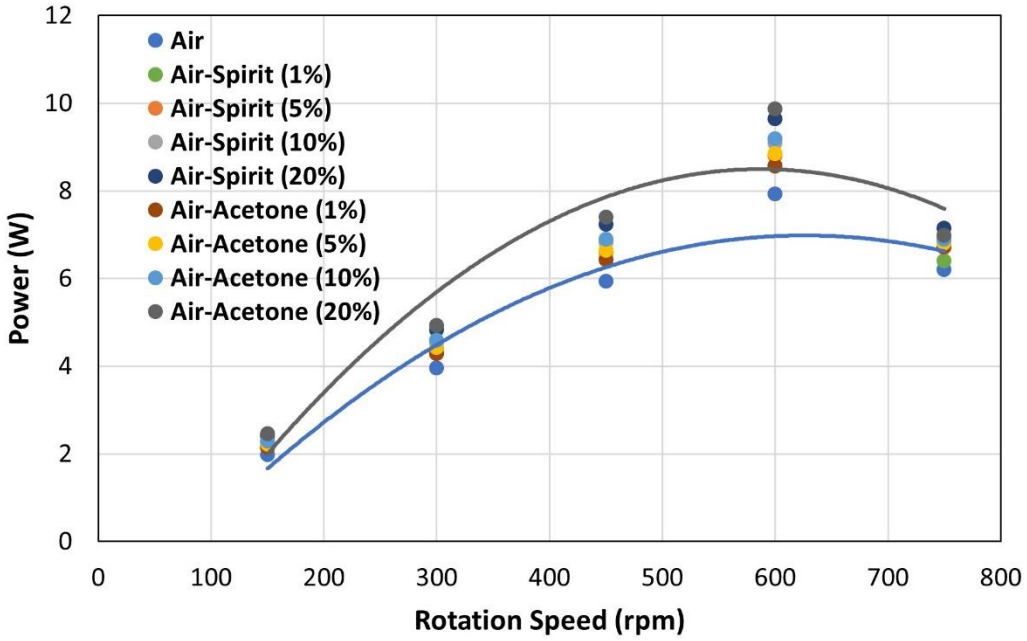

Figure 5-20: Power variation when add spirit and acetone into air with rotational speed effect

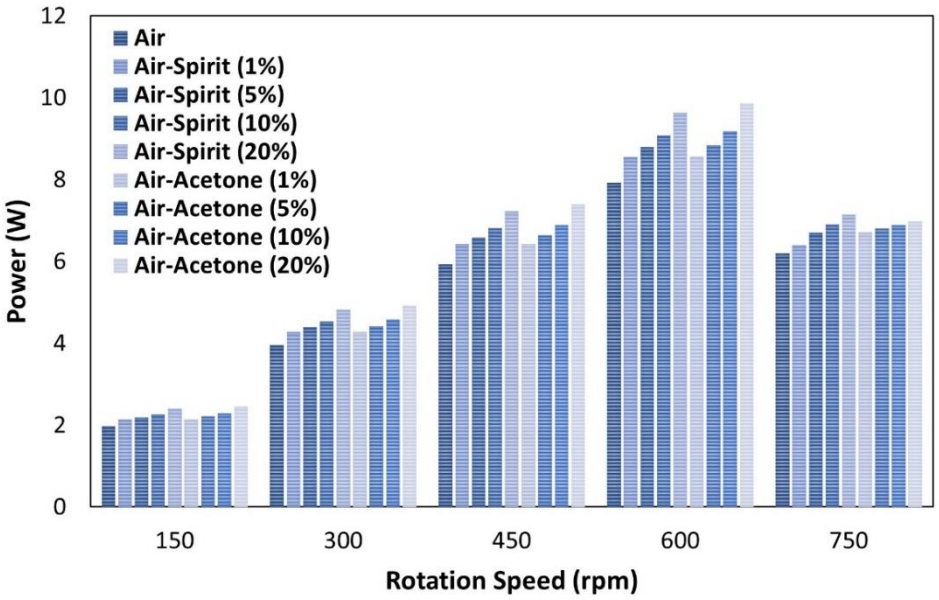

Figure 5-21: Output power variation with rotational speed

Figure (5-22) illustrates the relationship between engine torque and engine speed. Variations in engine torque based on different working fluid compositions within the 200-600 rotational speed range. The torque grows up to a specific engine speed and then decreases. The maximum torque production reached 0.16 Nm at 580 rpm.

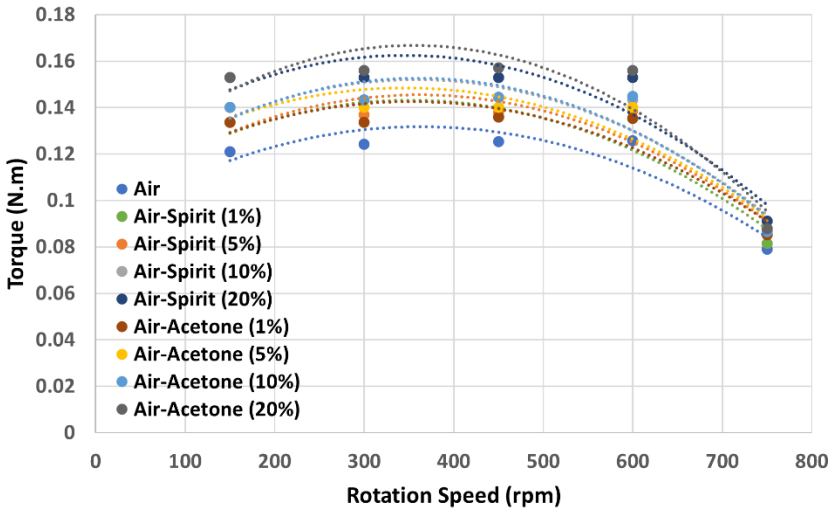

Figure 5-22: The effect of rotation speed on torque

The experimental tests results are presented in table (5-1).

Table 5-1: Experimental study results

Working fluid	Volume fraction (%)	Power (W)	Power gain (%)
Air	100%	8	-
Air-acetone mixture	1%	8.5	6,3
	5%	9	12,5
	10%	9.5	19
	20%	10	25
Air-spirit mixture	1%	8.25	2,5
	5%	8.5	6,3
	10%	9	13
	20%	9.5	19
Air-water mixture	1%	8.2	2,5
	5%	8.35	4,4
	10%	8.5	6,3
	20%	8.75	9,4

5.3. Mathematical modeling and simulation results

Numerical research includes two distinct analytical components. The first section encompasses the mathematical modeling conducted in MATLAB for three fundamental Stirling engine models. The second section includes a simulation of the ideal Stirling cycle performed in ASPEN-HYSYS. Both evaluations examine the impact of using a compound working fluid on power output and the efficiency of the Stirling engine. Different low-boiling liquids were put through a series of studies with varying concentrations in order to investigate the associated impacts.

5.3.1. Modeling results by MATLAB

The performance of the Gamma Stirling engine was investigated; this part presents the results of the numerical study for the ideal isothermal, ideal adiabatic, and actual adiabatic models, The study included an analysis of the engine performance in the case of a single and combined working fluid based on the engine parameters that are shown in (Table 4-2) and the mathematical modelling flowchart that is displayed in (Figure 5-23).

The analysis starts with initial conditions that are constant each time, and it continues in this manner until a cyclic steady state is obtained. The process starts with the crank angle being equal to zero and continues until the net value at the crank angle equal to 360° is attained. Therefore, the whole cycle is on the crank angle ranging from 0 to 2π, and the MATLAB program is responsible for coding and solving all the equations.

The Gamma engine operates under certain parameters, including a hot source temperature of 700 K, a cold sink temperature of 288 K, charge pressure of 1-3 bar, and nominal engine speed of 600 rpm.

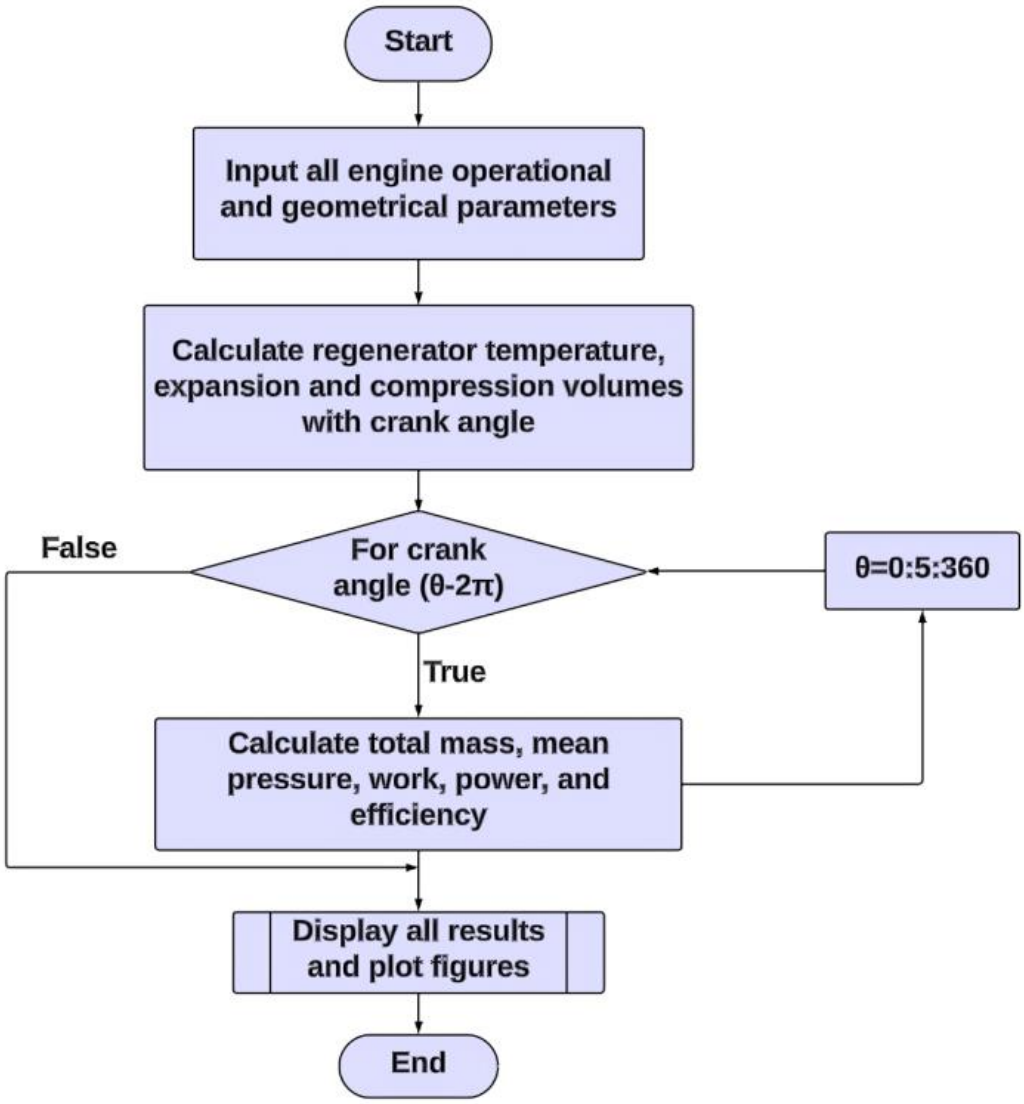

Figure 5-23: Mathematical modelling flowchart

5.3.1.1. Air as working fluid

The analysis starts by considering air as the only working fluid in the Stirling engine. The relation between pressure and total volume (P-V diagram) can be observed in (Figure 5-24). The entire work of the engine is obtained by integrating the area under the pressure-volume curve for one full cycle ($0 - 2\pi$). The engine net work is 0.87 J, with -0.6 J contributed by the compression region and 1.47 J by the expansion region, the output power is 8.7 W, the cycle efficiency is 58.8% and the

total mass of the air is 0.2 g. The P-V diagram provides a clear representation of the four distinct phases of the Stirling cycle: compression, heating, expansion, and cooling. Every step of the process corresponds to specific changes in pressure and volume, as the piston moves back and forth inside the engine chamber.

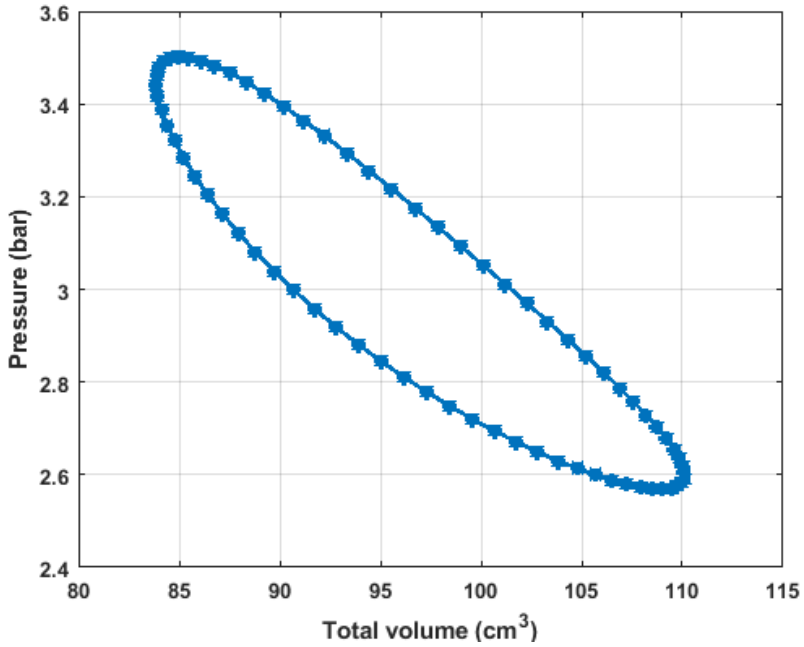

Figure 5-24: P-V diagram of the cycle when air is working fluid

The mean pressure fluctuates with the rotation of the crankshaft throughout the cycle. The initial pressure is 3 bar, the maximum pressure is 3.5 bar and the minimum pressure is 2.5 bar as shown in (Figure 5-25). The change in pressure is a result of temperature differences between the hot and cold sides. The Stirling engine is characterized by substantial fluctuations in sinusoidal volume during compression and expansion phases, which have a direct impact on all important parameters. During the cycle, variations in volume impact the rates of mass flow, heat transfer, pressure, work, and other related factors.

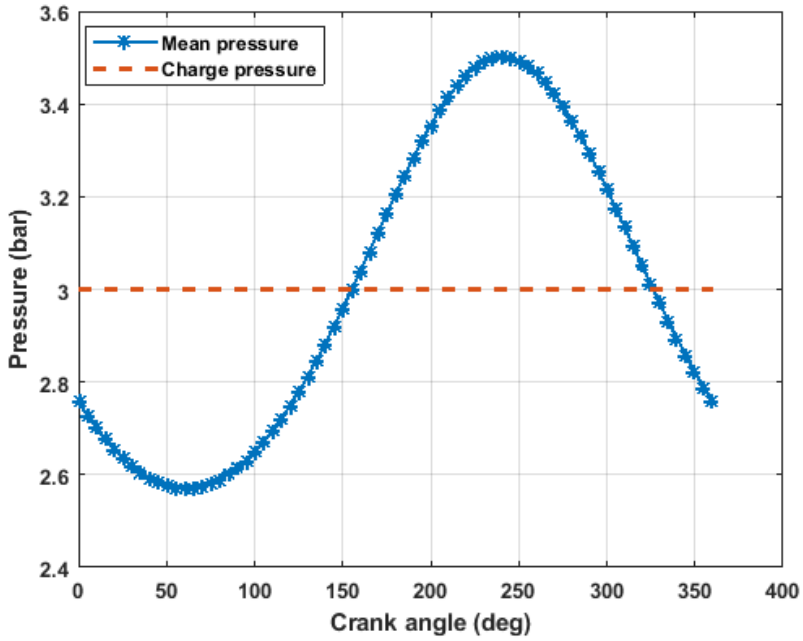

Figure 5-25: Pressure variation with crank angle

5.3.1.2. Air-acetone mixture

The air-acetone combination was used as the working fluid for the engine in this scenario. Four distinct acetone volume ratios (1%,5%, 10%, 20%) were examined to study their respective impacts on engine performance as shown in the P-V diagrams (Figures 5-26, 5-27, 5-28, 5-29). The utilization of air-acetone mixture as the operational substance in a Stirling engine might yield several consequences, dependent upon various factors such as the mixture's composition, engine configuration, and operational parameters.

Acetone has a lower boiling point relative to water, hence enhancing the efficiency of heat transfer in the heat exchangers of the engine. This may result in improved thermal performance and increased engine efficiency.

Also adding acetone into the air has the potential to enhance the power density of the engine since acetone has greater energy content per unit volume than pure air. This may lead to a simpler engine design or increased power output for a given size.

Furthermore, using an air-acetone combination offers greater flexibility in operational parameters, since acetone demonstrates efficient performance throughout a wider range of temperatures in comparison to water. This characteristic might be helpful in certain applications or settings. Acetone has greater environmental compatibility in comparison to some other organic compounds often used in Stirling engines. Due to its reduced toxicity and less environmental effect upon discharge, it is a more sustainable option.

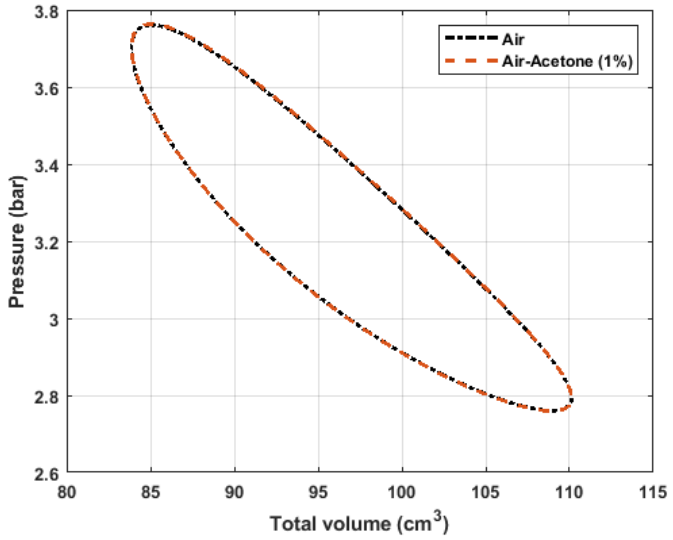

Figure 5-26: P-V diagram of air-acetone mixture (1%)

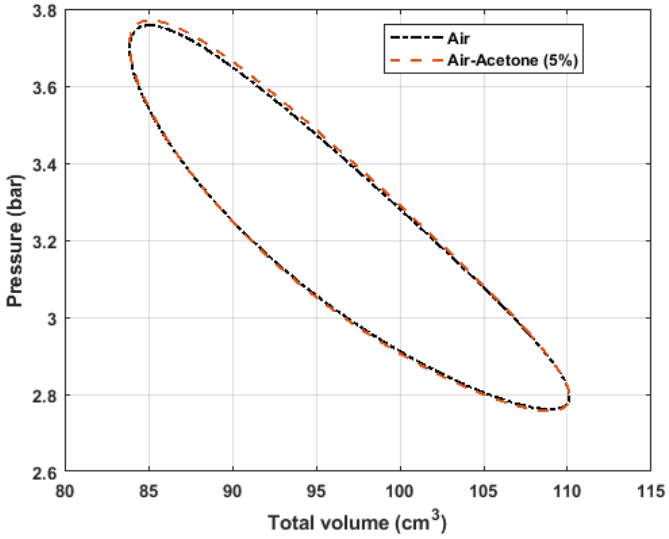

Figure 5-27: P-V diagram of air-acetone mixture (5%)

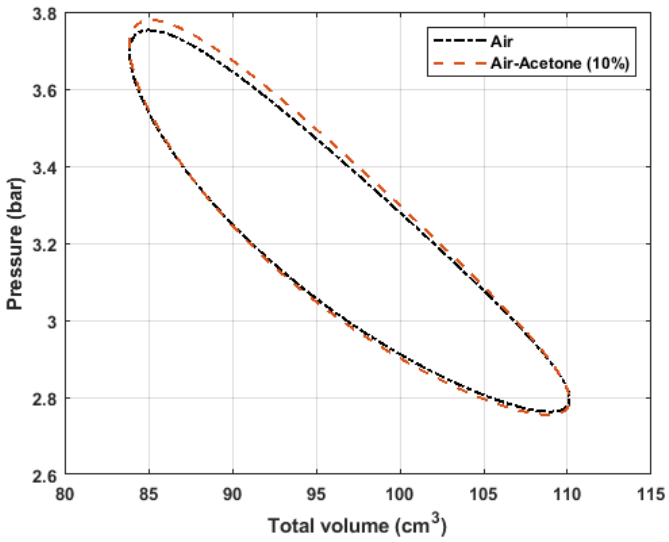

Figure 5-28: P-V diagram of air-acetone mixture (10%)

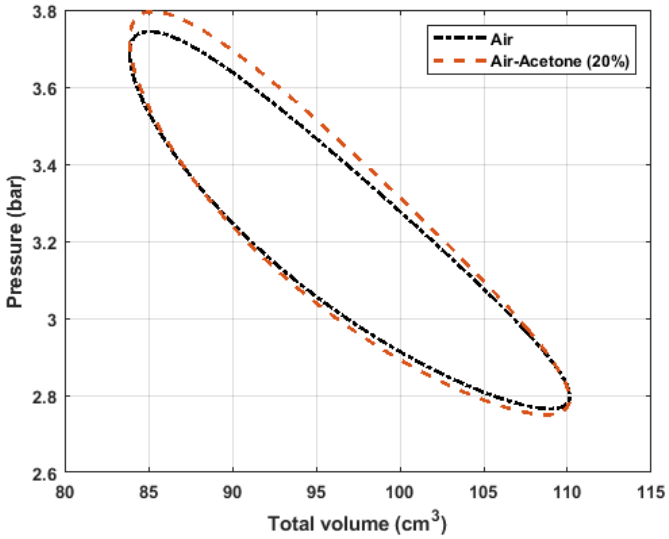

Figure 5-29: P-V diagram of air-acetone mixture (20%)

Figure (5-30) illustrates the impact of varying concentrations of acetone on work and power, which shows that by increasing the percentage of acetone, both work and power gradually increase. Acetone has a higher density of energy per unit volume in comparison to air alone. When combined with air, it enhances the total energy density of the working fluid. The increased energy content results in enhanced power generation during the engine operation. Additionally, acetone has enhanced thermal characteristics in comparison to air, including increased thermal

conductivity. Consequently, this leads to enhanced thermal conductivity inside the engine. Consequently, there is greater efficiency in harnessing heat input, resulting in a higher level of power output.

The effect of adding acetone on compression and expansion heat is shown in (Figure 5-31). Acetone often exhibits a lower specific heat capacity in comparison to air. This implies that it requires a lower amount of thermal energy to increase its temperature by a certain quantity. The introduction of acetone into air results in a reduction in the total specific heat capacity of the mixture. Consequently, a reduced amount of thermal energy is needed to compress the mixture during the compression stroke, resulting in a decrease in compression heat. Acetone has higher thermal conductivity compared to air. This can result in more efficient heat transfer within the mixture during compression and expansion strokes. While this may seem contradictory to the decrease in compression and expansion heat, it's essential to note that efficient heat transfer can lead to less heat being absorbed or released during the process. In compression stroke, less heat may be absorbed from the surroundings due to faster heat transfer, resulting in decreased compression heat. Similarly, during the expansion stroke, less heat may be released to the surroundings due to faster heat transfer, resulting in decreased expansion heat.

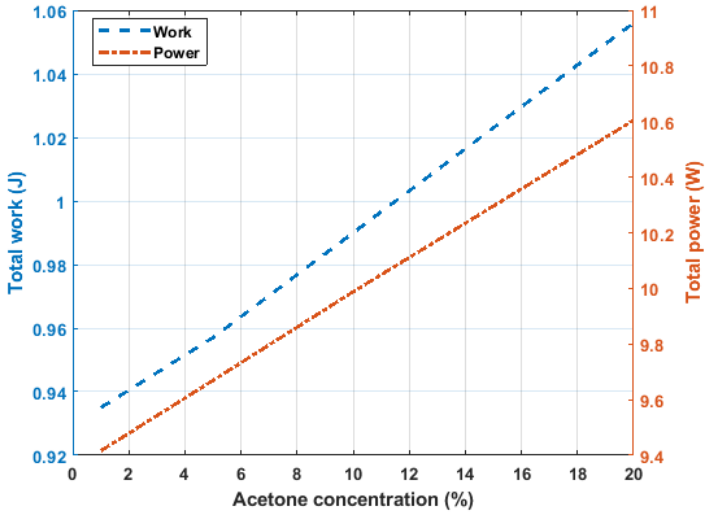

Figure 5-30: The effect of adding acetone on work and power

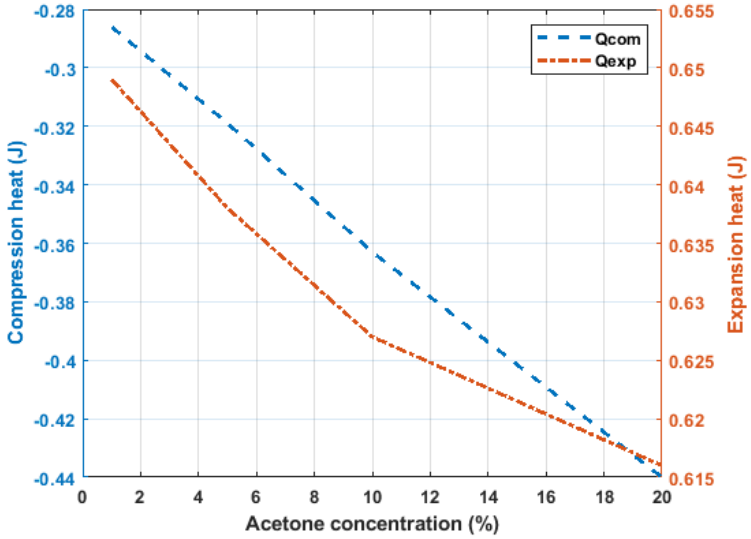

Figure 5-31: The effect of adding acetone on compression and expansion heat

5.3.1.3. Air-spirit mixture

The P-V diagrams of air-alcohol mixture are shown in Figures (5-32, 5-33, 5-34, 5-35) respectively, while Figures (5-36 and 5-37) show the effect of adding alcohol on work,power,compression and expansion heat.

Alcohol, such as ethanol or methanol, may enhance the combustion properties in comparison to air alone. This may lead to enhanced consumption of heat from the external heat source, resulting in a higher power output. Similar to an air-acetone mixture, using an air-spirit mixture may provide more flexibility in selecting operating conditions such as temperature and pressure. This can facilitate better optimization of engine performance according to specific application requirements.

In summary, using an air-spirit mixture as the working fluid in a Stirling engine can lead to various benefits, including improved combustion characteristics, higher energy density, enhanced heat transfer, increased power density, flexibility in operating conditions, and reduced environmental impact. However, it also presents challenges related to material compatibility, safety considerations, and engine design.

These factors should be carefully considered when implementing an air-alcohol mixture in Stirling engine applications.

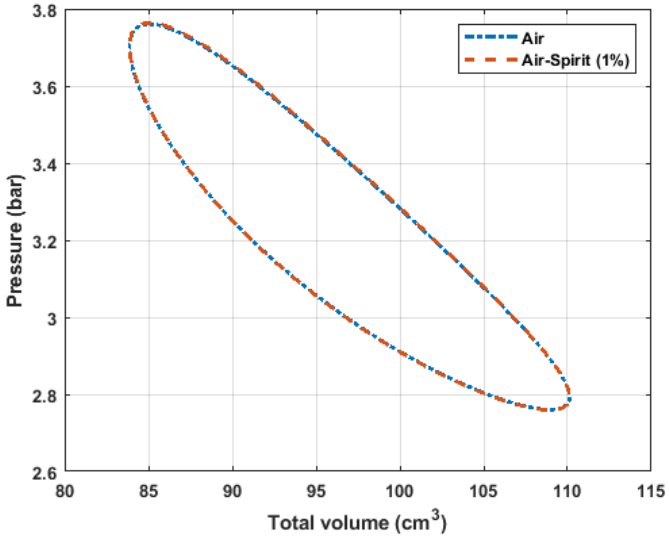

Figure 5-32: P-V diagram of air-spirit mixture (1%)

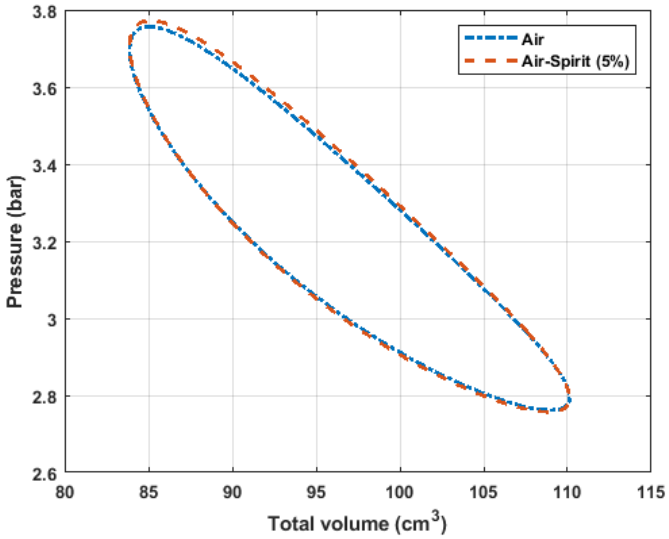

Figure 5-33: P-V diagram of air-spirit mixture (5%)

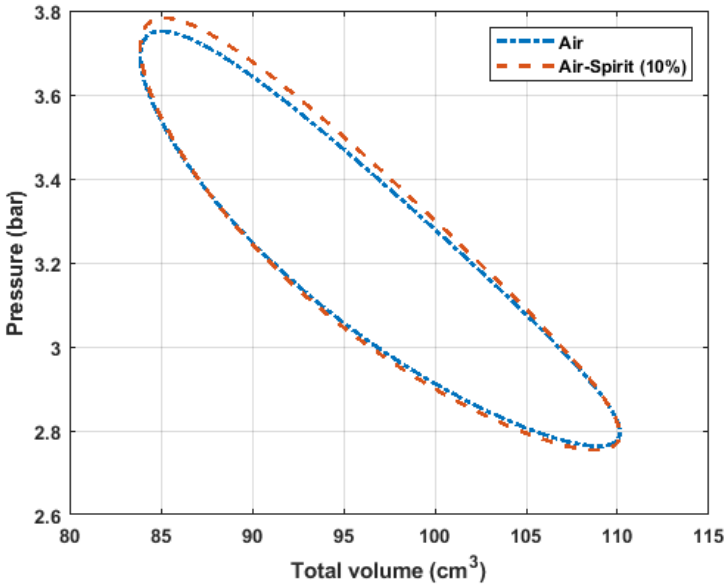

Figure 5-34: P-V diagram of air-spirit mixture (10%)

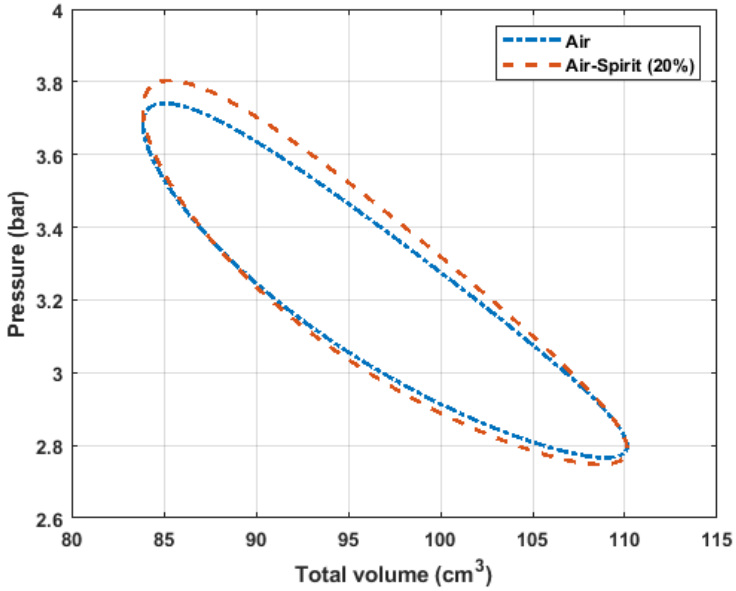

Figure 5-35: P-V diagram of air-spirit mixture (20%)

The combined effect of changes in compression and expansion heat, along with other factors determine heat transfer efficiency and combustion characteristics, ultimately determines the net work output of the Stirling engine.

While the addition of spirit may affect compression and expansion heat individually, the net work output depends on the overall efficiency of the engine thermodynamic cycle.

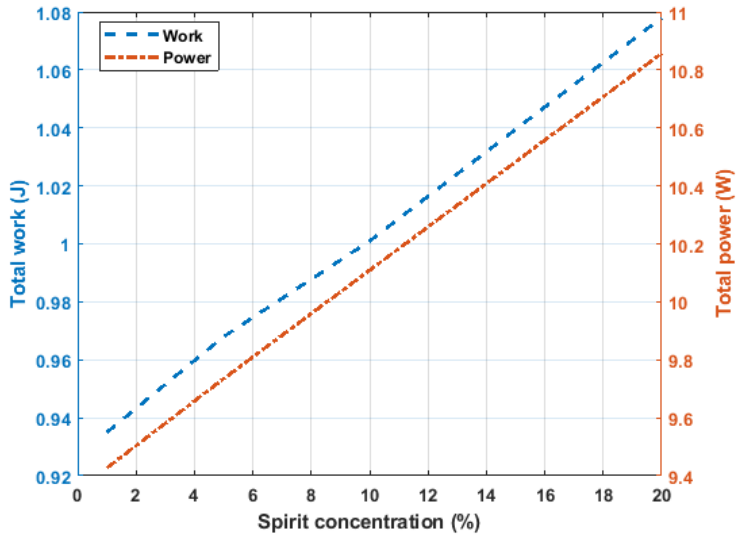

Figure 5-36: The effect of adding spirit on work and power

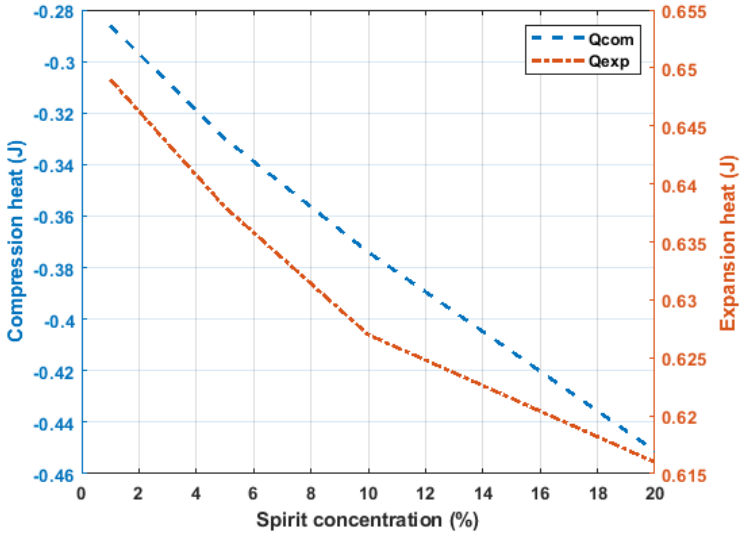

Figure 5-37: The effect of adding spirit on compression and expansion heat

Table 5-2: Results of working fluid mixtures

	Air	Acetone				Spirit			
		1%	5%	10%	20%	1%	5%	10%	20%
Qexp (J)	1.474	0.649	0.638	0.627	0.616	0.649	0.638	0.627	0.616
Qcom (J)	-0.605	-0.286	-0.319	-0.363	-0.440	-0.286	-0.33	-0.374	-0.462
Work (J)	0.869	0.935	0.957	0.99	1.056	0.935	0.968	1.001	1.078
Power (W)	8.712	9.416	9.669	9.988	10.6	9.427	9.735	10.11	10.86

5.3.1.4. Temperature distribution

In Stirling engine, the temperature distribution varies with the crank angle as the piston or displacer moves through its cycle. The temperature distribution changes due to the cyclic compression and expansion of the working fluid and the heat transfer processes within the engine.

The temperature distribution diagram in ideal adiabatic analysis in the compression and expansion area does not remain the same during the cycle; rather, it shifts and changes in response to the adiabatic compression and expansion that takes place in the workspaces as presented in (Figure 5-38). The cooler temperature is equal to the cold sink temperature (Tc=288 K) and the heater temperature is equal to the hot source temperature (Te=700 K) while the regenerator temperature is (Tr=463 K).

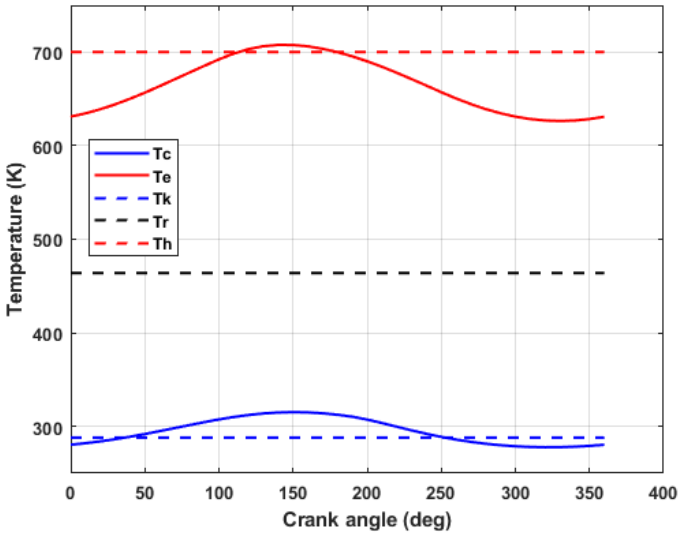

Figure 5-38: Temperature diagram in ideal adiabatic analysis

The temperature distribution in the engine in relation to the crank angle in non-ideal adiabatic analysis (Figure 5-39) shows that the temperature of the expansion and compression zones changes with crank angle throughout the cycle while the regenerator temperature stays constant. The heater wall temperature (Twh = 700 K) is greater than the engine working fluid temperature (Tgh = 677 K), but the cooler wall temperature (Twk= 288 K) is lower than the engine working fluid temperature (Tgk = 312 K).

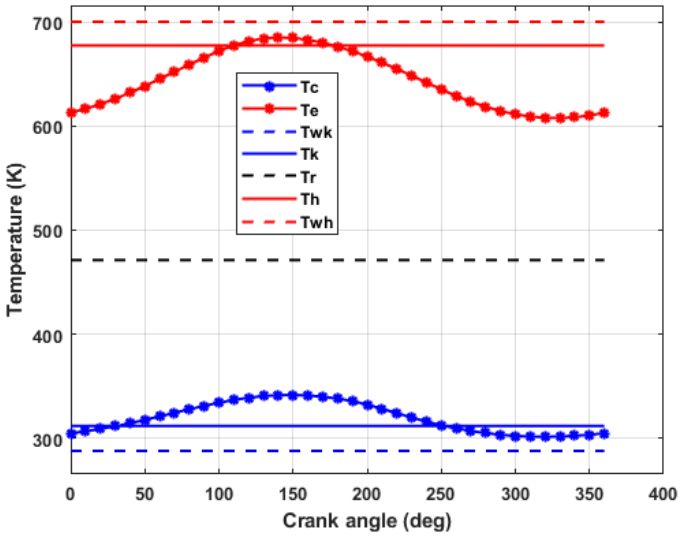

Figure 5-39: Temperature diagram in non-ideal adiabatic analysis

5.3.1.5. Effect of phase angle

The phase angle is a relative time between the movement of the pistons or displacers and the temperature differential throughout the engine. Performance of the engine is impacted by this timing. Figures (5-40, 5-41, 5-42, 5-43, 5-44, 5-45) illustrate how the amount of work and power varies regardless of the phase angle. The phase angle influences the pressure and volume changes within the engine working chambers. Optimal phase angles can maximize the pressure differentials between the hot and cold sides of the engine, resulting in increased mechanical work output. Efficient phase angle adjustment can enhance the engine overall efficiency. By synchronizing the movement of the pistons or displacers with the temperature gradients across the engine, the phase angle minimizes energy losses due to inefficient compression and expansion processes. Proper timing ensures that the engine effectively utilizes heat input to produce mechanical work while minimizing losses.

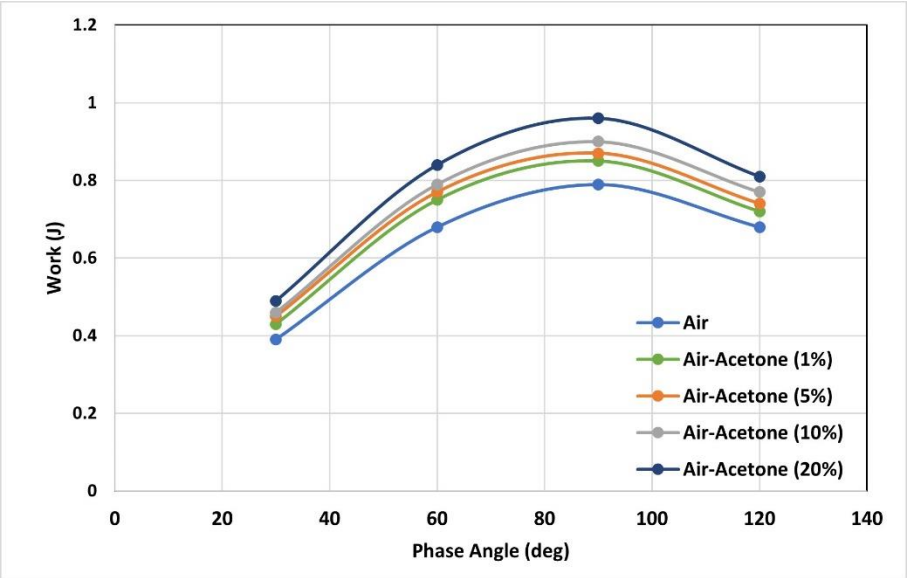

Figure 5-40: Work variation when add acetone with phase angle effect

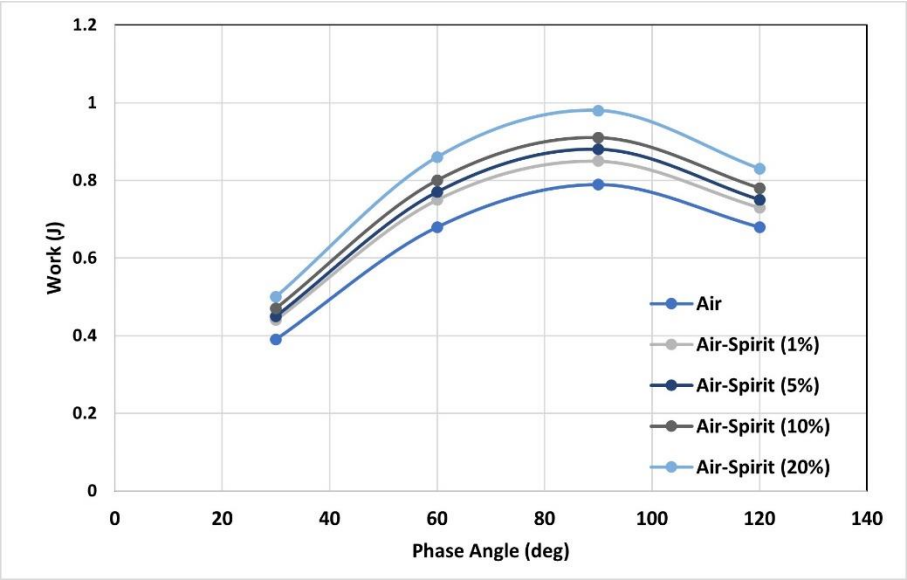

Figure 5-41: Work variation when add spirit with phase angle effect

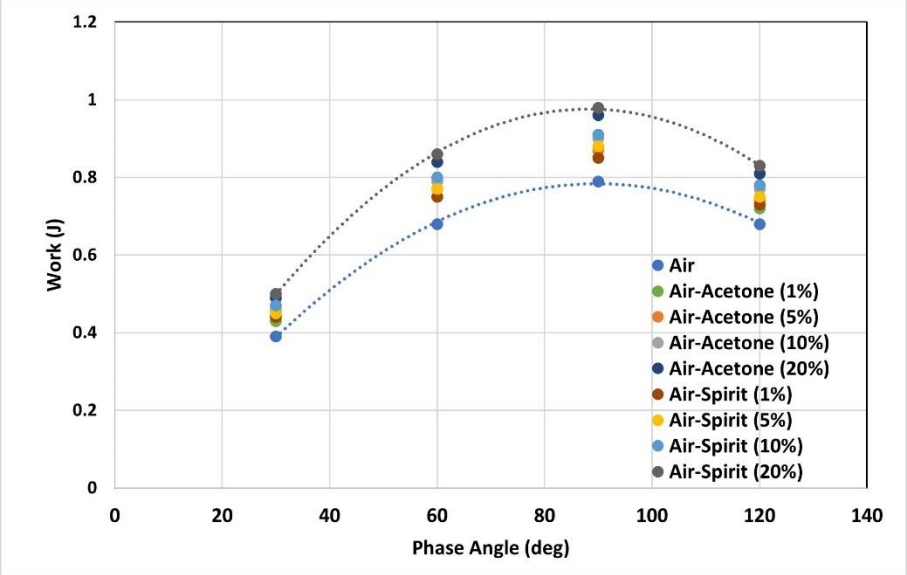

Figure 5-42: Work variation when add acetone and spirit into air with phase angle effect

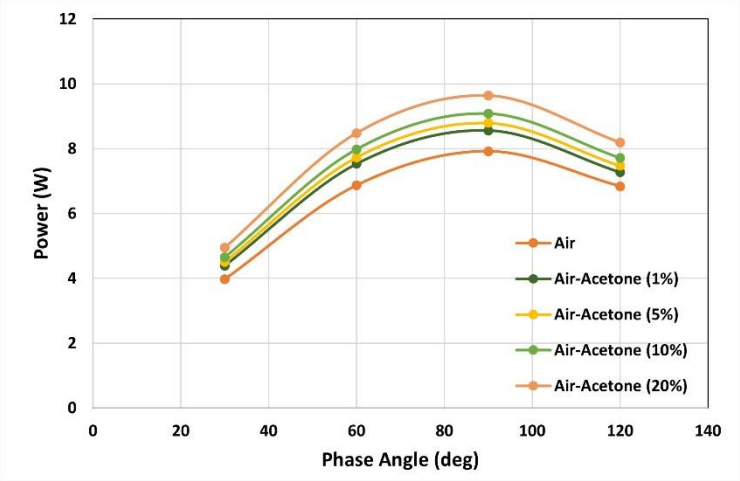

Figure 5-43: Power variation when add acetone with phase angle effect

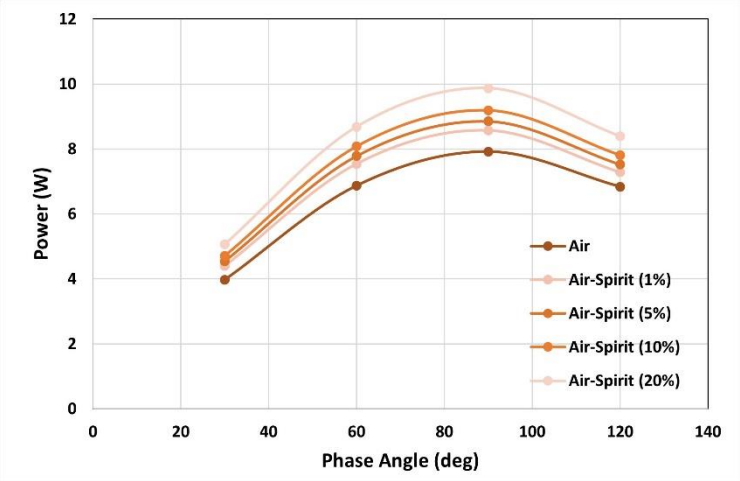

Figure 5-44: Power variation when add spirit with phase angle effect

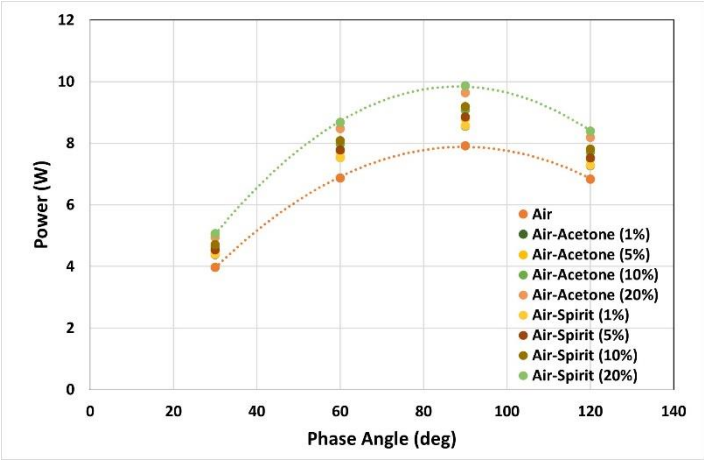

Figure 5-45: Power variation when add acetone and spirit into air with phase angle effect

As shown in the plots, the optimal phase angle is 90°, at this value the movement of the pistons or displacers is perfectly synchronized with the temperature difference between the hot and cold sides of the engine. This synchronization allows for optimal compression and expansion of the working fluid, maximizing the pressure difference between the hot and cold sides. As a result, this configuration maximizes the mechanical work output of the engine.

5.2.3. Simulation by ASPEN-HYSYS

This part includes modeling and simulating an ideal Stirling cycle using the ASPEN-HYSYS. Similarly, the effect of compound working fluid in Stirling engine was studied.

ASPEN-HYSYS is a powerful process simulation software developed by Aspen Technology. It is widely used in various industries, particularly in chemical engineering, petroleum refining, and other process industries. Aspen HYSYS allows engineers to model, simulate, and optimize processes, including chemical reactions, separations, heat exchange, and other unit operations.

The flowsheet of the Stirling cycle is shown in Figure (5-46) which consists of compression space, expansion space, cooler, and heater.

The simulation parameters are presented in Table (5-3). The working fluids (acetone, benzene, ethanol, and methanol) were tested in this simulation with mole fraction (1%, 5%, 10%, 20%) added to the air.

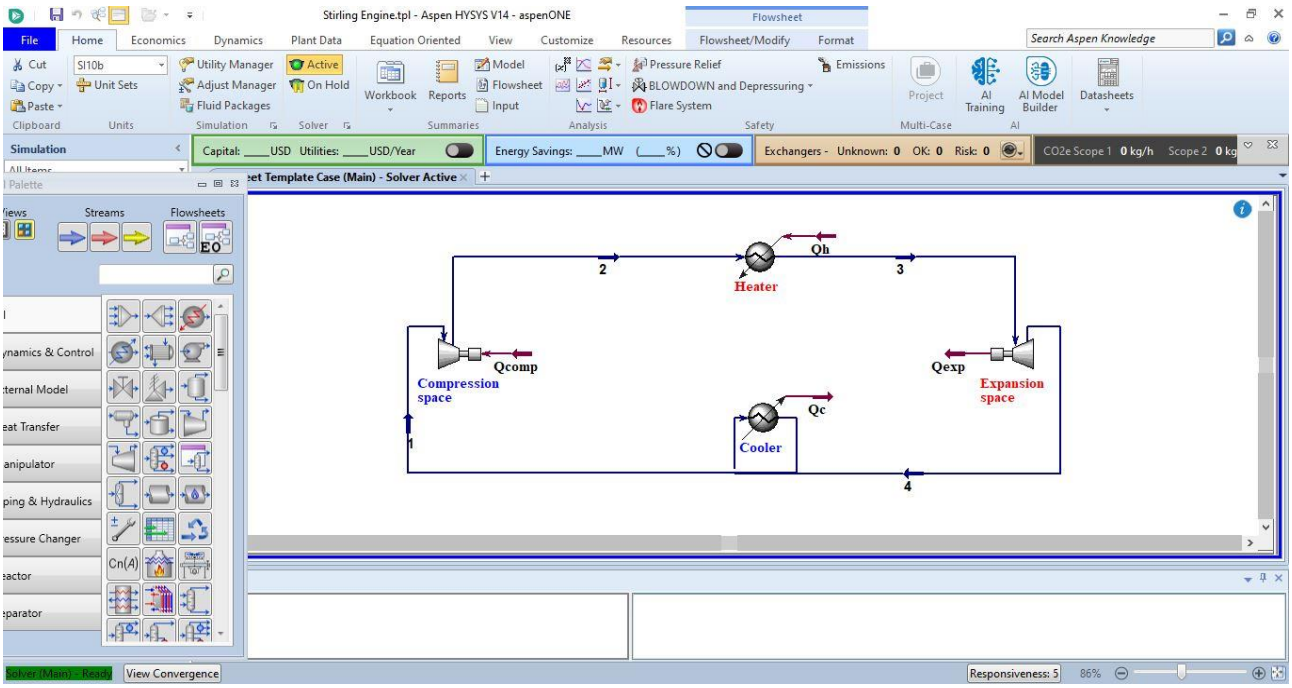

Figure 5-46: Main flowsheet of the Stirling cycle in ASPEN-HYSYS

Table 5-3: Simulation data

Parameter	Value
Pressure range	1-3 bar
Temperature range	288-700 K
Mole fraction	(1%, 5%, 10%, 20%)
Working fluids	air, acetone, benzene, ethanol, methanol, water

Figure (5-47) demonstrated the results of the first case obtained when use air only as working fluid. The consumed power is 38.15 W and heat flow 137.4 kJ/h while the generated power is 46.62 W and heat flow is 167.8 kJ/h then the net power is 8.47 W. In this analysis, we examine the energy flow and power characteristics of the compression space and expansion space within the Stirling engine model.

The compressor is responsible for increasing the pressure of the working fluid, while the expander decreases the pressure and generates mechanical work. The compressor receives low-pressure working fluid and compresses it to a higher

pressure. Energy is transferred to the fluid as mechanical work, increasing its enthalpy and temperature. The compressor consumes power to perform mechanical work on the working fluid. The power consumption of the compressor is calculated as the product of the compressor's power requirement and its efficiency. While the expander receives high-pressure working fluid and expands it to a lower pressure. Energy is extracted from the fluid as mechanical work, reducing its enthalpy and temperature. The expander generates power because of the expansion process. The power output of the expander is calculated based on the work done by the expanding fluid and the expander efficiency.

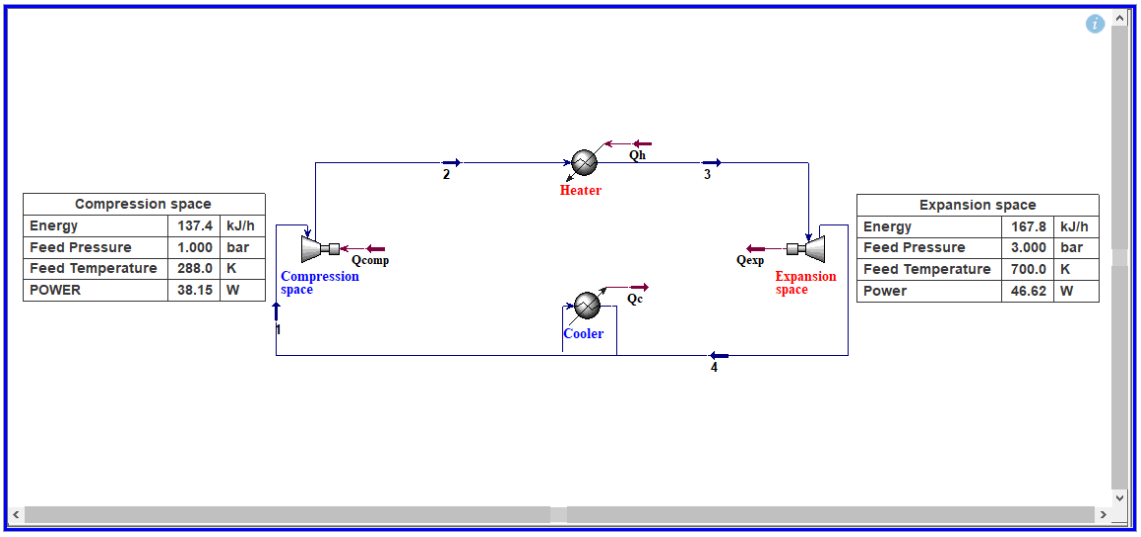

Figure 5-47: Stirling cycle output with air only

Figures (5-48, 5-49, 5-50, 5-51) confirmed the results obtained when use air-acetone mixture with four mole fractions as the working fluid. The power consumption is (38.11, 37.97, 37.8, 37.33) W, while the power generation is (46.70, 46.98, 47.24, 47.62) W. Therefore, the net power is (8.59, 9.01, 9.44, 10.29) W. The addition of acetone to air in a Stirling engine can lead to various thermodynamic advantages that contribute to increased power output. However, it's essential to carefully optimize the engine design and operating parameters to maximize the benefits of acetone addition and ensure efficient operation.

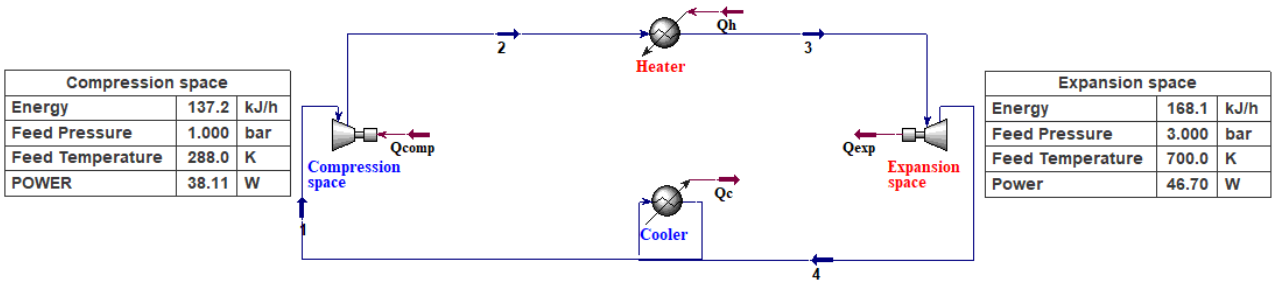

Compression space		
Energy	137.2	kJ/h
Feed Pressure	1.000	bar
Feed Temperature	288.0	K
POWER	38.11	W

Expansion space		
Energy	168.1	kJ/h
Feed Pressure	3.000	bar
Feed Temperature	700.0	K
Power	46.70	W

Figure 5-48: Stirling cycle output with air-acetone mixture (1%)

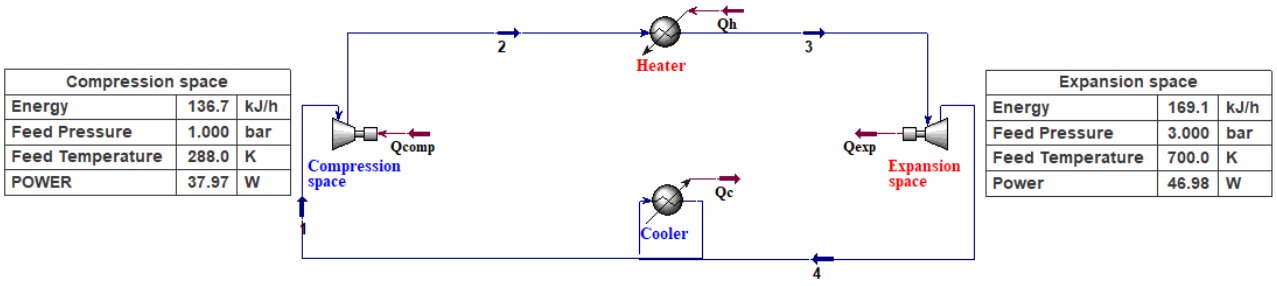

Compression space		
Energy	136.7	kJ/h
Feed Pressure	1.000	bar
Feed Temperature	288.0	K
POWER	37.97	W

Expansion space		
Energy	169.1	kJ/h
Feed Pressure	3.000	bar
Feed Temperature	700.0	K
Power	46.98	W

Figure 5-49: Stirling cycle output with air-acetone mixture (5%)

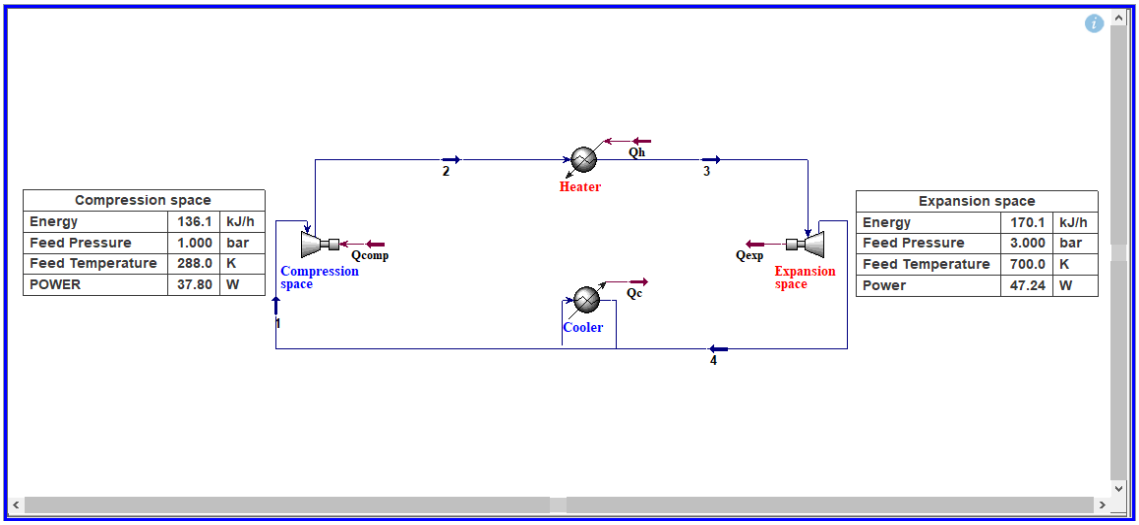

Compression space		
Energy	136.1	kJ/h
Feed Pressure	1.000	bar
Feed Temperature	288.0	K
POWER	37.80	W

Expansion space		
Energy	170.1	kJ/h
Feed Pressure	3.000	bar
Feed Temperature	700.0	K
Power	47.24	W

Figure 5-50: Stirling cycle output with air-acetone mixture (10%)

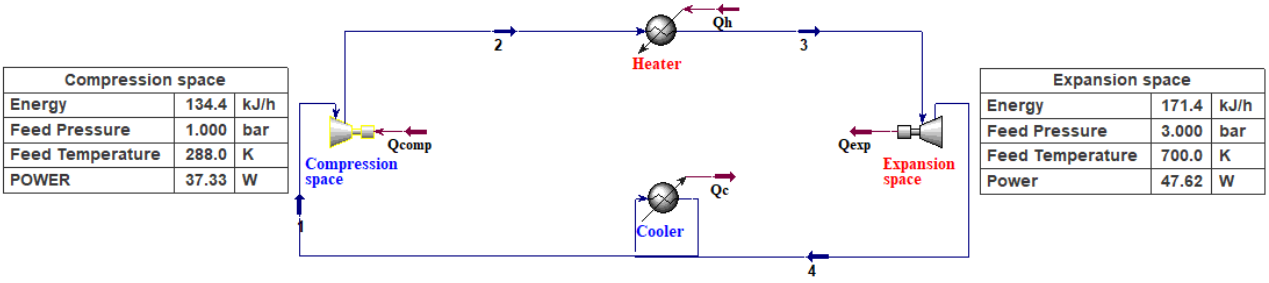

Figure 5-51: Stirling cycle output with air-acetone mixture (20%)

The third case is the air-benzene mixture as working fluid with the same mole fractions. The power in compression space is (38.11, 37.93, 36.15, 32.03) W and in expansion space is (46.73, 47.09, 47.41, 47.82) W, as shown in Figures (5-52, 5-53, 5-54, 5-55).

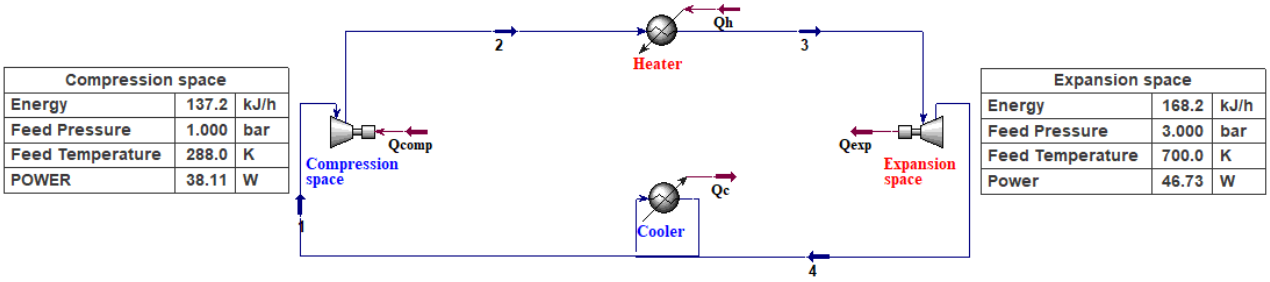

Figure 5-52: Stirling cycle output with air-benzene mixture (1%)

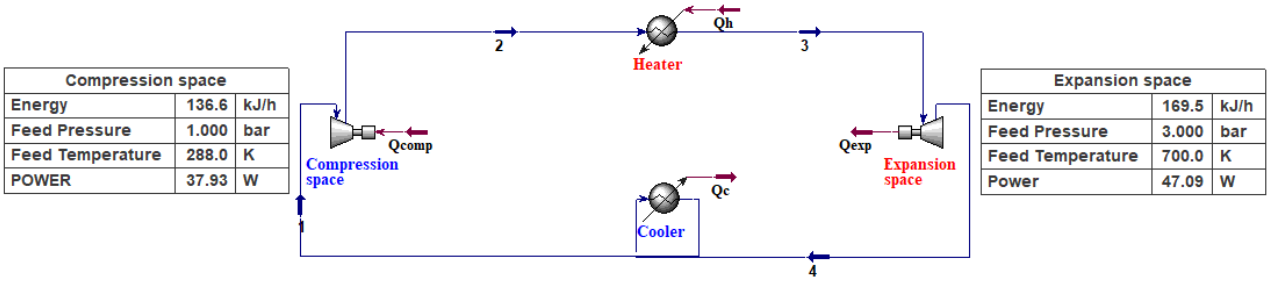

Figure 5-53: Stirling cycle output with air-benzene mixture (5%)

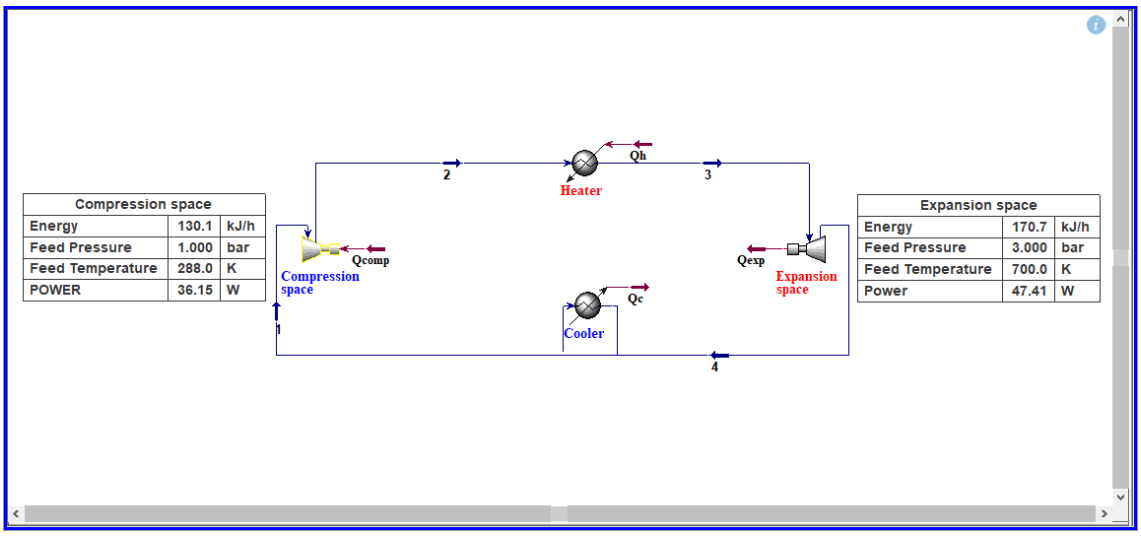

Figure 5-54: Stirling cycle output with air-benzene mixture (10%)

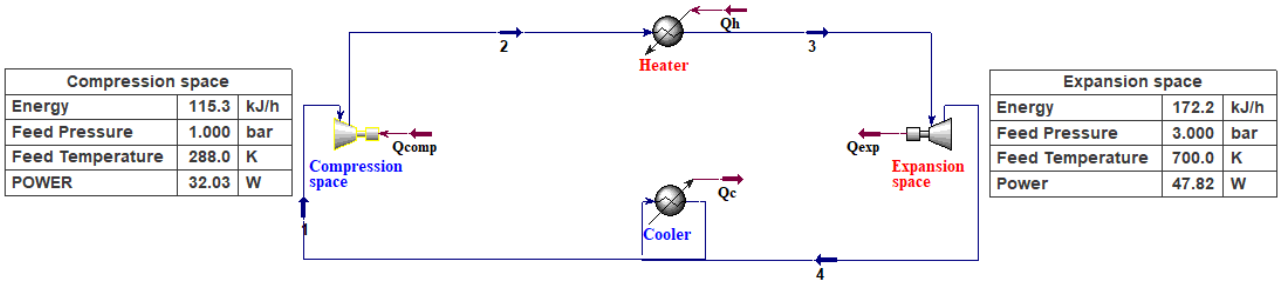

Figure 5-55: Stirling cycle output with air-benzene mixture (20%)

Ethanol and methanol, both organic molecules, are evaluated in this simulation since they belong to the category of alcohols. The results obtained are shown in Figures (5-56, 5-57, 5-58, 5-59) and Figures (5-60, 5-61, 5-62, 5-63). When compared to the power in expansion space, which is (46.69, 46.93, 47.17, 47.52) W, and the power in compression space is (38.12, 36.68, 34.57, 30.64) W. Additionally, when using a combination of air and ethanol as the working fluid, the total output power for this scenario is (8.57, 10.25, 12.6, 16.88) W.

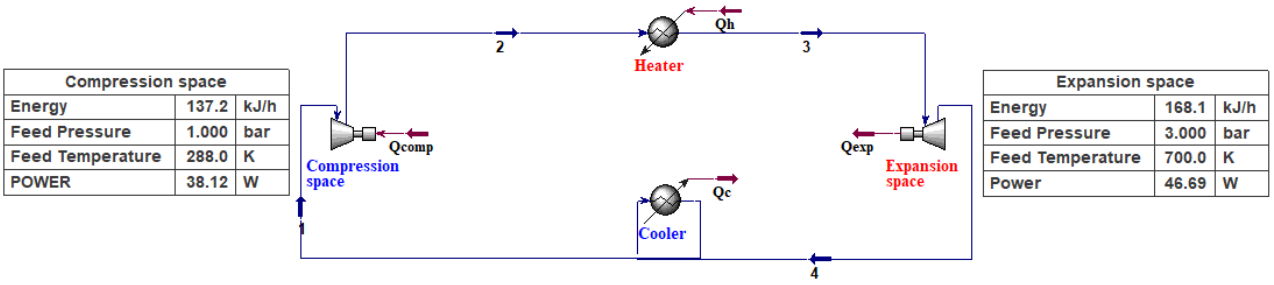

Compression space		
Energy	137.2	kJ/h
Feed Pressure	1.000	bar
Feed Temperature	288.0	K
POWER	38.12	W

Expansion space		
Energy	168.1	kJ/h
Feed Pressure	3.000	bar
Feed Temperature	700.0	K
Power	46.69	W

Figure 5-56: Stirling cycle output with air-ethanol mixture (1%)

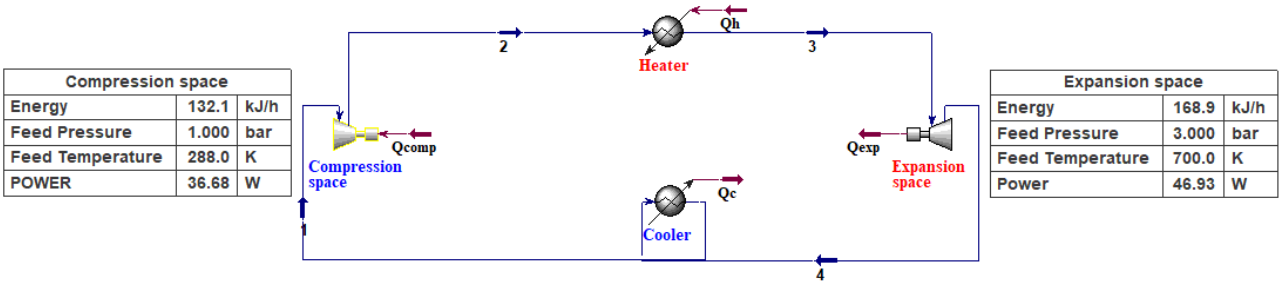

Compression space		
Energy	132.1	kJ/h
Feed Pressure	1.000	bar
Feed Temperature	288.0	K
POWER	36.68	W

Expansion space		
Energy	168.9	kJ/h
Feed Pressure	3.000	bar
Feed Temperature	700.0	K
Power	46.93	W

Figure 5-57: Stirling cycle output with air-ethanol mixture (5%)

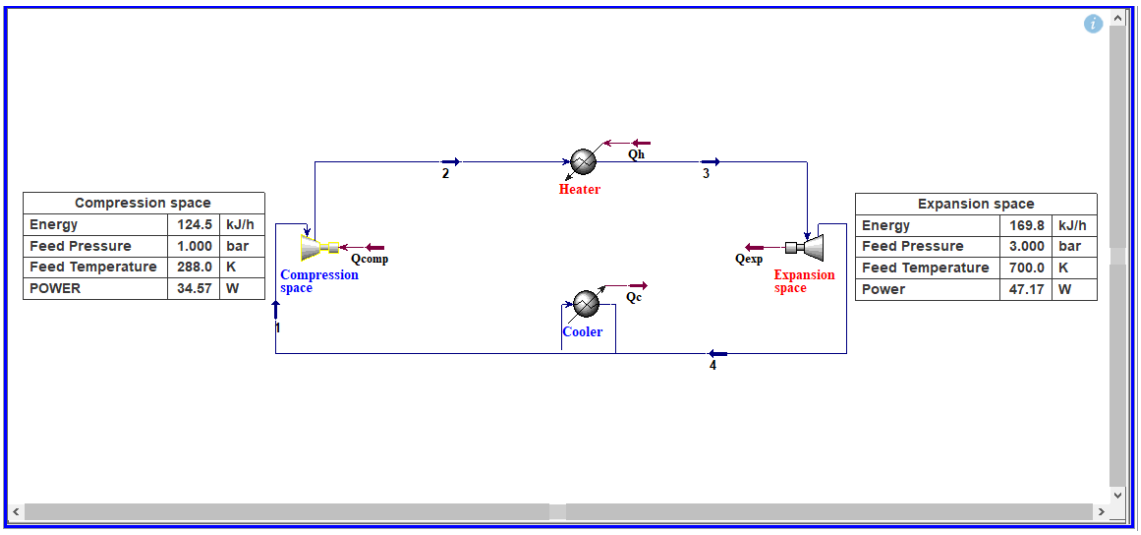

Compression space		
Energy	124.5	kJ/h
Feed Pressure	1.000	bar
Feed Temperature	288.0	K
POWER	34.57	W

Expansion space		
Energy	169.8	kJ/h
Feed Pressure	3.000	bar
Feed Temperature	700.0	K
Power	47.17	W

Figure 5-58: Stirling cycle output with air-ethanol mixture (10%)

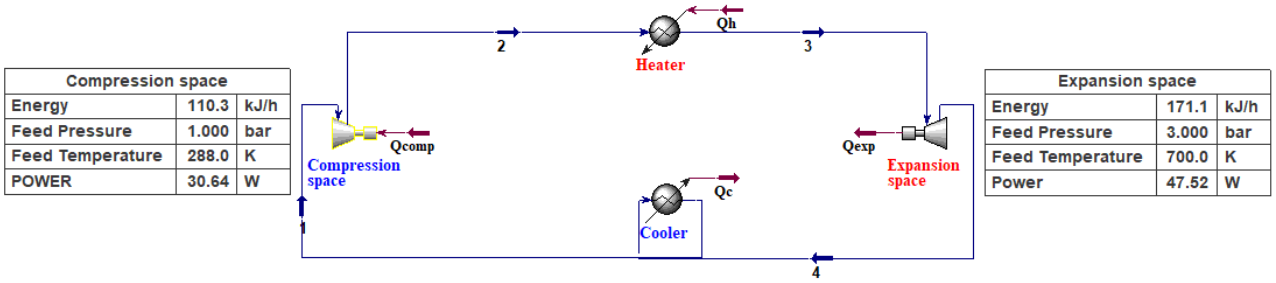

Figure 5-59: Stirling cycle output with air-ethanol mixture (20%)

When the working fluid is a mixture of air and methanol, the power in expansion space is (46.66, 46.78, 46.92, 47.14) W, while the power in compression space is (38.14, 38.07, 35.03, 31.05) W. This is because the expansion space is larger than the compression space. The overall output power for this scenario is (8.52, 8.71, 11.89, 16.09) W.

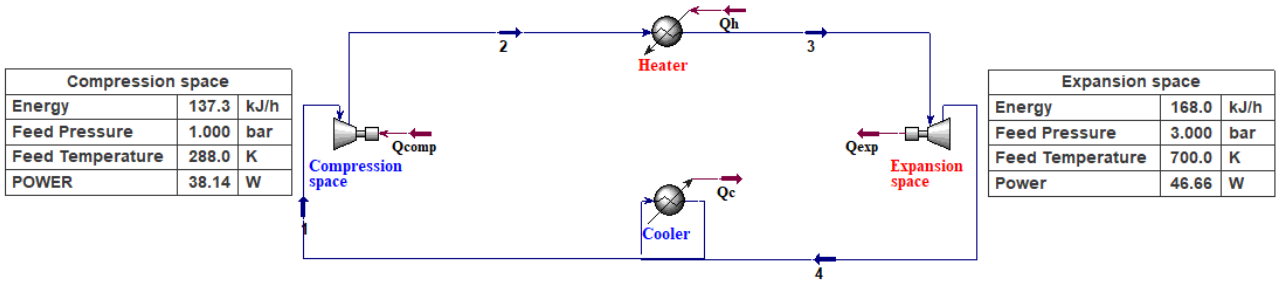

Figure 5-60: Stirling cycle output with air-methanol mixture (1%)

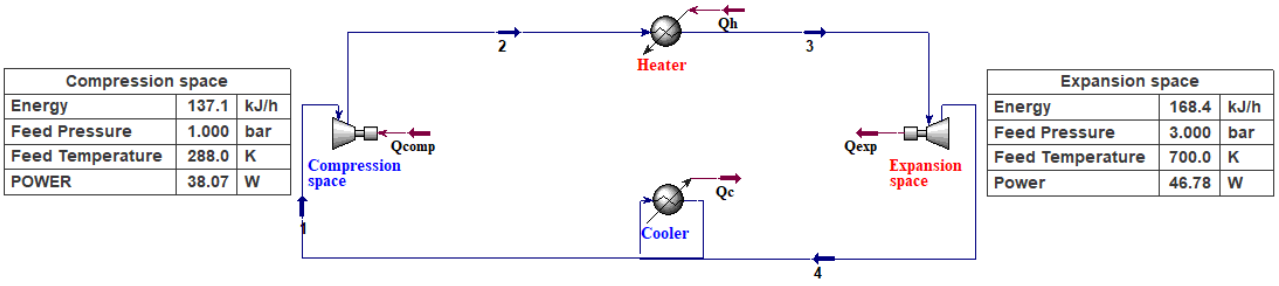

Figure 5-61: Stirling cycle output with air-methanol mixture (5%)

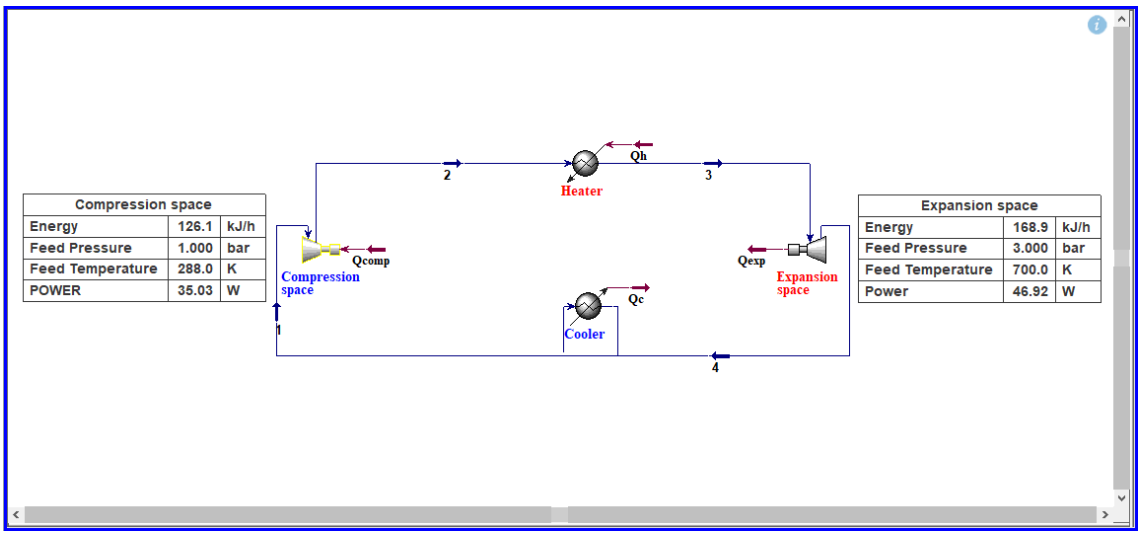

Figure 5-62: Stirling cycle output with air-methanol mixture (10%)

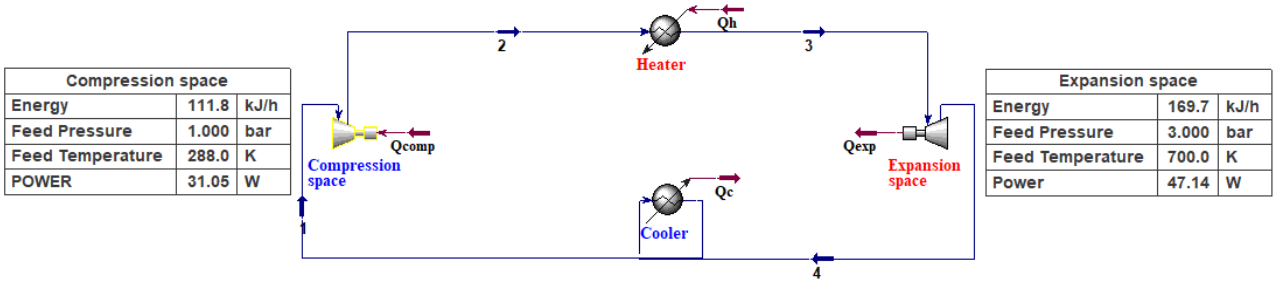

Figure 5-63: Stirling cycle output with air-methanol mixture (20%)

In this simulation, we investigate the influence of various working fluid compositions on the performance of Stirling engine. Five distinct cases are examined, each utilizing a different working fluid mixture: air only, air-acetone, air-benzene, air-ethanol, and air-methanol. Through comparative analysis, we aim to assess how the addition of different substances to air affects engine efficiency, power output, and overall performance.

In the first case, the Stirling engine operates using air as the only working fluid. In the second case, acetone is added to the air to assess its effect on engine performance. Acetone, with its favorable thermodynamic properties, is introduced to

enhance heat transfer within the engine. We examine how the inclusion of acetone alters power output compared to the air-only case.

The third case explores the utilization of a working fluid composed of air and benzene. Benzene, a non-polar aromatic hydrocarbon, is chosen for its high energy density and combustion properties. By incorporating benzene into the air mixture, we investigate its potential to enhance engine performance, particularly in terms of power output.

In the fourth case, ethanol is introduced into the air mixture to diversify the working fluid composition. Ethanol, a renewable biofuel, offers clean-burning properties and high-octane rating, making it a promising candidate for improving combustion efficiency and emissions reduction. We analyze how the addition of ethanol influences engine performance and thermal characteristics compared to the air-only case.

The fifth case examines the utilization of working fluid mixture comprising air and methanol. Methanol, another alcohol compound, is selected for its high energy content and combustion properties. Finally, the results obtained from this simulation are presented in Table (5-4).

Table 5-4: Numerical simulation results

Working fluid	**Mole fraction**	**Net power (W)**	**Total heat flow (kJ/h)**
Air	100%	8.47	30.4
Air-acetone mixture	1%	8.59	30.9
	5%	9.01	32.04
	10%	9.44	34
	20%	10.29	37
Air-benzene mixture	1%	8.62	31

	5%	9.16	32.9
	10%	11.26	40.6
	20%	15.79	56.9
Air-ethanol mixture	1%	8.57	30.9
	5%	10.25	36.8
	10%	12.6	45.3
	20%	16.88	60.8
Air-methanol mixture	1%	8.52	30.7
	5%	8.71	31.3
	10%	11.89	42.8
	20%	16.09	57.9
Air-water mixture	1%	8.48	30.6
	5%	10.76	38.7
	10%	12.72	45.8
	20%	16.63	59.8

5.4. Validation of mechanical power and electrical power

In Stirling engine, mechanical power is generated through the cyclic compression and expansion of working fluid, which drives piston or displacer. This mechanical power can be harnessed directly for various applications such as pumping water, driving machinery, or generating electricity.

On the other hand, electrical power generation in Stirling engines involves converting the mechanical power into electrical power through a generator or alternator. This process typically involves coupling the engine mechanical output to generator shaft, where the rotational motion is converted into electrical energy through electromagnetic induction.

This experiment aims to measure the electric power output generated by the gamma Stirling engine when coupled with miniature generator, in this case the air is the only working fluid. The setup involves connecting a voltmeter to the output terminals of the generator and placing a load resistor across them. The procedure includes starting the engine, recording voltage and current readings for varying electrical loads, and analyzing the data to calculate electric power output as shown in Figure (5-64).

Figure 5-64: Measurement setup of electrical power output

Figure (5-65) and table (5-5) show the mechanical and electrical power output of the gamma Stirling engine as a function of rotational speed. It demonstrates a direct proportionality between rotation speed and power, showcasing how increasing rotation speed typically leads to higher power output.

The results also highlight the engine optimal operating range and identifies the point of peak power output (7.92 and 6.97 W at 540 rpm), indicating the rotation speed at which the engine generates the maximum amount of power crucial for determining optimal operating conditions. Essentially, while higher rotation speeds

may initially result in more power generation, there are constraints and limitations to consider, such as thermal efficiency, mechanical restrictions, ideal operating conditions, and load dependence.

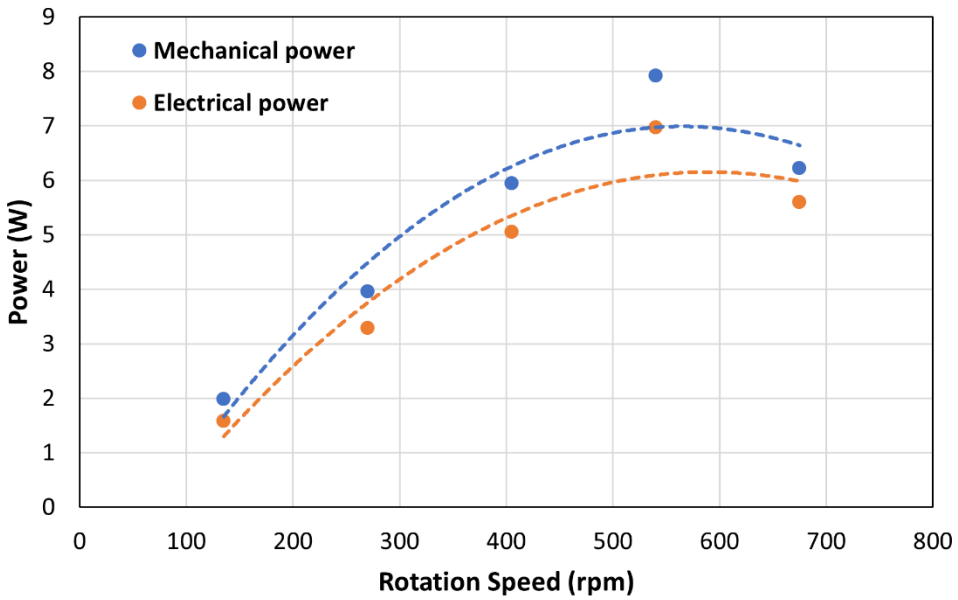

Figure 5-65: Mechanical and electrical power output of the gamma Stirling engine

Table (5-5): Results of electrical power output of the gamma Stirling engine

Rotation speed (rpm)	Mechanical power (W)	Electrical power (W)
135	1.98	1.58
270	3.96	3.29
405	5.94	5.05
540	7.92	6.97
675	6.22	5.60

Conclusions

This thesis studied the performance of gamma Stirling Engine using compound working fluid of air, air-acetone, air-spirit, and air-water through experimental and theoretical methods. The experimental phase involved constructing a prototype engine and conducting experiments to assess its performance in various operating conditions. The studies yielded useful data on the engine thermal efficiency, power output, and operational characteristics under various compositions of the working fluid.

The study theoretical part focused on creating mathematical models to replicate the Stirling engine performance with the compound working fluid. The models utilized thermodynamic principles, heat transfer mechanisms, and fluid dynamics to predict the engine performance and behavior. The experimental data were compared to theoretical predictions, showing a satisfactory agreement that confirmed the accuracy of the established models.

By analyzing both experimental data and theoretical simulations, several important discoveries have been made. The selection of working fluid has a substantial impact on the engine performance. The addition of acetone and ethanol to the working fluid improved thermal performance compared to using only air due to the better heat transfer characteristics and higher specific heat capacity of the compound mixture.

The testing results showed that it is crucial to adjust and optimize operational parameters including pressure, temperature, and rotation speed to enhance engine performance. Changes in these parameters resulted in notable alterations in the engine efficiency and power output, underscoring the importance of accurate management and modification during operation.

The theoretical models offered insights into the thermodynamic processes happening within the Stirling engine, helping to understand its activities and performance. Simulations were used to conduct sensitivity analysis, which helped

identify crucial elements influencing the engine work. This information can guide future design enhancements and optimization efforts.

The discoveries in this thesis expand Stirling engine technology by investigating the use of compound working fluids to improve performance. An in-depth examination of experimental and theoretical data highlights the significance of exploring different working fluid compositions for Stirling engines in sustainable energy production and thermal management.

In conclusion, we may summarize the main scientific and practical results as follows:

1. Based on an analysis of published works on the research and analysis of the thermodynamic and energy efficiency of Stirling engines in order to identify specific parameters that help improve its efficiency
2. For the first time, the possibility of using a complex working fluid consisting of a working gas with the addition of low-boiling liquids has been studied, allowing the use of elements of the Stirling (gas) and Rankine (steam) cycles in one technology.
3. Experimental studies were carried out on the effect of adding acetone, ethanol and water with concentrations from 1 to 20% volume into the composition of the working fluid in the working cylinder of the Stirling engine.
4. Addition of acetone in volume fractions of 1%, 5%, 10% and 20% resulted in an increase in power of 6.3%, 12.5%, 19%, and 25%, respectively. Adding alcohol resulted in power increases of 2.5%, 6.5%, 13%, and 19%. Adding water resulted in power increases of 2.5%, 4.4%, 6.3%, and 9.4%, respectively. Experimental data showed an increase in power output, especially significant when using low-boiling liquids.
5. A mathematical model has been developed for calculating the thermodynamic and energy efficiency of a Stirling engine with a complex working fluid in MATLAB software. Validation of the model showed satisfactory agreement

of the results with the experimental data, which makes it possible to further search for new compositions of working fluids without lengthy full-scale experiments.

6. A methodology has been developed for modeling thermodynamic and energy efficiency with complex working fluids using the ASPEN-HYSYS program code, which has shown satisfactory compliance with experimental and simulation data in MATLAB, which opens up prospects for a convenient preliminary analysis of the working fluids of a Stirling engine, consisting of multicomponent (more than 2) components.
7. A study was also conducted to test the mechanical and electrical power of a Gamma Stirling engine coupled with a miniature generator. In this case, the working fluid was air. The results show that power is directly related to rotation speed. additionally determine the optimal engine operating range and maximum power point (7.92 and 6.97 W at 540 rpm).
8. Directions for further research are suggested to improve modeling methods, optimize operating parameters and explore the possibilities of low-boiling liquids and other innovative working fluids for the development of Stirling engine technology.

Recommendations for the use of Research Materials:

Promoting and utilizing Stirling engines in Iraq can be beneficial due to their efficiency, reliability, and ability to operate using various heat sources, including solar energy, which Iraq has in abundance. Here are some steps to recommend and use Stirling engines effectively:

1. Solar Power Generation: Iraq experiences abundant sunlight throughout the year, making solar power a viable energy source. Stirling engines can be integrated with solar concentrators or parabolic dishes to efficiently convert solar heat into mechanical energy. This setup is particularly useful in remote or off-grid areas where access to conventional electricity grids is limited.

2. Heat Pumping and Refrigeration: Stirling engines can be employed in solar-driven heat pumps for residential or commercial cooling applications. In regions with high temperatures like Iraq, where cooling demands are significant, Stirling engines can efficiently operate heat pumps for air conditioning or refrigeration purposes. This reduces dependency on fossil fuels and lowers greenhouse gas emissions.
3. Water Pumping and Irrigation: Agriculture is a vital sector in Iraq, heavily dependent on irrigation. Stirling engines can power water pumps using solar thermal energy or biomass sources, ensuring reliable water supply for agricultural activities. This approach supports sustainable farming practices and mitigates the impact of water scarcity.

Considering Iraq's climatic conditions, the adoption of Stirling engines can leverage abundant solar energy resources while addressing energy security and sustainability goals. Strategic deployment in key sectors such as agriculture, industry, and rural electrification can maximize the socio-economic benefits of this technology, contributing to Iraq's overall development objectives.

NOMENCLATURE

Symbol	Description	Units
T	Temperature	K
p	Pressure	bar
V	Volume	m^3
Q	Heat	J
W	Work	J
M	Mass	kg
S	Entropy	J/K
R	Gas constant	J/kg
Cv	Heat capacity of gas at constant volume	J/kg.K
Cp	Heat capacity of gas at constant pressure	J/kg.K
Rt	Temperature ratio	
Rs	Swept volume ratio	
Rde	Expansion dead volume ratio	
Rdc	Compression dead volume ratio	
Rr	Regenerator dead volume ratio	
Ve	Expansion space volume	m^3
Vc	Compression space volume	m^3
Vse	Expansion swept volume	m^3
Vsc	Compression swept volume	m^3

Vde	Expansion dead volume	m^3
Vdc	Compression dead volume	m^3
Vb	Overlap volume	m^3
s,b	Constants	
pmean	Mean pressure	kPa
P	Power	W
N	Rotation speed	rpm
t	torque	N.m
NTU	Number of thermal units	
ST	Stanton number	
Awg	Internal wetted area	m^2
A	Area of internal free flow	m^2
h	Convection heat transfer coefficient	$W/m^2.K$
u	Velocity	m^2/s
Re	Reynolds number	
Pr	Prandtl number	
Bn	Beale number	
E	Regenerator effectiveness	
Qrloss	Regenerative enthalpy loss	J
Qcrloss	heat transfer loss between heater and cooler	J
freq	Frequency	Hz

K	Thermal conductivity	W/m.K
L	Heat exchanger length	mm
Twh	Heater wall temperature	K
Twk	Cooler wall temperature	K
f	Friction factor	
d	Hydraulic diameter	m
Qah	Heater actual heat input	J
Qak	Cooler actual heat output	J
Δp	Pressure drops	Pa
fD	Darcy friction factor	
Greek symbols		
η	Thermal efficiency	%
γ	Specific heat ratio	
α	Phase angle	deg
θ	Crank angle	deg
μ	Dynamic viscosity	kg/m.s
ρ	Density	kg/m³
βv	Coefficient of volumetric expansion	
β	Pressure phase angle	deg
Subscripts		
e	Expansion space	

c	Compression space	
k	Cooler heat exchanger	
h	Heater heat exchanger	
r	Regenerator	
he	Heater- expansion space interfaces	
ck	Compression space-cooler interfaces	
kr	Cooler – regenerator interfaces	
rh	Regenerator-heater interfaces	
g	Working gas	

REFERENCES

[1] "http://www.bekkoame.ne.jp/~khirata/english/history1.htm".

[2] "https://datahorizzonresearch.com/stirling-engine-generator-market-2361."

[3] S. Zhu, G. Yu, K. Liang, W. Dai, and E. Luo, "A review of Stirling-engine-based combined heat and power technology," Appl Energy, vol. 294, Jul. 2021, doi: 10.1016/j.apenergy.2021.116965.

[4] D. Menniti, N. Sorrentino, A. Pinnarelli, A. Burgio, G. Brusco, and G. Belli, "The concentrated solar power system with Stirling technology in a micro-grid: The simulation model," in 2014 International Symposium on Power Electronics, Electrical Drives, Automation and Motion, SPEEDAM 2014, IEEE Computer Society, 2014, pp. 253–260. doi: 10.1109/SPEEDAM.2014.6872095.

[5] G. Moonka, H. Surana, and H. R. Singh, “Study on some aspects of Stirling engine: A path to solar Stirling engines,” Mater Today Proc, vol. 63, pp. 737–744, Jan. 2022, doi: 10.1016/j.matpr.2022.05.107.

[6] L. Zhang, K. Han, Y. Wang, Y. Zhu, S. Zhong, and G. Zhong, “A bibliometric analysis of Stirling engine and in-depth review of its application for energy supply systems,” Energy Reviews, vol. 2, no. 4, p. 100048, Dec. 2023, doi: 10.1016/j.enrev.2023.100048.

[7] A. S. Nielsen, B. T. York, and B. D. MacDonald, “Stirling engine regenerators: How to attain over 95% regenerator effectiveness with sub-regenerators and thermal mass ratios,” Appl Energy, vol. 253, Nov. 2019, doi: 10.1016/j.apenergy.2019.113557.

[8] M. Gupta and V. Pundhir, “Solar Stirling Plant,” 2014. [Online]. Available: https://www.researchgate.net/publication/292139327

[9] M. Abbas, B. Boumeddane, N. Said, and A. Chikouche, “Dish Stirling technology: A 100 MW solar power plant using hydrogen for Algeria,” Int J Hydrogen Energy, vol. 36, no. 7, pp. 4305–4314, Apr. 2011, doi: 10.1016/j.ijhydene.2010.12.114.

[10] F. Sohail et al., “Design and Control of Generated Electricity Using Solar Powered Stirling Engine,” in Proceedings - 2020 23rd IEEE International Multi-Topic Conference, INMIC 2020, Institute of Electrical and Electronics Engineers Inc., Nov. 2020. doi: 10.1109/INMIC50486.2020.9318143.

[11] A. Boretti, “α-Stirling hydrogen engines for concentrated solar power,” International Journal of Hydrogen Energy, vol. 46, no. 29. Elsevier Ltd, pp. 16241–16247, Apr. 26, 2021. doi: 10.1016/j.ijhydene.2021.02.036.

[12] R. F. Costa and B. D. MacDonald, “Comparison of the net work output between Stirling and Ericsson cycles,” Energies (Basel), vol. 11, no. 3, Feb. 2018, doi: 10.3390/en11030670.

[13] A. O. Nayak, B. C. Fabien, J. C. Kramlich, and I. Novosselov, “Holistic Modeling, Design & Analysis of Integrated Stirling and Auxiliary Clean Energy Systems for Combined Heat and Power Applications,” 2015. Accessed: Dec. 03, 2023. [Online]. Available: http://hdl.handle.net/1773/34030

[14] F. Martins, C. Felgueiras, M. Smitkova, and N. Caetano, “Analysis of fossil fuel energy consumption and environmental impacts in european countries,” Energies (Basel), vol. 12, no. 6, 2019, doi: 10.3390/en12060964.

[15] X. Yu, C. She, F. Gholizadeh, and Y. P. Xu, “Numerical investigation of a new combined energy cycle based on Miller cycle, Organic Rankine cycle, Stirling engine and alkaline fuel cell,” Energy Reports, vol. 7, pp. 5406–5419, Nov. 2021, doi: 10.1016/j.egyr.2021.08.111.

[16] D. Maradin, “Advantages and disadvantages of renewable energy sources utilization,” International Journal of Energy Economics and Policy, vol. 11, no. 3, pp. 176–183, 2021, doi: 10.32479/ijeep.11027.

[17] K. Tromly, “Renewable Energy: An Overview. Energy Efficiency and Renewable Energy Clearinghouse (EREC) Brochure,” 2001.

[18] A. R. Mazhar, H. Z. Khan, M. K. Khan, A. Ahmed, and M. H. Yousaf, “Development and Analysis of a Liquid Piston Stirling Engine †,” Engineering Proceedings, vol. 23, no. 1, 2022, doi: 10.3390/engproc2022023034.

[19] N. Chekir, Y. Ben Salem, and I. Marzougui, “Small-scale solar stirling engine generator,” in 6th IEEE International Energy Conference, ENERGYCon 2020, Institute of Electrical and Electronics Engineers Inc., Sep. 2020, pp. 339–343. doi: 10.1109/ENERGYCon48941.2020.9236587.

[20] D. J. Kim and K. Sim, “Linear dynamic analysis of free-piston stirling engines on operable charge pressure and working frequency along with experimental verifications,” Applied Sciences (Switzerland), vol. 11, no. 11, Jun. 2021, doi: 10.3390/app11115205.

[21] M. Abbas, N. Said, and B. Boumeddane, “Thermal analysis of Stirling engine solar driven,” 2008.

[22] J. Boucher, F. Lanzetta, and P. Nika, “Optimization of a dual free piston Stirling engine,” Appl Therm Eng, vol. 27, no. 4, pp. 802–811, Mar. 2007, doi: 10.1016/j.applthermaleng.2006.10.021.

[23] M. Reckzügel, R.-G. Schmidt, and Aitziber Jiménez Abete, “Testing and optimization of the performance of a Stirling engine.,” 2013.

[24] Keith Strong and Roy Darlington, “Stirling and Hot Air Engines,” 2005.

[25] “Гостев, А. А. Двигатели внешнего сгорания: паровой двигатель и двигатель Стирлинга / А. А. Гостев, А. Е. Свистула // Совершенствование быстроходных двигателей : Сборник материалов научно-технической конференции студентов, аспирантов и профессорско-преподавательского состава кафедры «Двигатели внутреннего сгорания», посвященной 80-летию АлтГТУ, Барнаул, 02–03 июня 2022 года. – Барнаул: Алтайский государственный технический университет им. И.И. Ползунова, 2022. – С. 37-41. – EDN HLCPQO.”.

[26] J. Ni, “Research on the application of heat engine efficiency in reducing energy consumption,” Theoretical and Natural Science, vol. 9, no. 1, pp. 248–254, Nov. 2023, doi: 10.54254/2753-8818/9/20240768.

[27] H. ; A. Y. ; G. C. ; L. P. Ouerdane, “Continuity and boundary conditions in thermodynamics: From Carnot’s efficiency to efficiencies at maximum power,” Eur. Phys. J. Spec. Top. 2015 , 224, 5, 839–64..

[28] C. ; D. A. ; U. S. Bianciardia, “On the relationship between the economic process, the Carnot cycle and the entropy law,” Ecol. Econ. 1993, 8, 1, 7–10..

[29] C. Udriste, V. Golubyatnikov, and I. Tevy, “Economic cycles of carnot type,” Entropy, vol. 23, no. 10, Oct. 2021, doi: 10.3390/e23101344.

[30] Z. M. Farid, A. B. Rosli, and K. Kumaran, “Effects of phase angle setting, displacement, and eccentricity ratio based on determination of rhombic-drive primary geometrical parameters in beta-configuration Stirling engine,” in IOP Conference Series: Materials Science and Engineering, Institute of Physics Publishing, Jan. 2019. doi: 10.1088/1757-899X/469/1/012047.

[31] I. R. Kennedy and M. Hodzic, “Action and entropy in heat engines: An action revision of the carnot cycle,” Entropy, vol. 23, no. 7, Jul. 2021, doi: 10.3390/e23070860.

[32] H. Arif, A. Shah, T. A. H. Ratlamwala, K. Kamal, and M. A. Khan, “Effect of Material Change on Stirnol Engine: A Combination of NiTiNOL (Shape Memory Alloy) and Gamma Stirling Engine,” Materials, vol. 16, no. 8, Apr. 2023, doi: 10.3390/ma16083257.

[33] VINEETH C S, “STIRLING ENGINES: A BEGINEERS GUIDE.”

[34] C. Chi, J. Mou, M. Lin, R. Li, K. Jiao, and G. Hong, “Prediction on onset conditions of alpha, beta, and gamma type free piston Stirling generators,” Energy Sci Eng, vol. 11, no. 6, pp. 2052–2065, Jun. 2023, doi: 10.1002/ese3.1437.

[35] R. Stirling, “Stirling patent of 1816/1817,” in The Philips Stirling engine, Amsterdam, The Netherlands: Elsevier Science Publishers B.V., 1991, p. Appendix B., 1991.

[36] Nasrollah Naddaf, “Stirling engine cycle efficiency,” 2012.

[37] Y. Dubé et al., “Development of External Combustion Engine,” American Journal of Vehicle Design, vol. 1, no. 2, pp. 25–29, 2013, doi: 10.12691/ajvd-1-2-2.

[38] P. J. Zabalaga, E. Cardozo, L. A. C. Campero, and J. A. A. Ramos, “Performance analysis of a stirling engine hybrid power system,” Energies (Basel), vol. 13, no. 4, 2020, doi: 10.3390/en13040980.

[39] “ПЕРСПЕКТИВЫ ПРИМЕНЕНИЯ ДВИГАТЕЛЯ СТИРЛИНГА В КАЧЕСТВЕ ЗАМЕНЫ ДВИГАТЕЛЯ ВНУТРЕННЕГО СГОРАНИЯ PROSPECTS FOR USING THE STIRLING ENGINE AS A REPLACEMENT OF THE INTERNAL COMBUSTION ENGINE.”

[40] G. Walker and J. R. Senft, Free Piston Stirling Engines, vol. 12. in Lecture Notes in Engineering, vol. 12. Berlin, Heidelberg: Springer Berlin Heidelberg, 1985. doi: 10.1007/978-3-642-82526-2.

[41] P. Chen, P. Yang, L. Liu, and Y. Liu, “Parametric investigation of the phase characteristics of a beta-type free piston Stirling engine based on a thermodynamic-dynamic coupled model,” Energy, vol. 219, Mar. 2021, doi: 10.1016/j.energy.2020.119658.

[42] J. Mou and G. Hong, “A numerical model on thermodynamic analysis of free piston Stirling engines,” in IOP Conference Series: Materials Science and Engineering, Institute of Physics Publishing, Mar. 2017. doi: 10.1088/1757-899X/171/1/012090.

[43] T. Abishu Gelu, J. Luís Toste de Azevedo Edgar Caetano Fernandes, J. Alberto Caiado Falcão de Campos Supervisor, and E. Caetano Fernandes, “Analysis of Stirling engine and comparison with other technologies using low temperature heat sources Energy Engineering and Management Examination Committee,” 2014.

[44] J. R. Ávila Pérez, G. L. Gutiérrez Urueta, F. Tapia Rodríguez, and J. A. Araoz, “Modeling of a 1kW free piston Stirling engine: Opportunity for sustainable electricity production,” Ingeniería Investigación y Tecnología, vol. 21, no. 4, pp. 1–13, Oct. 2020, doi: 10.22201/fi.25940732e.2020.21.4.035.

[45] N. C. J. Chen and F. P. Griffin, “A Review of Stirling Engine Mathematical Models,” 1983.

[46] “Дюсегалиева, Қ. О. Стирлинг қозғалтқышын теориялық зерттеу / Қ. О. Дюсегалиева, Б. Т. Көпжасаров // Ғылым және білім. – 2022. – No. S2-2(67). – P. 127-134. – EDN NTRHGV.”.

[47] A. Ross, “Making Stirling Engines,” 1993.

[48] D. G. Thombare and S. K. Verma, “Technological development in the Stirling cycle engines,” Renewable and Sustainable Energy Reviews, vol. 12, no. 1. pp. 1–38, Jan. 2008. doi: 10.1016/j.rser.2006.07.001.

[49] J. Wang, C. Pan, T. Zhang, K. Luo, Y. Zhou, and J. Wang, “A novel method to hit the limit temperature of Stirling-type cryocooler,” J Appl Phys, vol. 123, no. 6, Feb. 2018, doi: 10.1063/1.5013602.

[50] J. Podešva and Z. Poruba, “The Stirling engine mechanism optimization,” Perspect Sci (Neth), vol. 7, pp. 341–346, Mar. 2016, doi: 10.1016/j.pisc.2015.11.052.

[51] A. Gaponenko, “MATHEMATICAL MODELING OF THE STIRLING ENGINE,” University News. North-Caucasian Region. Technical Sciences Series, no. 4, pp. 29–35, Dec. 2016, doi: 10.17213/0321-2653-2016-4-29-35.

[52] K. Migimatsu, H. Kada, and I. T. Tokuda, “Experimental study on entrainment of Stirling engines to an external pacemaker,” Nonlinear Theory and Its Applications, IEICE, vol. 8, no. 3, pp. 246–254, 2017, doi: 10.1587/nolta.8.246.

[53] Iker González Pino, “Modeling, expermental characterization and simulation of Stirling engine based micro-cogeneration plants for residential buildings,” 2019.

[54] D. Thimsen, “EPRI Project Manager Stirling Engine Assessment,” 2002. [Online]. Available: www.epri.com

[55] W. Ye, X. Wang, and Y. Liu, “Application of artificial neural network for predicting the dynamic performance of a free piston Stirling engine,” Energy, vol. 194, Mar. 2020, doi: 10.1016/j.energy.2020.116912.

[56] M. Majidniya, T. Boileau, B. Remy, and M. Zandi, “Performance simulation by a nonlinear thermodynamic model for a Free Piston Stirling Engine with a linear generator,” Appl Therm Eng, vol. 184, Feb. 2021, doi: 10.1016/j.applthermaleng.2020.116128.

[57] M. H. Ahmadi, M. A. Ahmadi, and F. Pourfayaz, “Thermal models for analysis of performance of Stirling engine: A review,” Renewable and Sustainable Energy Reviews, vol. 68. Elsevier Ltd, pp. 168–184, Feb. 01, 2017. doi: 10.1016/j.rser.2016.09.033.

[58] M. Lottmann et al., “Early Development Of A 100 Watt Low Temperature Difference Stirling Engine,” Robertson Library, University of Prince Edward Island, Sep. 2021. doi: 10.32393/csme.2021.193.

[59] H. Hachem et al., “Comparison based on exergetic analyses of two hot air engines: A Gamma type Stirling engine and an open joule cycle Ericsson engine,” Entropy, vol. 17, no. 11, pp. 7331–7348, 2015, doi: 10.3390/e17117331.

[60] “Юлдашев, А. А. Двигатель Стирлинга и его применение / А. А. Юлдашев // Аллея науки. – 2018. – Т. 2, № 11(27). – С. 111-117. – EDN YUVTFJ.”.

[61] “Лосинков, А. С. Двигатель Стирлинга – принцип работы и перспективы использования / А. С. Лосинков, К. С. Маркелова // Научное творчество студентов – развитию агропромышленного комплекса : Сборник студенческих научных работ, Брянск, 25 мая 2022 года. – Брянск: Брянский государственный аграрный университет, 2022. – С. 116-125. – EDN VLCJFT.”.

[62] H.-T. Le, H. Hoang Nghia, B. M. Huy, V. T. Phu, V. Bui, and H. Quyen, “STIRLING ENGINE: FROM DESIGN TO APPLICATION INTO PRACTICE AND EDUCATION ARTICLE INFORMATION ABSTRACT,” vol. 14, no. 1, 2022, doi: 10.5281/zenodo.64.

[63] C. Stumpf, “Parameter Optimization of a Low Temperature Difference Gamma-Type Stirling Engine to Maximize Shaft Power,” 2019. [Online]. Available: https://www.researchgate.net/publication/337011874

[64] M. Babaelahi and H. Sayyaadi, “A new thermal model based on polytropic numerical simulation of Stirling engines,” Appl Energy, vol. 141, pp. 143–159, Mar. 2015, doi: 10.1016/j.apenergy.2014.12.033.

[65] H. Karabulut, H. S. Yücesu, C. Çinar, and F. Aksoy, “An experimental study on the development of a β-type Stirling engine for low and moderate temperature heat sources,” Appl Energy, vol. 86, no. 1, pp. 68–73, 2009, doi: 10.1016/j.apenergy.2008.04.003.

[66] O. Taki, K. Senhaji Rhazi, and Y. Mejdoub, “Stirling engine optimization using artificial neural networks algorithm,” ITM Web of Conferences, vol. 52, p. 02010, 2023, doi: 10.1051/itmconf/20235202010.

[67] C. Çinar, “Thermodynamic analysis of an α-type stirling engine with variable phase angle,” Proc Inst Mech Eng C J Mech Eng Sci, vol. 221, no. 8, pp. 949–954, Aug. 2007, doi: 10.1243/09544062JMES572.

[68] G. Walker, “ Stirling-cycle machines,” Oxford University Press, 1973.

[69] Y. Ö. Özgören, S. Çetinkaya, S. Saridemir, A. Çiçek, and F. Kara, “Predictive modeling of performance of a helium charged Stirling engine using an artificial neural network,” Energy Convers Manag, vol. 67, pp. 357–368, 2013, doi: 10.1016/j.enconman.2012.12.007.

[70] F. De Monte, “Thermal analysis of the heat exchangers and regenerator in stirling cycle machines,” J Propuls Power, vol. 13, no. 3, pp. 404–411, 1997, doi: 10.2514/2.5178.

[71] Graham Walker and Babatunde Agbi, “Thermodynamic Aspects of Stirling Engines with Two-Phase, Two-Component Working Fluids,” Transactions of the Canadian Society for Mechanical Engineering Volume 2, , 1973.

[72] G. Walker, “Stirling engines (G Walker),” 1980.

[73] Aitziber Jiménez Abete, “Testing and Optimization of the performance of a Stirling engine.,” 2013.

[74] “Жилин, Р. А. Перспективное моделирование двигателя Стирлинга / Р. А. Жилин, Г. М. Картавцев, В. С. Ходцев // Высокие технологии в строительном комплексе. – 2023. – № 1. – С. 63-65. – EDN KWNULK.”.

[75] R. Singh, “Designing, construction and working of novel thermal pumps,” 2015. [Online]. Available: https://www.researchgate.net/publication/305655746

[76] K. Khatke, K. D. Pandey, and M. K. Dwivedi, “Thermodynamic Analysis of Stirling Engine and its Performance Challenges: A Review,” 2020. [Online]. Available: https://www.researchgate.net/publication/342419359

[77] Muhammad Kamran, “Fundamentals of Smart Grid Systems, Chapter 7 - Microgrid and hybrid energy systems,” Academic Press, 2023, Pages 299-363, ISBN 9780323995603,.

[78] A. Der Minassians and S. R. Sanders, “Multiphase stirling engines,” Journal of Solar Energy Engineering, Transactions of the ASME, vol. 131, no. 2, pp. 0210131–02101311, May 2009, doi: 10.1115/1.3097274.

[79] I. B. Gorshkov and V. V. Petrov, “Numerical simulation of stages number influence to the characteristics of a looped tube thermoacoustic Stirling engine,” Izvestiya of Saratov University. Physics, vol. 21, no. 2, pp. 133–144, 2021, doi: 10.18500/1817-3020-2021-21-2-133-144.

[80] R. Gheith, H. Hachem, F. Aloui, and S. Ben Nasrallah, “Experimental and theoretical investigation of Stirling engine heater: Parametrical optimization,” Energy Convers Manag, vol. 105, pp. 285–293, Aug. 2015, doi: 10.1016/j.enconman.2015.07.063.

[81] M. H. Khanjanpour, M. Rahnama, A. A. Javadi, M. Akrami, A. R. Tavakolpour-Saleh, and M. Iranmanesh, “An experimental study of a gamma-type MTD stirling engine,” Case Studies in Thermal Engineering, vol. 24, Apr. 2021, doi: 10.1016/j.csite.2021.100871.

[82] M. Kumar Sahu and P. Sai Cherla, “Battery Charger with Stirling Engine,” International Journal of Technology and Emerging Sciences on, vol. 14, 2022, [Online]. Available: www.mapscipub.com

[83] C. P. Speer, “Modifications to Reduce the Minimum Thermal Source Temperature of the ST05G-CNC Stirling Engine,” 2018.

[84] C. Stumpf, “Parameter Optimization of a Low Temperature Difference Gamma-Type Stirling Engine to Maximize Shaft Power,” 2019. [Online]. Available: https://www.researchgate.net/publication/337011874

[85] P. Durcansky, R. Nosek, and J. Jandacka, “Use of stirling engine for waste heat recovery,” Energies (Basel), vol. 13, no. 6, Aug. 2020, doi: 10.3390/en13164133.

[86] E. Bo, “Review of research on performance of stirling engine regenerators,” Theoretical and Natural Science, vol. 5, no. 1, pp. 922–928, May 2023, doi: 10.54254/2753-8818/5/20230552.

[87] Z. De Rouyan, C. Speer, and D. S. Nobes, “Preliminary Design of a Hollow Displacer for a Low Temperature Difference Stirling Engine,” 2021.

[88] S. M. Nguyen, “DETERMINATION OF A FREE-PISTON STIRLING ENGINE-GENERATOR OPERATING CURVE FOR APPLICATIONS IN ENERGY EXTRACTION,” 2022.

[89] “Ермакова, Е. В. Перспективы применения двигателей Стирлинга в малой энергетике / Е. В. Ермакова // Инновационные подходы к решению технико-экономических проблем, Москва, 25 ноября 2015 года / Главный редактор И.Г. Игнатова. – Москва: Национальный исследовательский университет ‘Московский институт электронной техники’, 2015. – С. 126-129. – EDN WCHSTL.”

[90] N. Patel, R. Bumataria, R. K. Bumataria, and N. K. Patel, “Review of Stirling Engines for Pumping Water using Solar Energy as a source of Power.” [Online]. Available: www.ijera.com

[91] M. Z. Malik et al., “A review on design parameters and specifications of parabolic solar dish Stirling systems and their applications,” Energy Reports, vol. 8. Elsevier Ltd, pp. 4128–4154, Nov. 01, 2022. doi: 10.1016/j.egyr.2022.03.031.

[92] A. Aditya, G. Balaji, B. C. Chengappa, K. Chethan Kumar, and S. A. Mohankrishna, “Design and development of Solar Stirling Engine for power generation,” in IOP Conference Series: Materials Science and Engineering, Institute of Physics Publishing, Jun. 2018. doi: 10.1088/1757-899X/376/1/012022.

[93] T. Mancini et al., “Dish-stirling systems: An overview of development and status,” Journal of Solar Energy Engineering, Transactions of the ASME, vol. 125, no. 2. pp. 135–151, May 2003. doi: 10.1115/1.1562634.

[94] D. Howard and R. G. Harley, “Modeling of dish-stirling solar thermal power generation,” in IEEE PES General Meeting, PES 2010, 2010. doi: 10.1109/PES.2010.5590188.

[95] H. Hachem, R. Gheith, F. Aloui, and S. Ben Nasrallah, “Technological challenges and optimization efforts of the Stirling machine: A review,” Energy Conversion and Management, vol. 171. Elsevier Ltd, pp. 1365–1387, Sep. 01, 2018. doi: 10.1016/j.enconman.2018.06.042.

[96] J. Yan, Y. D. Peng, Z. R. Cheng, F. M. Liu, and X. H. Tang, “Design and implementation of a 38 kW dish-Stirling concentrated solar power system,” in IOP Conference Series: Earth and Environmental Science, Institute of Physics Publishing, Nov. 2017. doi: 10.1088/1755-1315/93/1/012052.

[97] A. Yerbury, A. Coote, V. Garaniya, and H. Yu, “Design of a solar Stirling engine for marine and offshore applications,” International Journal of Renewable Energy Technology, vol. 7, no. 1, p. 1, 2016, doi: 10.1504/ijret.2016.073400.

[98] T. Tsoutsos, V. Gekas, and K. Marketaki, “Technical and economical evaluation of solar thermal power generation,” 2003. [Online]. Available: www.elsevier.com/locate/renene

[99] R. Binti, A. P. Melaka, C. K. Gan, M. Ruddin, and A. Ghani, “Development of Design Parameters for the Concentrator of Parabolic Dish (PD) Based Concentrating Solar Power (CSP) under Malaysia Environment,” 2017. [Online]. Available: https://www.researchgate.net/publication/273451435

[100] F. M. Mohamed, A. S. Jassim, Y. H. Mahmood, and M. A. K. Ahmed, “Design and Study of Portable Solar Dish Concentrator,” 2012.

[101] L. Geok Pheng, R. Affandi, M. R. Ab Ghani, C. K. Gan, and J. Zanariah, “Stirling Engine Technology for Parabolic Dish-Stirling System Based on Concentrating Solar Power (CSP),” Applied Mechanics and Materials, vol. 785, pp. 576–580, Aug. 2015, doi: 10.4028/www.scientific.net/amm.785.576.

[102] U. R. Singh and A. Kumar, “Review on solar Stirling engine: Development and performance,” Thermal Science and Engineering Progress, vol. 8. Elsevier Ltd, pp. 244–256, Dec. 01, 2018. doi: 10.1016/j.tsep.2018.08.016.

[103] O. Joshi and M. Tendolkar, “Numerical Investigations about Flow Resistance Values for Stirling Type Pulse Tube Cryocooler,” CFD Letters, vol. 14, no. 6, pp. 79–89, Jun. 2022, doi: 10.37934/cfdl.14.6.7989.

[104] D. Smirnov, F. M. Ibanez, and H. Ouerdane, “Junction temperature of CMOS electronics cooled by a Stirling cryocooler,” Case Studies in Thermal Engineering, vol. 52, Dec. 2023, doi: 10.1016/j.csite.2023.103688.

[105] K. Srinivasan, K. Venkatraman Srinivasan, M. Arunachalam, R. Pokale, and A. Mahalingam, “Mahalingam. Theoretical Analysis and Optimization of Regenerator of Stirling Cryocooler,” American Journal of Science and Technology, vol. 4, no. 4, pp. 67–73, 2017, [Online]. Available: http://www.aascit.org/journal/ajst

[106] D. J. M. Aguilar, J. A. A. Hidalgo, M. Eskubi, and P. Martínez, “Analysis of the operating parameters in a Stirling cryocooler,” in E3S Web of Conferences, EDP Sciences, Oct. 2021. doi: 10.1051/e3sconf/202131310002.

[107] J. Park et al., “Development of a kw-class Stirling cryocooler for liquefaction of natural gas (NG),” in IOP Conference Series: Materials Science and Engineering, Institute of Physics Publishing, Jun. 2020. doi: 10.1088/1757-899X/755/1/012035.

[108] J. W. and B. C. W. T. Beale, “Stirling engines for developing countries,” Intersociety energy conversion engineering conference. 15, pp. 1971-1975, 1980.

[109] G. Schmidt, “Classical analysis of operation of Stirling engine,” A report published in German engineering union (Original German), vol. 15, pp. 1-12, 1871.

[110] T. Finkelstein, “analogue simulation of Stirling engine,” Simulation, vol. 2, 1975.

[111] T. Finkelstein, “Generalized thermodynamic analysis of Stirling engines,” SAE Technical Paper 0148-7191, 1960.

[112] G. Walker, “An Optimization of the Principal Design Parameters of Stirling Cycle Machines,” J. Mech. Eng. Sci., vol. 4, no. 3, pp. 226–240, 1962.

[113] G. Walker, “Stirling cycle cooling engine with two-phase, twocomponent working fluid,” Cryogenics (Guildf)., vol. 14, no. 8, pp. 459–462, 1974.

[114] D. M. B. Israel Urieli, “Stirling cycle engine analysis,” 1983.

[115] J. R. Senft, “Mechanical efficiency of kinematic heat engines,” J. Franklin Inst., vol. 324, no. 2, pp. 273–290, 1987.

[116] J. R. Senft, “Optimum Stirling engine geometry,” International Journal of Energy Research, vol. 26, pp. 1087-1101, 2002.

[117] K. Hirata, S. Iwamoto, F. Toda, and K. Hamaguchi, “PERFORMANCE EVALUATION FOR A 100 W STIRLING ENGINE.”

[118] H. Hachem, R. Gheith, F. Aloui, and S. Ben Nasrallah, “Technological challenges and optimization efforts of the Stirling machine: A review,” Energy Conversion and Management, vol. 171. Elsevier Ltd, pp. 1365–1387, Sep. 01, 2018. doi: 10.1016/j.enconman.2018.06.042.

[119] Y. Timoumi, I. Tlili, and S. Ben Nasrallah, “Design and performance optimization of GPU-3 Stirling engines,” Energy, vol. 33, no. 7. Elsevier Ltd, pp. 1100–1114, 2008. doi: 10.1016/j.energy.2008.02.005.

[120] H. Snyman, T. M. Harms, and J. M. Strauss, “Design analysis methods for Stirling engines,” 2008.

[121] G. Lavinia, N. Martaj, L. Grosu, and P. Rochelle, “Thermodynamic Study of a Low Temperature Difference Stirling Engine at Steady State Operation,” Int. J. of Thermodynamics, vol. 10, no. 4, pp. 165–176, 2007, doi: 10.5541/ijot.200.

[122] E. Eid, “Performance of a beta-configuration heat engine having a regenerative displacer,” Renew Energy, vol. 34, no. 11, pp. 2404–2413, Nov. 2009, doi: 10.1016/j.renene.2009.03.016.

[123] D. J. Shendage, S. B. Kedare, and S. L. Bapat, “An analysis of beta type Stirling engine with rhombic drive mechanism,” Renew Energy, vol. 36, no. 1, pp. 289–297, Jan. 2011, doi: 10.1016/j.renene.2010.06.041.

[124] P. Puech and V. Tishkova, “Thermodynamic analysis of a Stirling engine including regenerator dead volume,” Renew Energy, vol. 36, no. 2, pp. 872–878, Feb. 2011, doi: 10.1016/j.renene.2010.07.013.

[125] M. C. Campos, J. V. C. Vargas, and J. C. Ordonez, “Thermodynamic optimization of a Stirling engine,” Energy, vol. 44, no. 1, pp. 902–910, 2012, doi: 10.1016/j.energy.2012.04.060.

[126] J. L. Salazar and W. L. Chen, “A computational fluid dynamics study on the heat transfer characteristics of the working cycle of a β-type Stirling engine,” Energy Convers Manag, vol. 88, pp. 177–188, 2014, doi: 10.1016/j.enconman.2014.08.040.

[127] H. Ferral-Smith, G. Giannakakis, J. Wilson, and J. Taylor, “Factors Influencing the Thermodynamic Efficiency of Stirling Engines,” PAM Review Energy

Science & Technology, vol. 4, pp. 17–29, Jun. 2017, doi: 10.5130/pamr.v4i0.1459.

[128] C. Cinar, S. Yucesu, T. Topgul, and M. Okur, “Beta-type Stirling engine operating at atmospheric pressure,” Appl Energy, vol. 81, no. 4, pp. 351–357, 2005, doi: 10.1016/j.apenergy.2004.08.004.

[129] D. Mishra and S. Chaudhary, “Thermodynamic Modeling And Performance Analysis of Stirling Engine Cycle,” 2014.

[130] M. Ni et al., “Improved Simple Analytical Model and experimental study of a 100 W β-type Stirling engine,” Appl Energy, vol. 169, pp. 768–787, May 2016, doi: 10.1016/j.apenergy.2016.02.069.

[131] S. Suyitno, A. Hissen, W. Endra Juwana, O. Dwi Hanggara Putra, and S. Huda, “Effects of Working Fluids on the Performance of Stirling Engine Optimization of solar updraft tower by using heliostat designed according to the physiography of Sabha city View project Performance Enhancement of Dye-Sensitized Solar Cells Using a Natural Sensitizer View project Effects of Working Fluids on the Performance of Stirling Engine,” 2013, doi: 10.13140/2.1.2365.3125.

[132] C. Yang, N. Zhuang, W. Du, H. Zhao, and X. Tang, “Modified Stirling cycle thermodynamic model IPD-MSM and its application,” Energy Convers Manag, vol. 260, May 2022, doi: 10.1016/j.enconman.2022.115630.

[133] H. Hachem, R. Gheith, and F. Aloui, “Theoretical investigations of Stirling engine performances for different filling gas properties,” Int J Energy Res, 2022, doi: 10.1002/er.7875.

[134] H. Hosseinzade and H. Sayyaadi, “CAFS: The Combined Adiabatic-Finite Speed thermal model for simulation and optimization of Stirling engines,”

Energy Convers Manag, vol. 91, pp. 32–53, 2015, doi: 10.1016/j.enconman.2014.11.049.

[135] A. Rahmati, S. M. Varedi-Koulaei, M. H. Ahmadi, and H. Ahmadi, “Dimensional synthesis of the Stirling engine based on optimizing the output work by evolutionary algorithms,” Energy Reports, vol. 6, pp. 1468–1486, Nov. 2020, doi: 10.1016/j.egyr.2020.05.030.

[136] K. Laazaar and N. Boutammachte, “New approach of decision support method for Stirling engine type choice towards a better exploitation of renewable energies,” Energy Convers Manag, vol. 223, Nov. 2020, doi: 10.1016/j.enconman.2020.113326.

[137] A. Abuelyamen and R. Ben-Mansour, “Energy efficiency comparison of Stirling engine types (α, β, and γ) using detailed CFD modeling,” International Journal of Thermal Sciences, vol. 132, pp. 411–423, Oct. 2018, doi: 10.1016/j.ijthermalsci.2018.06.026.

[138] R. Gheith, F. Aloui, M. Tazerout, and S. Ben Nasrallah, “Experimental investigations of a gamma Stirling engine,” Int J Energy Res, vol. 36, no. 12, pp. 1175–1182, Oct. 2012, doi: 10.1002/er.1872.

[139] L. S. Scollo, P. E. Valdez, S. R. Santamarina, M. R. Chini, and J. H. Barón, “Twin cylinder alpha stirling engine combined model and prototype redesign,” Int J Hydrogen Energy, vol. 38, no. 4, pp. 1988–1996, Feb. 2013, doi: 10.1016/j.ijhydene.2012.01.180.

[140] G. Féniès, F. Formosa, J. Ramousse, and A. Badel, “Double acting Stirling engine: Modeling, experiments and optimization,” Appl Energy, vol. 159, pp. 350–361, Dec. 2015, doi: 10.1016/j.apenergy.2015.08.128.

[141] R. Li, L. Grosu, and D. Queiros-Condé, “Losses effect on the performance of a Gamma type Stirling engine,” Energy Convers Manag, vol. 114, pp. 28–37, Apr. 2016, doi: 10.1016/j.enconman.2016.02.007.

[142] M. H. Ahmadi, M. A. Ahmadi, and M. Mehrpooya, “Investigation of the effect of design parameters on power output and thermal efficiency of a Stirling engine by thermodynamic analysis,” International Journal of Low-Carbon Technologies, vol. 11, no. 2, pp. 141–156, May 2016, doi: 10.1093/ijlct/ctu030.

[143] M. Chahartaghi and M. Sheykhi, “Energy and exergy analyses of beta-type Stirling engine at different working conditions,” Energy Convers Manag, vol. 169, pp. 279–290, Aug. 2018, doi: 10.1016/j.enconman.2018.05.064.

[144] S. Ranieri, G. A. O. Prado, and B. D. MacDonald, “Efficiency reduction in stirling engines resulting from sinusoidal motion,” Energies (Basel), vol. 11, no. 11, Nov. 2018, doi: 10.3390/en11112887.

[145] J. Egas and D. M. Clucas, “Stirling engine configuration selection,” Energies (Basel), vol. 11, no. 3, Feb. 2018, doi: 10.3390/en11030584.

[146] E. Rogdakis, P. Bitsikas, G. Dogkas, and G. Antonakos, “Three-dimensional CFD study of a β-type Stirling Engine,” Thermal Science and Engineering Progress, vol. 11, pp. 302–316, Jun. 2019, doi: 10.1016/j.tsep.2019.04.012.

[147] B. Rutczyk, I. Szczygieł, and Z. Buliński, “A zero-dimensional, real gas model of an α Stirling engine,” Energy Convers Manag, vol. 199, Nov. 2019, doi: 10.1016/j.enconman.2019.111995.

[148] Z. Buliński et al., “A Computational Fluid Dynamics analysis of the influence of the regenerator on the performance of the cold Stirling engine at different working conditions,” Energy Convers Manag, vol. 195, pp. 125–138, Sep. 2019, doi: 10.1016/j.enconman.2019.04.089.

[149] H. Hachem, R. Gheith, F. Aloui, and S. Ben Nasrallah, “Performance evaluation of Gamma type Stirling engine,” 2019.

[150] H. Raghavendra, P. Suryanarayana Raju, and K. Hemachandra Reddy, “Effect of Geometric and Operational Parameters on the Performance of a Beta-Type Stirling Engine: A Numerical Study,” Iranian Journal of Science and Technology - Transactions of Mechanical Engineering, vol. 46, no. 1. Springer Science and Business Media Deutschland GmbH, Mar. 01, 2022. doi: 10.1007/s40997-020-00406-0.

[151] J. Joseph, E. Mathew Louis, B. Thomas, K. Anurag, V. Sankar, and T. T. Pullan, “Fabrication and testing of a gamma type stirling engine,” in Materials Today: Proceedings, Elsevier Ltd, 2019, pp. 9641–9645. doi: 10.1016/j.matpr.2020.07.152.

[152] D. Erol and S. Çalışkan, “The examination of performance characteristics of a beta-type Stirling engine with a rhombic mechanism: The influence of various working fluids and displacer piston materials,” Int J Energy Res, vol. 45, no. 9, pp. 13726–13747, Jul. 2021, doi: 10.1002/er.6702.

[153] A. Romanelli, “Stirling engine operating at low temperature difference,” Am J Phys, vol. 88, no. 4, pp. 319–324, Apr. 2020, doi: 10.1119/10.0000832.

[154] C. Dobre, L. Grosu, M. Costea, and M. Constantin, “Beta type stirling engine. Schmidt and finite physical dimensions thermodynamics methods faced to experiments,” Entropy, vol. 22, no. 11, pp. 1–15, Nov. 2020, doi: 10.3390/e22111278.

[155] H. S. Yang and C. H. Cheng, “Development of a beta-type Stirling engine with rhombic-drive mechanism using a modified non-ideal adiabatic model,” Appl Energy, vol. 200, pp. 62–72, 2017, doi: 10.1016/j.apenergy.2017.05.075.

[156] D. Ipci, “Thermodynamic-dynamic analysis of gamma type free-piston stirling engine charged with hydrogen gas as working fluid,” Int J Green Energy, vol. 17, no. 12, pp. 805–815, Sep. 2020, doi: 10.1080/15435075.2020.1798771.

[157] R. Masser et al., “Optimized piston motion for an alpha-type stirling engine,” Entropy, vol. 22, no. 6, pp. 1–19, Jun. 2020, doi: 10.3390/e22060700.

[158] S. Alfarawi, “Thermodynamic analysis of rhombic-driven and crank-driven beta-type Stirling engines,” Int J Energy Res, vol. 44, no. 7, pp. 5596–5608, Jun. 2020, doi: 10.1002/er.5309.

[159] K. Mansuriya, B. D. Raja, A. R. Yıldız, A. Mudgal, and V. K. Patel, “Thermodynamic optimization of Stirling heat engine with methane gas using finite speed thermodynamic model,” Heat Transfer, vol. 50, no. 8, pp. 8155–8172, Dec. 2021, doi: 10.1002/htj.22271.

[160] M. A. Mukhtar, R. A. Bakar, and M. F. Zainudin, “Thermodynamic Analysis of a Gamma-configuration Stirling Engine,” Journal of Advanced Research in Fluid Mechanics and Thermal Sciences, vol. 83, no. 2, pp. 114–126, 2021, doi: 10.37934/ARFMTS.83.2.114126.

[161] T. Topgül, M. Okur, F. Şahin, and C. Çınar, “Experimental investigation of the effects of hot-end and cold-end connection on the performance of a gamma type Stirling engine,” Engineering Science and Technology, an International Journal, vol. 36, Dec. 2022, doi: 10.1016/j.jestch.2022.101152.

[162] P. Murti, A. Takizawa, E. Shoji, and T. Biwa, “Design guideline for multi-cylinder-type liquid-piston Stirling engine,” Appl Therm Eng, vol. 200, Jan. 2022, doi: 10.1016/j.applthermaleng.2021.117635.

[163] T. Kumaravelu, S. Saadon, and A. R. Abu Talib, “Heat transfer enhancement of a Stirling engine by using fins attachment in an energy recovery system,” Energy, vol. 239, Jan. 2022, doi: 10.1016/j.energy.2021.121881.

[164] K. M. Bataineh and M. F. Maqableh, “A new numerical thermodynamic model for a beta-type Stirling engine with a rhombic drive,” Thermal Science and Engineering Progress, vol. 28, Feb. 2022, doi: 10.1016/j.tsep.2021.101071.

[165] M. H. Katooli, R. Askari Moghadam, and M. Mehrpooya, “Design optimization of a heat-to-cool Stirling cycle using artificial neural network,” Int J Energy Res, Jun. 2022, doi: 10.1002/er.7890.

[166] W. Cao, Z. Chang, A. Zhou, X. Dou, G. Gao, and J. Gong, “Investigation into the Influence of Parallel Offset Wear on Stirling Engine Piston Rod Oil-Free Lubrication Seal,” Machines, vol. 10, no. 5, p. 350, May 2022, doi: 10.3390/machines10050350.

[167] M. Yu, C. Shi, J. Xie, P. Liu, Z. Liu, and W. Liu, “Constructal design of a circular micro-channel Stirling regenerator based on exergy destruction minimization,” Int J Heat Mass Transf, vol. 183, Feb. 2022, doi: 10.1016/j.ijheatmasstransfer.2021.122240.

[168] M. Ali Abro, M. Iqbal Soomro, A. Shakoor Shaikh, S. Khan Pathan, S. Zulfiqar Ali Bhutto Campus, and K. Mir, “An Experimental Study on Performance Investigation of Solar Dish Sterling Engine in Pakistan Surface Modification of Steels to improve High Temperature Corrosion View project HVAC systems View project An Experimental Study on Performance Investigation of Solar Dish Sterling Engine in Pakistan.” [Online]. Available: www.ijisrt.com730

[169] M. H. Babikir et al., “Simplified Modeling and Simulation of Electricity Production from a Dish/Stirling System,” International Journal of Photoenergy, vol. 2020, 2020, doi: 10.1155/2020/7398496.

[170] M. Vahidi Bidhendi and Y. Abbassi, “Exploring dynamic operation of a solar dish-stirling engine: Validation and implementation of a novel TRNSYS type,”

Sustainable Energy Technologies and Assessments, vol. 40, Aug. 2020, doi: 10.1016/j.seta.2020.100765.

[171] C. Zhang, Q. Xu, Y. Zhang, I. Arauzo, and C. Zou, “Performance analysis of different arrangements of a new layout dish-Stirling system,” Energy Reports, vol. 7, pp. 1798–1807, Nov. 2021, doi: 10.1016/j.egyr.2021.03.003.

[172] M. E. Zayed, J. Zhao, A. H. Elsheikh, Z. Zhao, S. Zhong, and A. E. Kabeel, “Comprehensive parametric analysis, design and performance assessment of a solar dish/Stirling system,” Process Safety and Environmental Protection, vol. 146, pp. 276–291, Feb. 2021, doi: 10.1016/j.psep.2020.09.007.

[173] V. İncili, G. Karaca Dolgun, A. Georgiev, A. Keçebaş, and N. S. Çetin, “Performance evaluation of novel photovoltaic and Stirling assisted hybrid micro combined heat and power system,” Renew Energy, vol. 189, pp. 129–138, Apr. 2022, doi: 10.1016/j.renene.2022.03.030.

[174] I. T. Sa’ed A.Musmar, “Numerical Investigation of Working Fluid Effect on Stirling Engine Performance,” International Journal of Thermal and Environmental Engineering, vol. 10, no. 1, 2015, doi: 10.5383/ijtee.10.01.005.

[175] W. R. Maltini Martir and E. R. Washif_Gtotl, “Stirling Engine Second Edition.”

[176] S. Alfarawi, “MODELLING AND OPTIMIZATION OF HIGH TEMPERATURE DIFFERENCE (HTD) GAMMA-TYPE STIRLING ENGINE PROTOTYPE,” 2017.

[177] J. R. Senft, “A simple derivation of the generalized Beale number,” IECEC ’82; Proceedings of the Seventeenth Intersociety Energy Conversion Engineering Conference, vol. - 1, pp. 1652–1655, 1982.

[178] G. Walker, “Stirling-cycle Engines,” Oxford: Clarendon Press, 1973.

[179] J. A. Araoz Ramos, Thermodynamic analysis of Stirling engine systems applications for combined heat and power. Industrial Engineering and Management, KTH Royal Institute of Technology, 2015.

[180] R. K. Ranjan and S. K. Verma, “Thermodynamic analysis and analytical simulation of the Rallis modified Stirling cycle,” Archives of Thermodynamics, vol. 40, no. 2, pp. 35–67, 2019, doi: 10.24425/ather.2019.129541.

[181] R. K. Bumataria and N. K. Patel, “STIRLING ENGINE PERFORMANCE PREDICTION USING SCHMIDT ANALYSIS BY CONSIDERING DIFFERENT LOSSES.” [Online]. Available: http://www.ijret.org

[182] P. L. and L. V. A. Organ, “Back-to-back test for determining the pumping losses in a Stirling cycle machine,” IECEC’82, pp. 1856-1861, 1985.

[183] T. Raymond et al., “Study on the phase angle effect for alpha type stirling engine thermodynamics behavior,” vol. 10, no. 17, 2015, [Online]. Available: https://www.researchgate.net/publication/283713190

[184] “ЭНЕРГЕТИЧЕСКАЯ ЭФФЕКТИВНОСТЬ ЦИКЛА ДВИГАТЕЛЯ СТИРЛИНГА В МОДИФИЦИРОВАННОЙ ТЕОРИИ ШМИДТА.”

[185] K. M. Bataineh, “Numerical thermodynamic model of alpha-type Stirling engine,” Case Studies in Thermal Engineering, vol. 12, pp. 104–116, Sep. 2018, doi: 10.1016/j.csite.2018.03.010.

[186] G. Antonakos, I. Koronaki, G. R. Domenikos, and S. Baltadouros, “Investigation of the Performance of Thermodynamic Analysis Models for a Cryocooler PPG-102 Stirling Engine,” Energies (Basel), vol. 16, no. 19, Oct. 2023, doi: 10.3390/en16196815.

[187] A. M. Gaponenko and A. A. Kagramanova, “Analysis of the Stirling engine in the Schmidt approximation,” in Journal of Physics: Conference Series, Institute of Physics Publishing, Dec. 2018. doi: 10.1088/1742-6596/1111/1/012019.

[188] M. K. Gussoli, J. C. D. de Oliveira, and M. Higa, “INVESTIGATION ON VOLUME VARIATION FOR ALPHA STIRLING ENGINES ON ISOTHERMAL MODEL,” Revista de Engenharia Térmica, vol. 19, no. 2, p. 10, Dec. 2020, doi: 10.5380/reterm.v19i2.78608.

[189] J. Li and F. Wang, “Numerical investigations on the Stirling engine power and the efficiency of Stirling engine generator,” Advances in Mechanical Engineering, vol. 14, no. 8, Aug. 2022, doi: 10.1177/16878132221117017.

[190] J. A. Auñón, J. M. Pérez, M. J. Martín, F. Auñón, and D. Nuñez, “Development and validation of a software application to analyze thermal and kinematic multimodels of Stirling engines,” Heliyon, vol. 9, no. 9, Sep. 2023, doi: 10.1016/j.heliyon.2023.e18487.

[191] S. Alfarawi, R. AL-Dadah, and S. Mahmoud, “Performance evaluation of gamma-type Stirling engine using combined Schmidt and mechanical loss model,” European Journal of Sustainable Development Research, vol. 8, no. 1, p. em0240, Nov. 2023, doi: 10.29333/ejosdr/13888.

[192] K. Hirata, “SCHMIDT THEORY FOR STIRLING ENGINES.” [Online]. Available: http://www.nmri.go.jp/env/khirata/

[193] F. Arsalan Siddiqui et al., “Effect of phase angle on the efficiency of beta type Stirling engine Special Issue ‘Advances in Agricultural Engineering Technologies and Application’ in ‘Agriculture’ journal (IF 2.93) View project Van de Graaff Generator View project EFFECT OF PHASE ANGLE ON THE EFFICIENCY OF BETA TYPE STIRLING ENGINE 1* 2 2 2 3,” 2015. [Online]. Available: www.pu.edu.pk/journals/index.php/jfet/index

[194] J. Sedlák, A. Glváč, and A. Czán, “Design of stirling engine operating at low temperature difference,” in MATEC Web of Conferences, EDP Sciences, Mar. 2018. doi: 10.1051/matecconf/201815704003.

[195] T. Topgül, “Design, Manufacturing, and Thermodynamic Analysis of a Gamma-type Stirling Engine Powered by Solar Energy,” Strojniski Vestnik/Journal of Mechanical Engineering, vol. 68, no. 12, pp. 757–770, 2022, doi: 10.5545/sv-jme.2022.368.

[196] D. Chrenko et al., “A numerical optimisation of a Stirling engine,” 2011. [Online]. Available: https://www.researchgate.net/publication/260198030

[197] C. J. Paul and A. Engeda, “Modelling a Complete Stirling Engine,” 2018. [Online]. Available: https://www.sciencedirect.com/science/article/pii/S0360544214013000

[198] Ana Carolina Ávila Santos, Fábio Alfaia da Cunha, and Augusto César de Mendonça Brasil, “NUMERIC ANALYSIS OF AN ADIABATIC MODEL IN A STIRLING ENGINE,” in Proceedings of the 23rd ABCM International Congress of Mechanical Engineering, ABCM Brazilian Society of Mechanical Sciences and Engineering, 2015. doi: 10.20906/cps/cob-2015-2178.

[199] M. Cavazzuti, Optimization methods: From theory to design scientific and technological aspects in mechanics. Springer Berlin Heidelberg, 2013. doi: 10.1007/978-3-642-31187-1.

[200] I. and Urieli and Berchowitz D M., “ Stirling cycle engine analysis. United Kingdom: ,” 1984.

[201] M. Babaelahi and H. Sayyaadi, “Simple-II: A new numerical thermal model for predicting thermal performance of Stirling engines,” Energy, vol. 69, pp. 873–890, May 2014, doi: 10.1016/j.energy.2014.03.084.

[202] F. Ahmed, H. Hulin, and A. M. Khan, “Numerical modeling and optimization of beta-type Stirling engine,” Appl Therm Eng, vol. 149, pp. 385–400, Feb. 2019, doi: 10.1016/j.applthermaleng.2018.12.003.

[203] J. Kropiwnicki and M. Furmanek, “A theoretical and experimental study of moderate temperature alfa type stirling engines,” Energies (Basel), vol. 13, no. 7, 2020, doi: 10.3390/en13071622.

[204] Sa’ed A. Musmar and Iskander Tlili, “Numerical Investigation of Working Fluid Effect on Stirling Engine Performance,” International Journal of Thermal and Environmental Engineering, vol. 10, no. 1, 2015, doi: 10.5383/ijtee.10.01.005.

[205] D. G. Thombare and S. V. Karmare, “Theoretical and experimental investigation of Alfa type bio mass Stirling engine with effect of regenerator effectiveness, heat transfer, and properties of working fluid,” Journal of Renewable and Sustainable Energy, vol. 4, no. 4, Jul. 2012, doi: 10.1063/1.4748809.

[206] O. Taki, K. S. Rhazi, and Y. Mejdoub, “A Study of Stirling Engine Efficiency Combined with Solar Energy,” Advances in Science, Technology and Engineering Systems Journal, vol. 6, no. 2, pp. 837–845, Apr. 2021, doi: 10.25046/aj060297.

[207] C. H. Cheng, H. S. Yang, and L. Keong, “Theoretical and experimental study of a 300-W beta-type Stirling engine,” Energy, vol. 59, pp. 590–599, Sep. 2013, doi: 10.1016/j.energy.2013.06.060.

[208] J. Kropiwnicki, “Application of Stirling Engine Type Alpha Powered by the Recovery Energy on Vessels,” Polish Maritime Research, vol. 27, no. 1, pp. 96–106, Mar. 2020, doi: 10.2478/pomr-2020-0010.

[209] M. Sheykhi and M. Mehregan, “Improvement of technical performance of heat regenerator of GPU-3 Stirling engine,” Energy Reports, vol. 9, pp. 607–620, Dec. 2023, doi: 10.1016/j.egyr.2022.12.029.

[210] A. Sowale and A. J. Kolios, “Thermodynamic performance of heat exchangers in a free piston Stirling engine,” Energies (Basel), vol. 11, no. 3, Feb. 2018, doi: 10.3390/en11030505.

[211] W. Jan and P. Marek, “Mathematical Modeling of the Stirling Engine,” in Procedia Engineering, Elsevier Ltd, 2016, pp. 349–356. doi: 10.1016/j.proeng.2016.08.376.

[212] M. Chahartaghi and M. Sheykhi, “Thermal modeling of a trigeneration system based on beta-type Stirling engine for reductions of fuel consumption and pollutant emission,” J Clean Prod, vol. 205, pp. 145–162, Dec. 2018, doi: 10.1016/j.jclepro.2018.09.008.

[213] A. C. Ferreira, J. Silva, S. Teixeira, J. C. Teixeira, and S. A. Nebra, “Assessment of the Stirling engine performance comparing two renewable energy sources: Solar energy and biomass,” Renew Energy, vol. 154, pp. 581–597, Jul. 2020, doi: 10.1016/j.renene.2020.03.020.

[214] B. Urieli, “Stirling Cycle Engine Analysis,” 1984.

[215] S. Alfarawi, R. Al-Dadah, and S. Mahmoud, “Enhanced thermodynamic modelling of a gamma-type Stirling engine,” Appl Therm Eng, vol. 106, pp. 1380–1390, Aug. 2016, doi: 10.1016/j.applthermaleng.2016.06.145.

[216] I. Tlili, “Thermodynamic study on optimal solar stirling engine cycle taking into account the irreversibilities effects,” in Energy Procedia, 2012, pp. 584–591. doi: 10.1016/j.egypro.2011.12.979.

[217] S. Toghyani, A. Kasaeian, and M. H. Ahmadi, “Multi-objective optimization of Stirling engine using non-ideal adiabatic method,” Energy Convers Manag, vol. 80, pp. 54–62, Apr. 2014, doi: 10.1016/j.enconman.2014.01.022.

[218] J. A. Araoz, M. Salomon, L. Alejo, and T. H. Fransson, “NON-IDEAL STIRLING ENGINE THERMODYNAMIC MODEL SUITABLE FOR THE

INTEGRATION INTO OVERALL ENERGY SYSTEMS.” [Online]. Available: http://ees.elsevier.com/ate/

[219] Johannes M Strauss and Robert T Dobson, “Evaluation of a second order simulation for Sterling engine design and optimisation,” Journal of Energy in Southern Africa • Vol 21 No 2 , 2010.

[220] M. Ni et al., “Improved Simple Analytical Model and experimental study of a 100 W β-type Stirling engine,” Appl Energy, vol. 169, pp. 768–787, May 2016, doi: 10.1016/j.apenergy.2016.02.069.

[221] J. M. Daoud and D. Friedrich, “A new duplex Stirling engine concept for solar-powered cooling,” Int J Energy Res, vol. 44, no. 7, pp. 6002–6014, Jun. 2020, doi: 10.1002/er.5190.

[222] G. T. Udeh, S. Michailos, D. Ingham, K. J. Hughes, L. Ma, and M. Pourkashanian, “A new non-ideal second order thermal model with additional loss effects for simulating beta Stirling engines,” Energy Convers Manag, vol. 206, Feb. 2020, doi: 10.1016/j.enconman.2020.112493.

[223] R. Gheith, H. Hachem, F. Aloui, and S. Ben Nasrallah, “Experimental and theoretical investigation of Stirling engine heater: Parametrical optimization,” Energy Convers Manag, vol. 105, pp. 285–293, Aug. 2015, doi: 10.1016/j.enconman.2015.07.063.

[224] F. Ahadi, M. Azadi, M. Biglari, and S. N. Madani, “Study of coating effects on the performance of Stirling engine by non-ideal adiabatic thermodynamics modeling,” Energy Reports, vol. 7, pp. 3688–3702, Nov. 2021, doi: 10.1016/j.egyr.2021.06.063.

[225] H. Qiu, K. Wang, P. Yu, M. Ni, and G. Xiao, “A third-order numerical model and transient characterization of a β-type Stirling engine,” Energy, vol. 222, May 2021, doi: 10.1016/j.energy.2021.119973.

[226] W. Zhao, R. Li, H. Li, Y. Zhang, and S. Qiu, “Numerical analysis of fluid dynamics and thermodynamics in a stirling engine,” Appl Therm Eng, vol. 189, May 2021, doi: 10.1016/j.applthermaleng.2021.116727.

[227] W. R. Martini, “STIRLING ENGINE DESIGN MANUAL,” 1978.

[228] S. P. Kumbhar, D. G. Thombare, and N. K. Chhapkhane, “CFD Simulation of Stirling Engine Heater,” vol. 3, 2013, [Online]. Available: www.ijesr.org

[229] S. Alfarawi, R. AL-Dadah, and S. Mahmoud, “Potentiality of new miniature-channels Stirling regenerator,” Energy Convers Manag, vol. 133, pp. 264–274, Feb. 2017, doi: 10.1016/j.enconman.2016.12.017.

[230] R. W. Dyson, S. D. Wilson, and R. C. Tew, “Review of Computational Stirling Analysis Methods,” 2004. [Online]. Available: http://www.sti.nasa.gov

[231] A. Najah EL Idrissi, M. Benbrahim, and N. Rassai, “Effect of the particle size argan nut shell (ANS) biomass on combustion parameters in stirling engine in Morocco,” Results in Engineering, vol. 18, Jun. 2023, doi: 10.1016/j.rineng.2023.101202.

APPENDIX A

Gamma Stirling engine schematic diagrams and details are shown in Figures below, it consists of hot expansion cylinder with displacer constructed from aluminum, cold compression cylinder with power piston constructed from steel, crankshaft, flywheel, small regenerator passage, connecting rods, cooling fins.

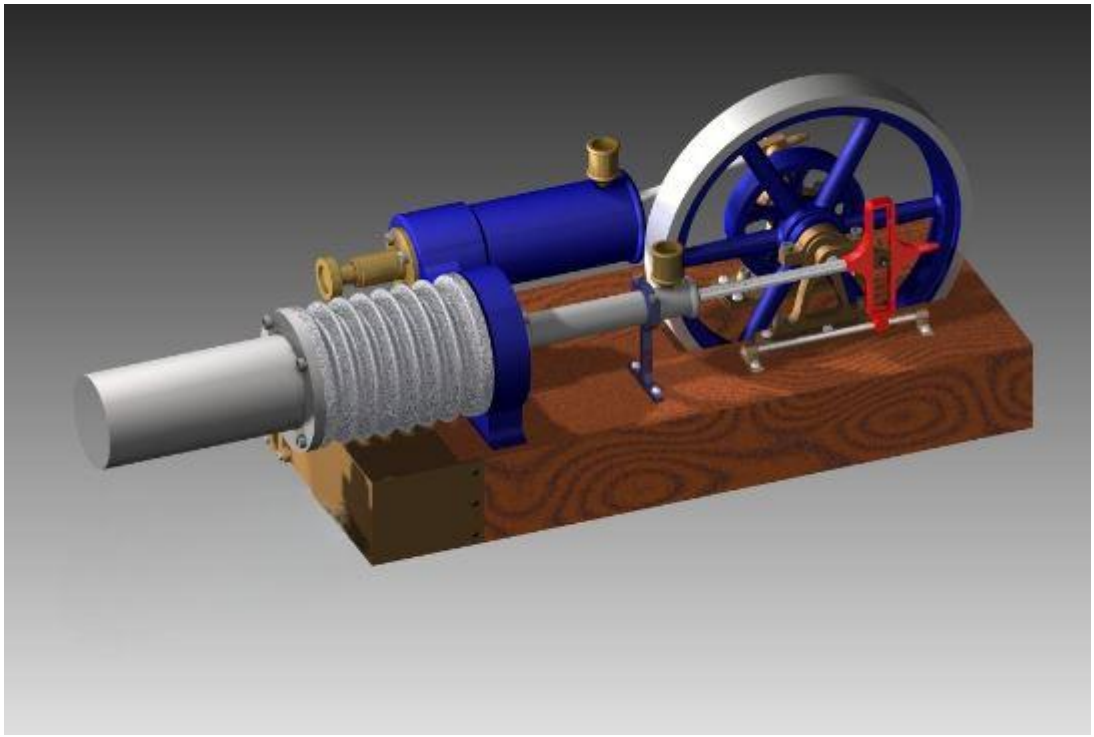

Figure (A-1): Drawing of Gamma Stirling engine

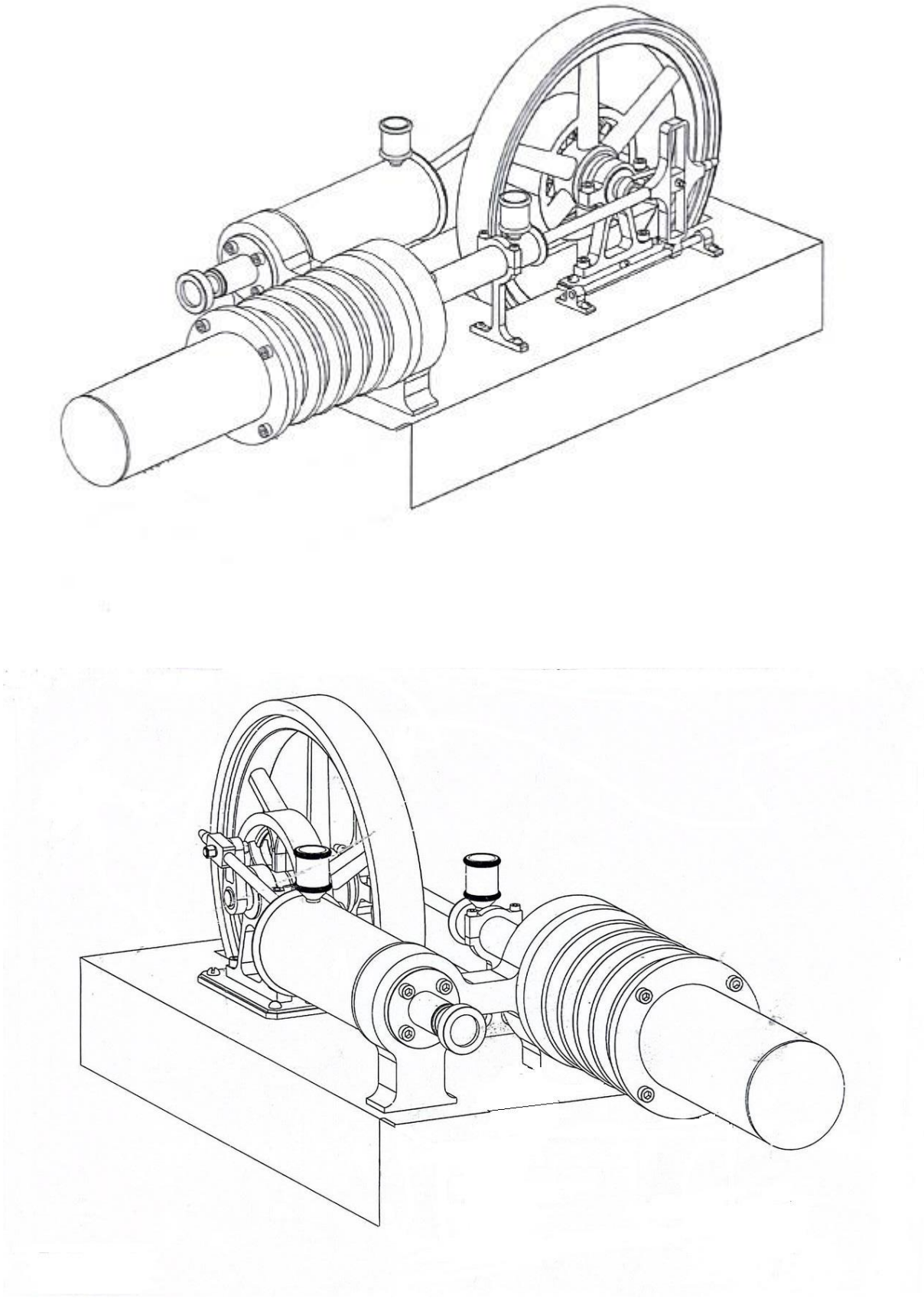

Figure (A-2): Schematic drawing of Gamma Stirling engine

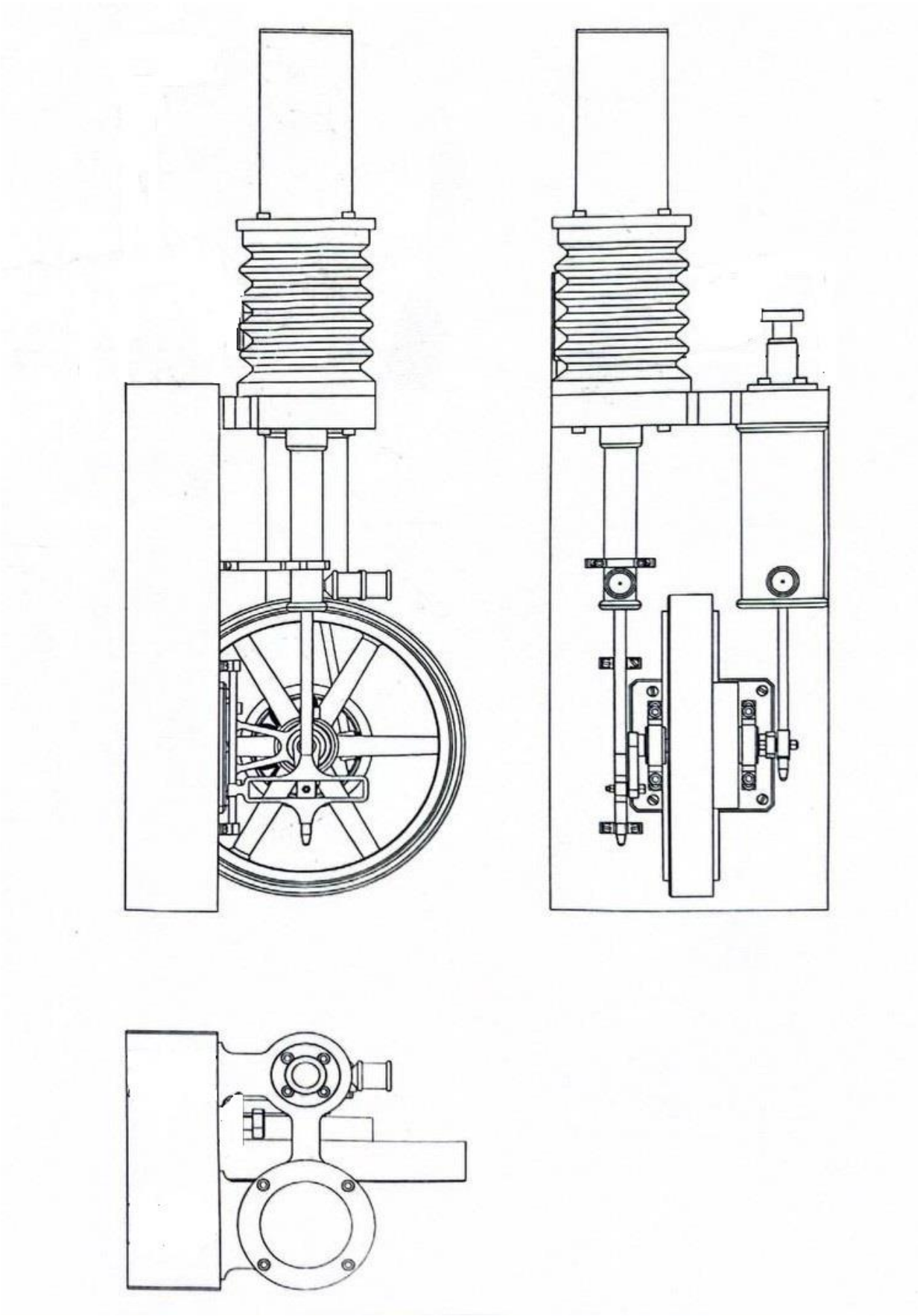

Figure (A-3): Top, front, and side view of Gamma Stirling engine

Expansion space

$Swept\ volume\ Vse = \frac{\pi}{4}\ d^2 l$ (A-1)

$l: displacer\ stroke$

$d: displacer\ diameter$

Compression space

$Swept\ volume\ Vsc = \frac{\pi}{4}\ d^2 l$ (A-2)

$l: power\ piston\ stroke$

$d: power\ piston\ diameter$

Heater

$Heater\ volume\ Vh = \frac{\pi}{4}\ d^2 l * n$ (A-3)

$l: passageways\ or\ tubes\ length$

$d: passageways\ or\ tubes\ diameter$

$n: passageways\ or\ tubes\ number$

Regenerator

$Regenerator\ volume\ Vr = porosity * A * l$ (A-4)

$A = \frac{\pi}{4}\ (dout^2 - din^2) * n$ (A-5)

$l: hight$

$A: matrix\ area$

$n: regenerators\ number$

Cooler

$Cooler\ volume\ Vk = \frac{\pi}{4}\ d^2 l * n$ (A-6)

$l: passageways\ or\ tubes\ length$

$d: passageways\ or\ tubes\ diameter$

$n: passageways\ or\ tubes\ number$

APPENDIX B

TABLE B-1: Molar mass, gas constant and ideal-gas specific heats of different fluids

Substance	Molar Mass M, kg/kmol	Gas Constant R, kJ/kg·K*	Specific Heat Data at 25°C		
			c_p, kJ/kg·K	c_v, kJ/kg·K	$k = c_p/c_v$
Air	28.97	0.2870	1.005	0.7180	1.400
Ammonia, NH_3	17.03	0.4882	2.093	1.605	1.304
Argon, Ar	39.95	0.2081	0.5203	0.3122	1.667
Bromine, Br_2	159.81	0.05202	0.2253	0.1732	1.300
Isobutane, C_4H_{10}	58.12	0.1430	1.663	1.520	1.094
n-Butane, C_4H_{10}	58.12	0.1430	1.694	1.551	1.092
Carbon dioxide, CO_2	44.01	0.1889	0.8439	0.6550	1.288
Carbon monoxide, CO	28.01	0.2968	1.039	0.7417	1.400
Chlorine, Cl_2	70.905	0.1173	0.4781	0.3608	1.325
Chlorodifluoromethane (R-22), $CHClF_2$	86.47	0.09615	0.6496	0.5535	1.174
Ethane, C_2H_6	30.070	0.2765	1.744	1.468	1.188
Ethylene, C_2H_4	28.054	0.2964	1.527	1.231	1.241
Fluorine, F_2	38.00	0.2187	0.8237	0.6050	1.362
Helium, He	4.003	2.077	5.193	3.116	1.667
n-Heptane, C_7H_{16}	100.20	0.08297	1.649	1.566	1.053
n-Hexane, C_6H_{14}	86.18	0.09647	1.654	1.558	1.062
Hydrogen, H_2	2.016	4.124	14.30	10.18	1.405
Krypton, Kr	83.80	0.09921	0.2480	0.1488	1.667
Methane, CH_4	16.04	0.5182	2.226	1.708	1.303
Neon, Ne	20.183	0.4119	1.030	0.6180	1.667
Nitrogen, N_2	28.01	0.2968	1.040	0.7429	1.400
Nitric oxide, NO	30.006	0.2771	0.9992	0.7221	1.384
Nitrogen dioxide, NO_2	46.006	0.1889	0.8060	0.6171	1.306
Oxygen, O_2	32.00	0.2598	0.9180	0.6582	1.395
n-Pentane, C_5H_{12}	72.15	0.1152	1.664	1.549	1.074
Propane, C_3H_8	44.097	0.1885	1.669	1.480	1.127
Propylene, C_3H_6	42.08	0.1976	1.531	1.333	1.148
Steam, H_2O	18.015	0.4615	1.865	1.403	1.329
Sulfur dioxide, SO_2	64.06	0.1298	0.6228	0.4930	1.263
Tetrachloromethane, CCl_4	153.82	0.05405	0.5415	0.4875	1.111
Tetrafluoroethane (R-134a), $C_2H_2F_4$	102.03	0.08149	0.8334	0.7519	1.108
Trifluoroethane (R-143a), $C_2H_3F_3$	84.04	0.09893	0.9291	0.8302	1.119
Xenon, Xe	131.30	0.06332	0.1583	0.09499	1.667

TABLE B–2: Different fluid properties relate to boiling points.

	Boiling Data at I atm		Freezing Data		Liquid Properties		
Substance	Normal Boiling Point, °C	Latent Heat of Vaporization h_{fg}, kJ/kg	Freezing Point, °C	Latent Heat of Fusion h_{if}, kJ/kg	Temperature, °C	Density ρ, kg/m^3	Specific Heat c_p, kJ/kg·K
Ammonia	−33.3	1357	−77.7	322.4	−33.3	682	4.43
					−20	665	4.52
					0	639	4.60
					25	602	4.80
Argon	−185.9	161.6	−189.3	28	−185.6	1394	1.14
Benzene	80.2	394	5.5	126	20	879	1.72
Brine (20% sodium chloride by mass)	103.9	—	−17.4	—	20	1150	3.11
n-Butane	−0.5	385.2	−138.5	80.3	−0.5	601	2.31
Carbon dioxide	−78.4*	230.5 (at 0°C)	−56.6		0	298	0.59
Ethanol	78.2	838.3	−114.2	109	25	783	2.46
Ethyl alcohol	78.6	855	−156	108	20	789	2.84
Ethylene glycol	198.1	800.1	−10.8	181.1	20	1109	2.84
Glycerine	179.9	974	18.9	200.6	20	1261	2.32
Helium	−268.9	22.8	—	—	−268.9	146.2	22.8
Hydrogen	−252.8	445.7	−259.2	59.5	−252.8	70.7	10.0
Isobutane	−11.7	367.1	−160	105.7	−11.7	593.8	2.28
Kerosene	204–293	251	−24.9	—	20	820	2.00
Mercury	356.7	294.7	−38.9	11.4	25	13,560	0.139
Methane	−161.5	510.4	−182.2	58.4	−161.5	423	3.49
					−100	301	5.79
Methanol	64.5	1100	−97.7	99.2	25	787	2.55
Nitrogen	−195.8	198.6	−210	25.3	−195.8	809	2.06
					−160	596	2.97
Octane	124.8	306.3	−57.5	180.7	20	703	2.10
Oil (light)					25	910	1.80
Oxygen	−183	212.7	−218.8	13.7	−183	1141	1.71
Petroleum	—	230–384			20	640	2.0
Propane	−42.1	427.8	−187.7	80.0	−42.1	581	2.25
					0	529	2.53
					50	449	3.13
Refrigerant-134a	−26.1	216.8	−96.6	—	−50	1443	1.23
					−26.1	1374	1.27
					0	1295	1.34
					25	1207	1.43
Water	100	2257	0.0	333.7	0	1000	4.22
					25	997	4.18
					50	988	4.18
					75	975	4.19
					100	958	4.22